Title
Characterizing meiotic mechanisms in C. elegans

Author
Kasad, Roshni

Publication Date
2010

Peer reviewed|Thesis/dissertation

Characterizing meiotic mechanisms in *C. elegans*

by

Roshni Adi Kasad

A dissertation submitted in partial satisfaction of the

requirements for the degree of

Doctor of Philosophy

in

Molecular and Cell Biology

in the

Graduate Division

of the

University of California, Berkeley

Committee in charge:

Professor Abby F. Dernburg, Chair
Professor W. Zacheus Cande
Professor Daniel Fletcher
Professor Karsten Weis

Spring 2010

Abstract

Characterizing meiotic mechanisms in *C. elegans*

by

Roshni Adi Kasad

Doctor of Philosophy in Molecular and Cell Biology

University of California, Berkeley

Professor Abby F. Dernburg, Chair

Meiosis is the specialized cell division by which haploid egg and sperm cells are generated from mitotically dividing diploid germ cells. During early prophase, the environment of the nucleus is dynamic, as a given chromosome will undergo a series of encounters with homologous and nonhomologous chromosomes. A fundamental problem is how each chromosome is able to discriminate and accurately pair and form stabilized interactions via the synaptonemal complex only with its appropriate partner. It is only within this context of homologous interactions that recombination can take place, which is what allows for genetic diversity among sexually reproducing species.

In Chapters 1 and 2, I will focus on homolog pairing and synapsis and will discuss experiments that point towards the Pairing Center protein HIM-8 functioning as a molecular link that couples these two events. In Chapter 3, I will discuss the role of the chromatin factor GAK-1 in meiosis. I will show that GAK-1 plays a role at multiple steps in meiosis, including recombination and maintenance of the synaptonemal complex. The data suggest that GAK-1 may function as a transcription factor for meiosis-specific genes, which would explain the pleiotropic effects seen in meiosis. These studies will hopefully further our understanding of the molecular basis of aneuploidies.

Table of contents

List of Figures and Tables

Acknowledgments

Thank you to Sara Jover-Gil for performing the initial experiments and analysis that led to the work presented in Chapter 3, to Abby Dernburg for her mentorship during my graduate career, and to all past and present members of the Dernburg lab for their support and guidance over the past six years.

Introduction:
Achieving homologous interactions

Meiosis is the basis of sexual reproduction

The observation that fertilization involves the penetration of an egg cell by sperm was first observed in sea urchins by Oscar Hertwig in 1876 (Churchill, 1970). During the latter part of the nineteenth century, scientists reasoned that a specialized mechanism had to exist to prevent genome doubling at fertilization, which thereby allowed maintenance of diploidy in somatic cells (Scherthan, 2001). In 1887, August Weismann hypothesized the existence of 'Reduktionstheilung' or reductional division to explain the haploid number of chromosomes in germ cells. Through basic cytology, scientists first described key events of reductional division, including polarized rearrangement of chromatin, homolog pairing, and intimate homolog associations that were coined as synapsis (discussed below).

The hallmark of sexual reproduction is meiosis. In this specialized type of cell division, a population of progenitor cells goes through two rounds of division to produce sperm or egg, which have half the number of chromosomes. It is essential that the chromosome number is halved so that the proper diploid complement of chromosomes is restored in the zygote when the sperm fertilizes the egg. During meiosis, maternal and paternal chromosomes, known as homologs, undergo highly regulated interactions to ensure that they eventually segregate away from each other.

In meiosis, a single round of DNA replication is followed by meiosis I, the first round of division where homologs segregate away from each other to two daughter cells. In the next round of division, meiosis II, sister chromatids segregate away from each other, which is similar to what occurs in mitosis. During meiotic prophase, three key events occur that create physical links between homologs, which are often required for proper chromosome segregation. Homologs must first find each other and pair. In most organisms, this pairing is then stabilized by synapsis, which is the formation of the synaptonemal complex (SC), a proteinaceous complex that forms between homologs. In the context of the SC, reciprocal recombination events are completed, allowing an exchange of genetic information and also establishing a physical linkage between paired homologs. It is these exchanges of chromosomal segments, known as crossovers, that allow for genetic diversity among sexually reproducing species. Some organisms have dispensed with synapsis or even recombination; however, it seems that pairing between homologs is universally required to enable them to biorient on the meiosis I spindle so that they accurately segregate away from each other.

Meiosis has profound consequences when it goes awry. Defects in meiosis can result in aneuploidy, where a gamete carries either too many or too few of a particular chromosome. In most situations, dosage imbalance of an entire chromosome is not tolerated, and the zygote dies early in development. In *Saccharomyces cerevisiae*, the rate of nondisjunction (failure of homologs to segregate away from each other) is roughly 1 in 1,000 to 1 in 10,000 viable spores (Sears et al., 1992; Sora et al., 1982). In *C. elegans,* ~0.2% of all meioses result in nondisjunction of the X chromosome (Hodgkin et al., 1979). In mouse, the incidence of aneuploid fertilized eggs ranges from 1-2% (Hassold and Hunt, 2001). The nondisjunction rate in humans is astonishingly high compared to other species. In humans, 10-30% of fertilized eggs are aneuploid with the majority being either trisomic or monosomic for a particular chromosome.

Aneuploidy is the leading cause of miscarriages, accounting for roughly 30%. Given such a high incidence of meiotic failure in humans, understanding the principles that govern proper chromosome segregation in meiosis is of high interest.

It has been difficult to dissect the underlying molecular causes of nondisjunction in humans. A strong correlation is seen between aneuploidy and increased maternal age, known as the maternal age effect. Defects in executing homolog pairing, synapsis, and/or recombination have been shown to increase the chances of aneuploid daughter cells in humans and model systems. In humans, studies show that achiasmate (non-recombinant) homologs and/or homologs where crossovers occur close to telomeres can lead to aneuploidy in oogenesis (Hassold et al., 2007). A reduction in the number of crossovers is also associated with male infertility in humans. As will be apparent below, we have gained much insight into the molecular mechanisms of homolog pairing, synapsis, and recombination and how they are all coordinated to achieve proper segregation of chromosomes through the study of model organisms.

Homolog pairing can be double-strand break-dependent or –independent

Organisms have evolved divergent mechanisms for achieving homolog pairing and synapsis. One class of mechanisms is double-strand break (DSB)-dependent, which is utilized by budding yeast, Arabidopsis, and mice (Baudat et al., 2000; Giroux et al., 1989; Grelon et al., 2001; Romanienko and Camerini-Otero, 2000). These mechanisms require the initiation of recombination, which occurs when Spo11 generates a DSB in one sister chromatid (Keeney et al., 1997). Homology is presumably assessed through complementary base pairing, and pairing is stabilized by SC polymerization (Gerton and Hawley, 2005). In organisms relying predominantly on DSB-dependent pairing, the absence of Spo11 results in loss of pairing and synapsis.

In contrast, *Drosophila* and *C. elegans* have evolved primarily DSB-independent pairing mechanisms (Dernburg et al., 1998; McKim and Hayashi-Hagihara, 1998). In the absence of recombination, homologs pair and synapse efficiently. Stable pairing relies on *cis*-acting chromosomal sites called Pairing Centers (PCs) in worms (MacQueen et al., 2005; McKim et al., 1993; Villeneuve, 1994). In female flies, it is specifically heterochromatic regions of homologous chromosomes that pair (Dernburg et al., 1996; Karpen et al., 1996), and in male flies, the rDNA locus seems to mediate pairing of the sex chromosomes (McKee and Karpen, 1990).

***cis*-acting DNA elements mediate homolog pairing**

A number of organisms have evolved various pairing center-like sites to assist in establishment or maintenance of homolog pairing. In *Drosophila* males, the rDNA locus on the sex chromosomes functions as the X-Y pairing site (McKee and Karpen, 1990). Two chromatin factors, SNM (a cohesin-like protein) and MNM (a zinc-finger protein), bind to this locus and are required for proper segregation (Thomas et al., 2005). In *Saccharomyces cerevisiae*, pairing centers *per se* do not exist, but evidence points towards centromeres as sites that promote homolog pairing and synapsis initiation (Kemp et al., 2004; Tsubouchi and Roeder, 2005). Additionally, telomeres play a large role in mediating homologous interactions (discussed below).

In *C. elegans*, PCs have been mapped to sub-telomeric regions near one end of each chromosome (McKim et al., 1993; Villeneuve, 1994). PCs promote the stabilization of homolog

pairing and synapsis initiation (MacQueen et al., 2005) In addition, a family of zinc-finger proteins that bind to the PCs is essential for stabilizing pairing. Specifically, HIM-8 binds to the X Chromosome PC (Phillips et al., 2005), while three paralogs, ZIM-1, -2, and -3 (zinc-finger in meiosis), bind to autosomal PCs (Phillips and Dernburg, 2006). ZIM-1 localizes to chromosomes II and III PCs, ZIM-2 localizes to the chromosome V PC, and ZIM-3 localizes to chromosomes I and IV PCs. Mutations that disrupt PCs or the *him-8/zim* gene family abrogate pairing, which results in synapsis and chromosome segregation defects. *him-8* and X chromosome PC deficiencies cause a Him (High incidence of males) phenotype. *C. elegans* has two sexes: hermaphrodites (*XX*) and males (*XO*), which arise among the self-progeny of hermaphrodites due to missegregation of the X. Wild type animals give rise to roughly 0.2% males, while meiotic mutants in worms that lead to increased missegregation of Xs also result in an elevated number of male progeny, known as a Him phenotype (Hodgkin et al., 1979). Mutations in *zim* genes are associated with high levels of embryonic lethality due to missegregation of autosomes. A previous study points towards Pairing Centers as the sites of synapsis initiation (MacQueen et al., 2005), but which proteins (whether PC proteins or others) coordinate synapsis initiation remain unknown.

Synapsis reinforces and stabilizes interactions between homologs

Homolog pairing is stabilized by synapsis. The synaptonemal complex is made of lateral elements that form along the lengths of each homolog and transverse filaments that span the 100 nm gap between the axis of homologs (Colaiacovo, 2006). Lateral elements that load onto unpaired DNA are called axial elements. In *C. elegans*, four axial elements have been identified (HIM-3 and HTP-1-3), which all share the common feature of having a HORMA domain, a motif that is also found in cell-cycle checkpoint proteins. Budding yeast appears to have only one transverse filament protein, but in *C. elegans*, four different components, SYP-1-4 have been identified (Colaiacovo et al., 2003; MacQueen et al., 2002; Smolikov et al., 2007; Smolikov et al., 2009). Synapsis is defined by the loading of these transverse elements to the axis of paired DNA.

Mutations in a number of SC components (e.g., *htp-1*, *him-3*, and *syp-4*) result in synapsis between nonhomologous regions. Additionally, studies using reciprocal translocations show that synapsis can proceed robustly in the absence of homology in *C. elegans*. MacQueen *et al.* (2005) show that chromosome pairs that share the same PC efficiently synapse even if the remaining portions of the chromosomes are nonhomologous and are of different physical lengths. All together, the above data suggest that synapsis does not require homology and that it must therefore be regulated to prevent its occurrence between inappropriate partners.

Pairing and synapsis are coupled via the meiotic "bouquet"

In many organisms, during the leptotene/zygotene stage of early meiotic prophase, chromosomes adopt a bouquet formation, in which the telomeres of all chromosomes are associated with the nuclear periphery and are often clustered at one side of the nucleus (Zickler and Kleckner, 1998). In budding yeast, mutations that disrupt bouquet formation (*e.g.*, *ndj1*Δ) also perturb homolog pairing (Trelles-Sticken et al., 2000). This led to the hypothesis that bouquet formation facilitates pairing by bringing homologs in close proximity via telomere attachments to the nuclear periphery. More recently, bouquet formation has been thought to play an integral role in restricting nonhomologous interactions (Koszul and Kleckner, 2009). In fission yeast, mutations that disrupt bouquet formation have reduced homolog pairing, but

ectopic recombination (recombination between non-allelic sites) is elevated (Davis and Smith, 2006; Niwa et al., 2000). In maize, mutations that abrogate bouquet formation also lead to nonhomologous synapsis (Golubovskaya et al., 2002).

A nuclear organization analogous to the bouquet is observed in *C. elegans* during leptotene/zygotene, or the transition zone (TZ). During this stage, PCs are tethered to the nuclear envelope (NE), causing all the chromatin to be asymmetrically localized towards one side of the nucleus (Albertson, 1997; Phillips and Dernburg, 2006). In mutants that never achieve a polarized state of chromatin (*e.g.*, *chk-2*Δ), pairing and synapsis are disrupted, providing evidence that this analogous state in worms may also facilitate pairing (MacQueen and Villeneuve, 2001). HIM-8/ZIMs may play a role in this process by tethering PC ends to the NE. In the TZ, extensive colocalization occurs between HIM-8/ZIMs and two NE proteins, ZYG-12 and SUN-1. ZYG-12 is an outer-membrane protein that is required for centrosome attachment to the nucleus in mitosis and mediates interactions with microtubules (Malone et al., 2003). SUN-1 is an inner nuclear envelope protein and is necessary for ZYG-12 localization to the NE (Fridkin et al., 2004; Malone et al., 2003). A point mutation in *sun-1* mutants also confers a Him phenotype, and deletion alleles genetically interact with X PC deficiencies. Sato et al. (2009) have perturbed various components of this nuclear envelope network and have proposed a model whereby microtubules facilitate homolog pairing and nuclear envelope patch components function both to promote pairing and synapsis and to inhibit nonhomologous interactions .

The recombination pathway

In the context of paired and synapsed homologous chromosomes, crossover recombination can occur where there is reciprocal exchange of genetic material between homologs. The first step in meiotic recombination is to initiate programmed double-strand breaks (DSBs) in one sister chromatid. This is accomplished by Spo11, which has orthologs in a range of species, including *C. elegans*, budding yeast, humans, and mice (Dernburg et al., 1998; Keeney et al., 1997; Metzler-Guillemain and de Massy, 2000; Romanienko and Camerini-Otero, 1999). Spo11 cuts DNA via a topoisomerase-like reaction to generate a covalent attachment between itself and the 5' DNA ends on either side of the DSB (Keeney and Kleckner, 1995). The Mre11-Rad50-Xrs2 complex then releases Spo11-bound short oligonucleotides. This is followed by 5' to 3' resection of DNA, which leaves 3'-single-stranded DNA (ssDNA) tails. The endonucleases required for this resection have been difficult to identify; though, recent evidence implicates proteins involved in mitotic DNA repair, namely the Exo1 nuclease and the Sgs1 helicase (Manfrini et al., 2010).

The 3'-ssDNA overhangs are then coated with RPA, which is then replaced by the RecA-like proteins, Rad51 and Dmc1, which assist in strand invasion (Bishop et al., 1992; Osman et al., 2009; Shinohara et al., 1992). Rad51/Dmc1-coated ssDNA invades a chromatid of the homolog to form heteroduplex DNA. Subsequent capture of the second DSB end, DNA synthesis, and ligation of broken ends leads to the formation of the classical double Holliday junction (Neale and Keeney, 2006). Recently, a number of molecules, including SLX4 and GEN1 in humans and HIM-18 in *C. elegans* have been proposed and/or identified as Holliday junction resolvases that lead to the formation of mature crossovers (Fekairi et al., 2009; Ip et al., 2008; Saito et al., 2009). Not all DSBs are converted to crossovers; a subset of breaks never form double Holliday junctions and are instead shunted down a noncrossover pathway in which local gene conversion occurs, but flanking markers are not exchanged (Neale and Keeney, 2006).

The various steps of the recombination pathway present many opportunities for imposing regulation of a process that is seemingly harmful to the genome.

Regulating the number and placement of crossovers

Deliberately inducing DNA damage via meiotic double-strand breaks could potentially be hazardous for genome integrity; yet, initiating recombination is necessary for two reasons: 1) to generate a physical linkage, the chiasma, which allows for proper alignment of homologs at the metaphase I plate to ensure proper segregation, and 2) to generate diversity among sexually reproducing species. Many levels of regulation are in place at various stages of the recombination pathway to maintain genome stability.

The first level of control is exerted at the step of DSB initiation. Meiotic recombination can only occur properly if DNA replication and sister chromatid cohesion have been established (Murakami and Keeney, 2008). To ensure proper timing, studies have found that various cell-cycle checkpoints prevent initiation of DSBs before completion of DNA replication. Additionally, some level of control is exerted on the distribution of DSBs throughout the genome, as they tend to be enriched in specific regions of the genome known as DSB hotspots (Petes, 2001). DSBs are often associated with active chromatin (H3K4me3) and are more frequently found in gene promoters and sub-telomeric regions in budding yeast (Blitzblau et al., 2007; Borde et al., 2009; Wu and Lichten, 1994). Whether DSB hotspots exist in *C. elegans* is unknown, but is currently being investigated.

Another level of control on meiotic recombination is through a phenomenon known as crossover interference, which was first observed in *Drosophila* (Muller, 1916; Sturtevant, 1915). When crossovers are spaced further apart on a chromosome than expected by chance, interference is said to be taking place. *C. elegans* exhibit an extreme form of interference where exactly one crossover occurs per homolog pair (Hillers and Villeneuve, 2003). One hypothesis for why interference exists may be to ensure that each homolog pair undergoes recombination. Assuming that a limited number of crossovers can occur in a given meiocyte, a random distribution of crossovers could result in smaller chromosomes being more unlikely to receive a crossover, leading to nondisjunction (Kaback et al., 1999).

The mechanism(s) by which interference is established has been enigmatic. Kleckner et al. (2004) proposed that stress forces in the axes promote crossovers, which in turn relieve axial stress locally, thereby suppressing further crossovers and thus, promoting interference. Other evidence suggests that the synaptonemal complex, itself, promotes interference (Sym and Roeder, 1994). In *C. elegans*, mutations that alter chromatin compaction are correlated with a reduction of interference (Mets and Meyer, 2009). Youds et al. recently showed that the RTEL-1 protein has anti-recombinase activity, which promotes interference in *C. elegans* (Barber et al., 2008; Youds et al., 2010). Additionally, defects in pairing of one homolog pair have also been associated with loss of crossover control on the remaining chromosomes (Carlton et al., 2006).

Finally, another level of regulation within the recombination pathway is through the distribution of crossovers throughout the genome. In budding yeast, crossovers are suppressed at centromeres and telomeres (Chen et al., 2008; Mancera et al., 2008). In humans and mice, PRMD9 is a chromatin-binding factor that recognizes particular sequence motifs and is a major determinant of crossover hotspots (Baudat et al., 2010). *C. elegans* also has a nonrandom distribution of crossovers. The organization of the *C. elegans* genome differs from that of mammals, yeast, and other model systems. First, there are no specified centromeric regions; instead, centromere activity is distributed along the length of the chromosomes (Maddox et al.,

2004). Protein coding genes are clustered towards the centers of each of the five autosomes and are more evenly dispersed along the X chromosome (Brenner, 1974). Meiotic crossovers show a biased distribution towards the gene-poor regions in the arms of the chromosomes (Barnes et al., 1995; Rockman and Kruglyak, 2009). A mutation in the *rec-1* gene results in a redistribution of crossovers more evenly across the physical length of the chromosome; however, it does not alter the total number of crossovers, nor does it result in elevated nondisjunction (Zetka and Rose, 1995).

Concluding Remarks

Model systems such as *C. elegans* are amenable to studying the molecular mechanisms of meiosis because they are easily manipulated for genetics and also because all stages of meiocytes can be observed cytologically in fixed samples. In the following chapters, I will discuss studies done in *C. elegans* to better understand how pairing, synapsis, and recombination are coordinated so that chromosome interactions only take place between homologous partners. The work presented in Chapters 1 and 2 focuses on homolog pairing and synapsis. Specifically, my experiments demonstrate that the Pairing Center protein HIM-8 contributes to both pairing and synapsis, providing evidence for a molecular link that may couple these two events. In Chapter 3, I will present my analysis of the role of a chromatin component, GAK-1, which seems to have pleiotropic effects on meiosis in *C. elegans*.

References

Albertson, D.G., Rose, A.M., and Villeneuve, A.M. (1997). Chromosome organization, mitosis, and meiosis. C elegans II (eds DL Riddle et al), 47-78.

Barber, L.J., Youds, J.L., Ward, J.D., McIlwraith, M.J., O'Neil, N.J., Petalcorin, M.I., Martin, J.S., Collis, S.J., Cantor, S.B., Auclair, M.*, et al.* (2008). RTEL1 maintains genomic stability by suppressing homologous recombination. Cell *135*, 261-271.

Barnes, T.M., Kohara, Y., Coulson, A., and Hekimi, S. (1995). Meiotic recombination, noncoding DNA and genomic organization in Caenorhabditis elegans. Genetics *141*, 159-179.

Baudat, F., Buard, J., Grey, C., Fledel-Alon, A., Ober, C., Przeworski, M., Coop, G., and de Massy, B. (2010). PRDM9 is a major determinant of meiotic recombination hotspots in humans and mice. Science *327*, 836-840.

Baudat, F., Manova, K., Yuen, J.P., Jasin, M., and Keeney, S. (2000). Chromosome synapsis defects and sexually dimorphic meiotic progression in mice lacking Spo11. Mol Cell *6*, 989-998.

Bishop, D.K., Park, D., Xu, L., and Kleckner, N. (1992). DMC1: a meiosis-specific yeast homolog of E. coli recA required for recombination, synaptonemal complex formation, and cell cycle progression. Cell *69*, 439-456.

Blitzblau, H.G., Bell, G.W., Rodriguez, J., Bell, S.P., and Hochwagen, A. (2007). Mapping of meiotic single-stranded DNA reveals double-stranded-break hotspots near centromeres and telomeres. Curr Biol *17*, 2003-2012.

Borde, V., Robine, N., Lin, W., Bonfils, S., Geli, V., and Nicolas, A. (2009). Histone H3 lysine 4 trimethylation marks meiotic recombination initiation sites. EMBO J *28*, 99-111.

Brenner, S. (1974). The genetics of Caenorhabditis elegans. Genetics *77*, 71-94.

Carlton, P.M., Farruggio, A.P., and Dernburg, A.F. (2006). A link between meiotic prophase progression and crossover control. PLoS Genet *2*, e12.

Chen, S.Y., Tsubouchi, T., Rockmill, B., Sandler, J.S., Richards, D.R., Vader, G., Hochwagen, A., Roeder, G.S., and Fung, J.C. (2008). Global analysis of the meiotic crossover landscape. Dev Cell *15*, 401-415.

Churchill, F.B. (1970). Hertwig, Weismann, and the meaning of reduction division circa 1890. Isis *61*, 429-457.

Colaiacovo, M.P. (2006). The many facets of SC function during C. elegans meiosis. Chromosoma *115*, 195-211.

Colaiacovo, M.P., MacQueen, A.J., Martinez-Perez, E., McDonald, K., Adamo, A., La Volpe, A., and Villeneuve, A.M. (2003). Synaptonemal complex assembly in C. elegans is dispensable for loading strand-exchange proteins but critical for proper completion of recombination. Dev Cell *5*, 463-474.

Davis, L., and Smith, G.R. (2006). The meiotic bouquet promotes homolog interactions and restricts ectopic recombination in Schizosaccharomyces pombe. Genetics *174*, 167-177.

Dernburg, A.F., McDonald, K., Moulder, G., Barstead, R., Dresser, M., and Villeneuve, A.M. (1998). Meiotic recombination in C. elegans initiates by a conserved mechanism and is dispensable for homologous chromosome synapsis. Cell *94*, 387-398.

Dernburg, A.F., Sedat, J.W., and Hawley, R.S. (1996). Direct evidence of a role for heterochromatin in meiotic chromosome segregation. Cell *86*, 135-146.

Fekairi, S., Scaglione, S., Chahwan, C., Taylor, E.R., Tissier, A., Coulon, S., Dong, M.Q., Ruse, C., Yates, J.R., 3rd, Russell, P.*, et al.* (2009). Human SLX4 is a Holliday junction resolvase subunit that binds multiple DNA repair/recombination endonucleases. Cell *138*, 78-89.

Fridkin, A., Mills, E., Margalit, A., Neufeld, E., Lee, K.K., Feinstein, N., Cohen, M., Wilson, K.L., and Gruenbaum, Y. (2004). Matefin, a Caenorhabditis elegans germ line-specific SUN-domain nuclear membrane protein, is essential for early embryonic and germ cell development. Proc Natl Acad Sci U S A *101*, 6987-6992.
Gerton, J.L., and Hawley, R.S. (2005). Homologous chromosome interactions in meiosis: diversity amidst conservation. Nat Rev Genet *6*, 477-487.
Giroux, C.N., Dresser, M.E., and Tiano, H.F. (1989). Genetic control of chromosome synapsis in yeast meiosis. Genome *31*, 88-94.
Golubovskaya, I.N., Harper, L.C., Pawlowski, W.P., Schichnes, D., and Cande, W.Z. (2002). The pam1 gene is required for meiotic bouquet formation and efficient homologous synapsis in maize (Zea mays L.). Genetics *162*, 1979-1993.
Grelon, M., Vezon, D., Gendrot, G., and Pelletier, G. (2001). AtSPO11-1 is necessary for efficient meiotic recombination in plants. Embo J *20*, 589-600.
Hassold, T., Hall, H., and Hunt, P. (2007). The origin of human aneuploidy: where we have been, where we are going. Hum Mol Genet *16 Spec No. 2*, R203-208.
Hassold, T., and Hunt, P. (2001). To err (meiotically) is human: the genesis of human aneuploidy. Nat Rev Genet *2*, 280-291.
Hillers, K.J., and Villeneuve, A.M. (2003). Chromosome-wide control of meiotic crossing over in C. elegans. Curr Biol *13*, 1641-1647.
Hodgkin, J., Horvitz, H.R., and Brenner, S. (1979). Nondisjunction Mutants of the Nematode CAENORHABDITIS ELEGANS. Genetics *91*, 67-94.
Ip, S.C., Rass, U., Blanco, M.G., Flynn, H.R., Skehel, J.M., and West, S.C. (2008). Identification of Holliday junction resolvases from humans and yeast. Nature *456*, 357-361.
Kaback, D.B., Barber, D., Mahon, J., Lamb, J., and You, J. (1999). Chromosome size-dependent control of meiotic reciprocal recombination in Saccharomyces cerevisiae: the role of crossover interference. Genetics *152*, 1475-1486.
Karpen, G.H., Le, M.H., and Le, H. (1996). Centric heterochromatin and the efficiency of achiasmate disjunction in Drosophila female meiosis. Science *273*, 118-122.
Keeney, S., Giroux, C.N., and Kleckner, N. (1997). Meiosis-specific DNA double-strand breaks are catalyzed by Spo11, a member of a widely conserved protein family. Cell *88*, 375-384.
Keeney, S., and Kleckner, N. (1995). Covalent protein-DNA complexes at the 5' strand termini of meiosis-specific double-strand breaks in yeast. Proc Natl Acad Sci U S A *92*, 11274-11278.
Kemp, B., Boumil, R.M., Stewart, M.N., and Dawson, D.S. (2004). A role for centromere pairing in meiotic chromosome segregation. Genes Dev *18*, 1946-1951.
Kleckner, N., Zickler, D., Jones, G.H., Dekker, J., Padmore, R., Henle, J., and Hutchinson, J. (2004). A mechanical basis for chromosome function. Proc Natl Acad Sci U S A *101*, 12592-12597.
Koszul, R., and Kleckner, N. (2009). Dynamic chromosome movements during meiosis: a way to eliminate unwanted connections? Trends Cell Biol *19*, 716-724.
MacQueen, A.J., Colaiacovo, M.P., McDonald, K., and Villeneuve, A.M. (2002). Synapsis-dependent and -independent mechanisms stabilize homolog pairing during meiotic prophase in C. elegans. Genes Dev *16*, 2428-2442.
MacQueen, A.J., Phillips, C.M., Bhalla, N., Weiser, P., Villeneuve, A.M., and Dernburg, A.F. (2005). Chromosome sites play dual roles to establish homologous synapsis during meiosis in C. elegans. Cell *123*, 1037-1050.

MacQueen, A.J., and Villeneuve, A.M. (2001). Nuclear reorganization and homologous chromosome pairing during meiotic prophase require C. elegans chk-2. Genes Dev *15*, 1674-1687.
Maddox, P.S., Oegema, K., Desai, A., and Cheeseman, I.M. (2004). "Holo"er than thou: chromosome segregation and kinetochore function in C. elegans. Chromosome Res *12*, 641-653.
Malone, C.J., Misner, L., Le Bot, N., Tsai, M.C., Campbell, J.M., Ahringer, J., and White, J.G. (2003). The C. elegans hook protein, ZYG-12, mediates the essential attachment between the centrosome and nucleus. Cell *115*, 825-836.
Mancera, E., Bourgon, R., Brozzi, A., Huber, W., and Steinmetz, L.M. (2008). High-resolution mapping of meiotic crossovers and non-crossovers in yeast. Nature *454*, 479-485.
Manfrini, N., Guerini, I., Citterio, A., Lucchini, G., and Longhese, M.P. (2010). Processing of meiotic DNA double strand breaks requires cyclin-dependent kinase and multiple nucleases. J Biol Chem *285*, 11628-11637.
McKee, B.D., and Karpen, G.H. (1990). Drosophila ribosomal RNA genes function as an X-Y pairing site during male meiosis. Cell *61*, 61-72.
McKim, K.S., and Hayashi-Hagihara, A. (1998). mei-W68 in Drosophila melanogaster encodes a Spo11 homolog: evidence that the mechanism for initiating meiotic recombination is conserved. Genes Dev *12*, 2932-2942.
McKim, K.S., Peters, K., and Rose, A.M. (1993). Two types of sites required for meiotic chromosome pairing in Caenorhabditis elegans. Genetics *134*, 749-768.
Mets, D.G., and Meyer, B.J. (2009). Condensins regulate meiotic DNA break distribution, thus crossover frequency, by controlling chromosome structure. Cell *139*, 73-86.
Metzler-Guillemain, C., and de Massy, B. (2000). Identification and characterization of an SPO11 homolog in the mouse. Chromosoma *109*, 133-138.
Muller, H.J. (1916). The mechanism of crossing over. Am Nat *50*, 193-221; 284-305; 350-366; 421-434.
Murakami, H., and Keeney, S. (2008). Regulating the formation of DNA double-strand breaks in meiosis. Genes Dev *22*, 286-292.
Neale, M.J., and Keeney, S. (2006). Clarifying the mechanics of DNA strand exchange in meiotic recombination. Nature *442*, 153-158.
Niwa, O., Shimanuki, M., and Miki, F. (2000). Telomere-led bouquet formation facilitates homologous chromosome pairing and restricts ectopic interaction in fission yeast meiosis. EMBO J *19*, 3831-3840.
Osman, K., Sanchez-Moran, E., Mann, S.C., Jones, G.H., and Franklin, F.C. (2009). Replication protein A (AtRPA1a) is required for class I crossover formation but is dispensable for meiotic DNA break repair. EMBO J *28*, 394-404.
Petes, T.D. (2001). Meiotic recombination hot spots and cold spots. Nat Rev Genet *2*, 360-369.
Phillips, C.M., and Dernburg, A.F. (2006). A family of zinc-finger proteins is required for chromosome-specific pairing and synapsis during meiosis in C. elegans. Dev Cell *11*, 817-829.
Phillips, C.M., Wong, C., Bhalla, N., Carlton, P.M., Weiser, P., Meneely, P.M., and Dernburg, A.F. (2005). HIM-8 binds to the X chromosome pairing center and mediates chromosome-specific meiotic synapsis. Cell *123*, 1051-1063.
Rockman, M.V., and Kruglyak, L. (2009). Recombinational landscape and population genomics of Caenorhabditis elegans. PLoS Genet *5*, e1000419.
Romanienko, P.J., and Camerini-Otero, R.D. (1999). Cloning, characterization, and localization of mouse and human SPO11. Genomics *61*, 156-169.

Romanienko, P.J., and Camerini-Otero, R.D. (2000). The mouse Spo11 gene is required for meiotic chromosome synapsis. Mol Cell *6*, 975-987.
Saito, T.T., Youds, J.L., Boulton, S.J., and Colaiacovo, M.P. (2009). Caenorhabditis elegans HIM-18/SLX-4 interacts with SLX-1 and XPF-1 and maintains genomic integrity in the germline by processing recombination intermediates. PLoS Genet *5*, e1000735.
Sato, A., Isaac, B., Phillips, C.M., Rillo, R., Carlton, P.M., Wynne, D.J., Kasad, R.A., and Dernburg, A.F. (2009). Cytoskeletal forces span the nuclear envelope to coordinate meiotic chromosome pairing and synapsis. Cell *139*, 907-919.
Scherthan, H. (2001). A bouquet makes ends meet. Nat Rev Mol Cell Biol *2*, 621-627.
Sears, D.D., Hegemann, J.H., and Hieter, P. (1992). Meiotic recombination and segregation of human-derived artificial chromosomes in Saccharomyces cerevisiae. Proc Natl Acad Sci U S A *89*, 5296-5300.
Shinohara, A., Ogawa, H., and Ogawa, T. (1992). Rad51 protein involved in repair and recombination in S. cerevisiae is a RecA-like protein. Cell *69*, 457-470.
Smolikov, S., Eizinger, A., Schild-Prufert, K., Hurlburt, A., McDonald, K., Engebrecht, J., Villeneuve, A.M., and Colaiacovo, M.P. (2007). SYP-3 restricts synaptonemal complex assembly to bridge paired chromosome axes during meiosis in Caenorhabditis elegans. Genetics *176*, 2015-2025.
Smolikov, S., Schild-Prufert, K., and Colaiacovo, M.P. (2009). A yeast two-hybrid screen for SYP-3 interactors identifies SYP-4, a component required for synaptonemal complex assembly and chiasma formation in Caenorhabditis elegans meiosis. PLoS Genet *5*, e1000669.
Sora, S., Lucchini, G., and Magni, G.E. (1982). Meiotic Diploid Progeny and Meiotic Nondisjunction in SACCHAROMYCES CEREVISIAE. Genetics *101*, 17-33.
Sturtevant, A.H. (1915). The behavior of chromosomes as studied through linkage. Z Indukt Abstammungs Vererbungsl *13*, 234-287.
Sym, M., and Roeder, G.S. (1994). Crossover interference is abolished in the absence of a synaptonemal complex protein. Cell *79*, 283-292.
Thomas, S.E., Soltani-Bejnood, M., Roth, P., Dorn, R., Logsdon, J.M., Jr., and McKee, B.D. (2005). Identification of two proteins required for conjunction and regular segregation of achiasmate homologs in Drosophila male meiosis. Cell *123*, 555-568.
Trelles-Sticken, E., Dresser, M.E., and Scherthan, H. (2000). Meiotic telomere protein Ndj1p is required for meiosis-specific telomere distribution, bouquet formation and efficient homologue pairing. J Cell Biol *151*, 95-106.
Tsubouchi, T., and Roeder, G.S. (2005). A synaptonemal complex protein promotes homology-independent centromere coupling. Science *308*, 870-873.
Villeneuve, A.M. (1994). A cis-acting locus that promotes crossing over between X chromosomes in Caenorhabditis elegans. Genetics *136*, 887-902.
Wu, T.C., and Lichten, M. (1994). Meiosis-induced double-strand break sites determined by yeast chromatin structure. Science *263*, 515-518.
Youds, J.L., Mets, D.G., McIlwraith, M.J., Martin, J.S., Ward, J.D., NJ, O.N., Rose, A.M., West, S.C., Meyer, B.J., and Boulton, S.J. (2010). RTEL-1 enforces meiotic crossover interference and homeostasis. Science *327*, 1254-1258.
Zetka, M.C., and Rose, A.M. (1995). Mutant rec-1 eliminates the meiotic pattern of crossing over in Caenorhabditis elegans. Genetics *141*, 1339-1349.
Zickler, D., and Kleckner, N. (1998). The leptotene-zygotene transition of meiosis. Annu Rev Genet *32*, 619-697.

Chapter 1: Analysis of an attached X chromosome reveals links between homolog pairing and synapsis

Summary

Homolog pairing and synapsis initiation are tightly linked processes that are essential for accurate segregation in meiosis. A fundamental problem is how each chromosome is able to discriminate and accurately synapse only with its appropriate partner. In *C. elegans*, *cis*-acting chromosomal loci and a family of zinc-finger proteins, Pairing Center (PC) proteins that bind to these loci, are essential for establishing homolog pairing. Genetic lesions that disrupt PC proteins result in pairing defects and missegregation of chromosomes. These proteins clearly play a role in stabilizing homolog interactions, but their role in synapsis initiation remains unknown. In addition to chromosomal elements, cytoskeletal components have also been implicated in pairing and synapsis. Microtubules and motor proteins, via connections to PCs through specific nuclear envelope components, seem to provide a mechanical force to facilitate pairing and synapsis. Here, I examine the role of PC proteins in initiating synapsis and identify a molecular link between pairing and synapsis. Through analysis of a strain carrying an artificially paired set of X chromosomes, I bypass the need of the PC proteins' function in pairing and am able to examine their role in synapsis initiation. My results indicate that PC proteins are required for synapsis initiation between homologs. Additionally, in our modified system where pairing is artificially achieved, nuclear envelope components do not seem to be as critical for promoting synapsis. I also examine the role of PC proteins in initiation of nonhomologous synapsis and find that they are dispensable for such aberrant interactions. Inadvertently, I obtained preliminary data that indicates that simultaneously abrogating the function of multiple PCs causes nonhomologous synapsis.

Introduction

An interesting question is just how a chromosome is able to distinguish between homolog and nonhomolog and to form stable interactions via the synaptonemal complex (SC) only with its appropriate partner. We know of mutant situations where pairing and synapsis are uncoupled (Couteau et al., 2004; Martinez-Perez and Villeneuve, 2005; Smolikov et al., 2007); therefore, the two processes must be tightly regulated. One possibility is that molecules involved in pairing are also involved in initiating synapsis.

In *C. elegans*, *cis*-acting chromosomal loci and a family of zinc-finger proteins, Pairing Center (PC) proteins that bind to these loci, are essential for establishing homolog pairing (MacQueen et al., 2005; Phillips and Dernburg, 2006; Phillips et al., 2005). Genetic lesions that disrupt PC proteins result in pairing defects and missegregation of chromosomes. For example, HIM-8 binds to the X chromosome PC and regulates its pairing. A mutation in *him-8* or a deletion of the X PC region results in an absence of pairing of the X, as observed by FISH. Consequently, the X does not undergo synapsis, recombination, or proper segregation.

Recent work has uncovered a network of proteins that tethers PCs to microtubules via the nuclear envelope (Penkner et al., 2007; Penkner et al., 2009; Sato et al., 2009). The SUN domain protein, SUN-1, is an inner nuclear envelope protein that interacts with the KASH domain protein, ZYG-12, which is at the outer nuclear envelope. These two proteins are normally uniformly diffuse around the nuclear envelope, but upon entry into meiosis at the transition zone, SUN-1 and ZYG-12 form patches that colocalize with PCs. ZYG-12, itself, interacts with microtubules (Malone et al., 2003). Perturbations of any part of this network using colchicine to inhibit microtubules and genetic mutants to disrupt patch components dramatically affect pairing and synapsis (Sato et al., 2009). These findings have led to a model whereby microtubules promote homologous pairing and synapsis, while SUN-1 seems to provide a barrier to precocious nonhomologous synapsis.

PC proteins clearly play a role in stabilizing homolog interactions, but their role in synapsis initiation remains unknown. Based on translocation studies, we know that PCs are involved not only in pairing, but also seem to be the sites of synapsis initiation (MacQueen et al., 2005). The molecular link between pairing and synapsis could be PC proteins like HIM-8. Previously, we could not test this hypothesis because knocking out a PC protein resulted in a pairing defect, which prevented us from seeing its effect on synapsis. The attached X, allows us to bypass the role of HIM-8 in pairing and examine its role in synapsis. In this strain, the two Xs are translocated together with both PCs proximal to the fusion site. In this genetic background where the Xs are artificially paired, I find that HIM-8 is required for synapsis initiation, providing a molecular link for pairing and synapsis. Through analysis of a point mutation in *him-8*, I also find that the link between Pairing Centers and microtubules via nuclear envelope patch components does not seem to be as critical for promoting synapsis once pairing is already achieved. Finally, I inadvertently discovered that abrogating PC function of multiple chromosomes results in nonhomologous synapsis of the affected chromosomes.

Results

The *X^X* strain is a tool that allows for direct examination of synapsis

Because Pairing Center proteins are required for pairing, it is difficult to assess their role in synapsis. Fortuitously, a strain was recovered from a mutagenesis screen that carried a duplicated portion of the left end of the X chromosome—the region where the Pairing Center is located (Hodgkin and Albertson, 1995). This translocated chromosome presumably recombined with the "endogenous" X PC locus on another X chromosome, resulting in a strain carrying an attached X, referred to from hereon as *X^X* (Figure 1A).

I performed basic cytological assays to ensure that the X^X behaved similarly to two independent Xs in meiosis. The synaptonemal complex is comprised of axial elements that load onto chromosomes prior to pairing and central elements that "zipper up" paired homologs (Colaiacovo, 2006). By early prophase, the axial element, HTP-3, and the central element, SYP-1, load normally onto the X^X, which is marked by the X PC protein, HIM-8 (Figure 1B, i). Each nucleus has a stretch of SYP-1 with a single cluster of right-end FISH probe foci at one end, (Figure 1B, ii). This is evidence that the X^X undergoes wild type synapsis, as opposed to fold over (one homolog folding over on itself) or sister synapsis (between sister chromatids), which have been observed in various mutants (Couteau et al., 2004; Martinez-Perez and Villeneuve, 2005; Smolikov et al., 2007).

HIM-8 plays a role in synapsis initiation

Taking advantage of the X^X chromosome, I bypassed the need of HIM-8's function in pairing and was able to examine its role in synapsis initiation of the X. Since nuclei progress spatially through the length of the gonad over time, a time-course analysis of synapsis on fixed samples could be performed (Figure 2B). The gonad was divided up into five regions and progression of synapsis was examined from the distal tip where nuclei are dividing mitotically (zone 1), into the transition zone where nuclei first enter meiosis and begin to synapse (zone 2), and through the end of pachytene (zone 5), by which point chromosomes have fully synapsed (Figure 2C). The genetic lesion in *him-8(tm611)* mutants results in an early stop codon. A truncated version of the protein is made, which does not concentrate at the X PC, but is instead nuclear diffuse. This mutant fails to achieve wild type levels of synapsis (Phillips et al., 2005). In the *X^X;tm611* background, a maximum of 20% of nuclei achieve full synapsis (Figures 2A and 2B). This is higher than the *tm611* mutation on its own, which achieves 5% synapsis, but is nowhere near the 100% synapsis levels achieved in wild type animals in the presence of wild type HIM-8. Thus, when pairing is artificially induced by the attachment, fully functional HIM-8 is still required for wild type levels of synapsis.

Nuclear envelope components are not as critical for promoting synapsis of chromosomes that are already paired

Interestingly, another allele of *him-8* yielded different results in the *X^X* background. The *him-8(me4)* allele results in a missense mutation in the N-terminus of the gene, a region distinct from the zinc-finger motifs that potentially regulates protein-protein interactions. In this mutant, HIM-8 protein is made, and it localizes to the X Pairing Centers, but pairing is defective. Consequently, it behaves similarly to the *tm611* allele, and only 5% levels of synapsis are achieved. In my experiments, I observed that the X^X seemed to suppress the *him-8(me4)* synapsis defect, yielding on average 70% synapsis (Figure 2B). Complete synapsis of the X^X in the *me4* background was delayed compared to wild type, but by zone 5 (late pachytene), some gonads showed as high as 100% synapsed nuclei (raw data not shown).

It has already been shown that in *him-8(me4)*, the mutant HIM-8 protein, while localized to PCs, does not colocalize with nuclear envelope patches, which are critical in facilitating normal pairing and synapsis (Sato et al., 2009). I found that in the *X^X;him-8(me4)* strain, mutant HIM-8 protein again fails to colocalize with nuclear envelope patches (Figures 3A and 3B); though, it does colocalize with lamin (LMN-1), indicating that the X PCs are at least in contact with the nuclear envelope (Figure 3C). The *X^X;him-8(me4)* result is striking because it is the first time we have seen such high levels of synapsis (though, not quite at wild type levels) without association with a nuclear envelope patch.

I then examined the behavior of the X^X in a situation where nuclear envelope patch formation is defective. In the *zyg-12(ct350)* temperature-sensitive strain, smaller nuclear envelope patches are made, and pairing and synapsis are severely delayed and/or defective (Sato et al., 2009). Based on the ability of the X^X to synapse in the *him-8(me4)* background without association with a patch, I wondered whether it would be able to synapses in a patch-defective mutant like *zyg-12(ct350)*. At the non-permissive temperature, the X^X (marked by HIM-8) did not synapse in the *zyg-12(ct350)* background (Figure 4A). SYP-1 remained in a polycomplex in all pachytene nuclei, which typically occurs in synapsis-defective mutants (Colaiacovo, 2006).

The attached X rescues the nonhomologous phenotype seen in *sun-1* mutants

SUN-1 is a component of the nuclear envelope patches that form in the transition zone where pairing and synapsis are normally initiated (Penkner et al., 2007; Sato et al., 2009). SUN-1 has been shown to provide a barrier to nonhomologous interactions, as the *sun-1* mutant undergoes extensive, precocious nonhomologous synapsis. The *sun-1* mutation causes sterility, and thus, it is maintained as a heterozygote over the *nT1* balancer. The *X^X; sun-1/nT1* strain shows wild type synapsis of the X, as HIM-8 foci are paired and attached to a stretch of SYP-1, and X right-end FISH signals are also paired (Figure 4B, i and iv). The *sun-1* mutant exhibits the previously reported phenotype of nonhomologous synapsis of the X, as there are many nuclei with unpaired HIM-8 foci and X right-end FISH signals attached to independent SYP-1 stretches (Figure 4B, ii and v). Similarly to *sun-1*, the Xs appear to be completely synapsed in *X^X;sun-1*, as seen by complete colocalization of HTP-3 and SYP-1 in all nuclei (Figure 4B, iii). Interestingly, in the *X^X;sun-1* background, this synapsis is now wild type, as it is between homologs (Figure 4B, vi). I quantified X chromosome pairing using a FISH probe to the right end of X to prove that the synapsis is homologous (Figure 4C). The pairing levels of the right ends of the X in *X^X;sun-1* are comparable to those in the control, *X^X;sun-1/nT1*. The level of pairing is roughly 80% of nuclei, which is low only because of our stringent cut-off for pairing (FISH signals in one nucleus being 0.7 μm apart).

Nonhomologous synapsis does not require Pairing Center proteins

After concluding that PC proteins (at least HIM-8) are required for synapsis initiation between homologs, I set out to examine the role of PC proteins in initiating nonhomologous synapsis. In various axial element mutants, pairing and synapsis are uncoupled, as SYP-1 is loaded precociously between nonhomologs (Couteau et al., 2004; Martinez-Perez and Villeneuve, 2005). Specifically, in *htp-1* mutants, all autosomes engage in nonhomologous interactions, while the Xs are surprisingly unaffected and pair and synapse properly (Figure 5A, ii and v). I first monitored synapsis (coincident loading of HTP-3 and SYP-1) of the X (marked by a FISH probe to the right end) in *htp-1;him-8* mutants (Figure 5A, iii). In the absence of HIM-8, Xs underwent nonhomologous interactions, as unpaired right-end probes are bound to

two independent stretches of SYP-1. I next examined initiation of nonhomologous synapsis of an autosome (Figure 5A, vi). In *htp-1;zim-2* mutants, the chromosome V Pairing Center function is abrogated; yet, chromosome *V* still undergoes nonhomologous synapsis.

Both of the above results indicate that PC proteins are not required for initiation of nonhomologous synapsis in a mutant situation. In fact, in the case of the X, the presence of its PC protein seems to even protect it from undergoing aberrant, nonhomologous interactions, since Xs pair and synapse appropriately in *htp-1* single mutants. One caveat to these experiments is that in the *htp-1;him-8* mutant, while the X PC would not be able to initiate synapsis, the PC of the interacting nonhomologous partner could be what is initiating synapsis. This could also hold true in the *htp-1;zim-2* mutant.

To determine whether nonhomologous synapsis can in fact occur between two chromosomes that *both* lacked PC function, I examined a situation where multiple PCs were simultaneously knocked out in the *htp-1* background. *him-8* and the *zim*s are all found within an operon and are thus, tightly linked, making it difficult to create double and triple mutants. I attempted to knockout PC function for three chromosomes by combining a *zim-1* mutant, which knocks out PC function of II and III, with *meDf2*, which is a deficiency of the X chromosome PC region (Villeneuve, 1994). This triple PC knockout in the *htp-1* mutant background behaves similarly to *htp-1* single mutants, but is more severe in that the X also undergoes nonhomologous interactions (data not shown). The surprising finding was that the *zim-1;meDf2* strain on its own also had substantial nonhomologous interactions (Figure 5B). Nonhomologous synapsis was monitored by simultaneously looking at SYP-1 and pairing of FISH probes to the right end of the X and the left end of chromosome II. In *zim-1;meDf2*, nuclei with unpaired XR and IIL FISH signals attached to stretches of SYP-1 are evidence of nonhomologous synapsis. More recent technologies have allowed for generating the *him-8/zim* quadruple knockout, and the results are consistent; when function of all four PCs is abrogated, aberrant intra-chromosomal synapsis ensues, as homologs fold over on themselves (R. Rillo and A.F. Dernburg unpublished data).

Discussion

HIM-8 may function as a molecular link for coordinating pairing and synapsis between homologs

It has previously been shown that HIM-8 is required for stabilizing X chromosome pairing (Phillips et al., 2005). In this current study, I found that the PC protein HIM-8 is required for synapsis initiation. We already have evidence that synapsis initiates at PCs (MacQueen et al., 2005). An attractive hypothesis is that once pairing is achieved, a signal is sent to HIM-8, which then recruits SC components to initiate synapsis. *C. elegans* is among a class of organisms that is able to pair and synapse its homologs even in the absence of recombination; thus, homology assessment and stabilized pairing does not require strand invasion.

In organisms like *Saccharomyces Cerivisiae,* synapsis is dependent on recombination. In the absence of Zip1 (the central element component of the SC in budding yeast), synapsis and recombination are abrogated (Lynn et al., 2007). Zip1 is a member of a family of proteins called ZMM proteins, which also includes proteins involved in processing recombination intermediates and in mismatch repair. ZMM proteins are defined by the fact that they are all required for crossover recombination. ZMM proteins also colocalize along chromosome axis and are members of what is called the synapsis initiation complex (SIC). SICs form along the

chromosome axis and are thought to be the sites of synapsis initiation, since Zip1 is found there prior to its polymerization along axis (Fung et al., 2004). Thus, coordination between recombination, which can assess homology/pairing, and synapsis occurs at the molecular level at SICs in budding yeast. Similarly, in *C. elegans*, the Pairing Center, could coordinate pairing and synapsis by receiving a signal from PC proteins to initiate synapsis and to ultimately commit a homolog pair to the synapsed state.

HIM-8 thus, seems to be a molecular link that can help explain how pairing and synapsis are mechanistically coupled. How HIM-8 functions as that link remains to be uncovered. An enticing possibility is that HIM-8 is able to directly recruit central element proteins of the synaptonemal complex after pairing is stabilized. In Chapter 2, attempts are made to address this model. Unfortunately, experimental difficulties prevented me from fully testing this hypothesis.

Uncoupling synapsis from nuclear envelope patches

In the *him-8(me4)* mutant, the X^X synapsed about 70% of the time. In some gonads synapsis levels reached 100% by the end of pachytene. To date, this is the first scenario where a set of chromosomes achieved such a high frequency of synapsis despite the fact that it was not connected to the microtubule network via SUN-1/ZYG-12 nuclear envelope patches. This is an interesting anomaly, as this connection of meiotic chromosomes to the nuclear envelope is highly conserved across species from fission yeast to mice (Ding et al., 2007; Niwa et al., 2000). The *me4* data indicates that once pairing is already achieved, the nuclear envelope patches may not be as critical for initiating synapsis.

Since the X^X could synapse efficiently in the *me4* background without association with an NE patch, there was reason to believe that it may also synapse in a situation where patch formation is defective (e.g., *zyg-12(ct350)* at the nonpermissive temperature). There are a variety of possibilities for why the X^X synapsed in the *me4* background but not in the *zyg-12(ct350)* background. One explanation is that in *him-8(me4)*, all the autosomes are still linked to nuclear envelope patches through their functional PCs and are thus, presumably moving. These dynamic chromosomes will likely bump into the X^X, and this residual movement of the X^X may be just enough to allow it to achieve synapsis. In contrast, in the *zyg-12(ct350)* background, all the chromosomes are probably static, since none of them are attached to a patch, and thus, none are linked to microtubules. In this latter situation, the autosomes will not provide any residual movement to the X^X, and thus, it is not able to synapse. An alternative explanation is that it is just simply not possible for only one pair of chromosomes to synapse in the *ct350* background. In synapsis-defective mutants like *zyg-12(ct350)*, SYP-1 polycomplexes form. Formation of polycomplexes is not well understood, and it is not clear whether or not polycomplexes are so highly stable that their formation could oppose the loading of SYP-1 onto a single set of paired chromosomes.

Examining the behavior of the X^X in a *sun-1* mutant presented another scenario where PCs were unattached from the NE network. In the *sun-1* single mutant, synapsis occurs precociously between nonhomologous chromosomes. In the *X^X;sun-1* mutant, the artificially paired Xs are able to overcome the absence of wild type SUN-1 and are able to homologously synapse. Sato et al. (2009) showed that in *sun-1(jf-18);syp-2(RNAi)* mutants where synapsis is defective due to loss of a central element protein, the Xs are partially proficient for pairing. They conclude that in the absence of SUN-1, it is the precocious nonhomologous synapsis phenotype that results in low levels of pairing; thus, SUN-1, itself, is not directly playing a role in pairing *per se*. In the *X^X;sun-1* mutant, the Xs are permanently committed to the paired

state, making them more competent at avoiding nonhomologous synapsis compared to the *sun-1* single mutant.

Nonhomologous synapsis does not require Pairing Center function

Mutations in axial elements in budding yeast and *C. elegans* lead to nonhomologous synapsis (Leu et al., 1998; Martinez-Perez and Villeneuve, 2005). When combining a mutation in the axial element component HTP-1 with mutations in a number of other Pairing Center proteins, nonhomologous synapsis ensued. Thus, while PC proteins, namely HIM-8, seem to be required for homologous synapsis, they are dispensable for synapsis that occurs inappropriately between nonhomologous partners.

Single Pairing Center mutants result in asynapsis of the affected chromosomes (MacQueen et al., 2005; Phillips and Dernburg, 2006; Phillips et al., 2005). Inadvertently, while investigating the role of PCs in nonhomologous synapsis initiation, I gathered preliminary data suggesting that the absence of multiple PCs results in nonhomologous interactions. More recent examination of a *him-8/zim-1-3*Δ mutant corroborates these results and suggests that the unpaired chromosomes are folding over on themselves and synapsing (R. Rillo and A.F. Dernburg unpublished data). How the cell senses that multiple Pairing Centers are inactivated and why it then chooses to execute nonhomologous synapsis instead of remaining in an unsynapsed state remains an unknown.

Methods and Materials

Genetics and strains

All strains were maintained under standard conditions at 20°C, unless otherwise noted (Brenner 1974). Unless otherwise indicated, Bristol N2 worms were used as the wild type strain. The *X^X* strain was recovered after EMS mutagenesis created a duplication of the left end of the X chromosome that translocated to the left end of an intact X. This translocation presumably recombined with an intact X, resulting in the *X^X* strain (Hodgkin and Albertson 1995). HIM-8 binds to the regions proximal to the attachment site. Animals carrying the X^X have roughly 50% embryonic lethality, as embryos will only survive if one gamete carries the X^X and the other gamete is nullo X (data not shown). At a low frequency, the X^X breaks down, presumably due to recombination events, yielding *X0* male progeny. Animals used in this study were confirmed to have the X^X by two ways: 1) having paired HIM-8 foci (marking the X PC) in the premeiotic region where Xs are not usually paired, and/or 2) having male siblings, which is evidence that at least the parent was carrying the X^X. *X^X* strains were generated by first crossing *X^X* animals to animals carrying the *mIs11* insertion, which marks *him-8* in trans and has a pharyngeal GFP marker. *X^X* F2s that were homozygous for *mIs11* were crossed to *him-8(me4)* or *him-8(tm611)* worms. Animals used in this study were always progeny of *him-8* heterozygotes, so as to ensure that the presence of males was always due to the X^X breaking down and not the *him-8* mutation, which also throws male progeny.

The *sun-1(jf18)* strain was generated by Verena Jantsch and was maintained as a balanced heterozygote with the *nT1* balancer (Penkner et al., 2007). Chris Malone generated *zyg-12(ct350)*, which is viable at the permissive temperature of 15°C and inviable at the nonpermissive temperature of 25°C (Malone et al., 2003). *X^X;zyg-12(ct350)* animals were generated by crossing *X^X* hermaphrodites to *zyg-12(ct350)/mIs12(II)* males. F1 *X^X;zyg-*

12(ct350/+) animals were selfed. F2 *X^X;zyg-12(ct350)* animals were identified by whether they threw F3s that do not survive at 25°C. *htp-1* mutants were maintained as heterozygotes with the *nT1* balancer. When relevant, homozygous mutant progeny that were analyzed came from heterozygous balanced parents. The *meDf2;mnDp66* strain was generated by Anne Villeneuve and contains a deficiency of the left end of the X chromosome (Villeneuve, 1994). *mnDp66* is a duplication of the left end of the X that is fused to chromosome I and is necessary for viability in the *meDf2* background (Herman and Kari, 1989).

Immunofluorescence, FISH, and microscopy

For immunofluorescence, worms were picked at the L4 stage, and 20-24 hours later, they were dissected on glass cover slips in Egg Buffer (25 mM HEPES-NaOH, pH 7.4, 0.118 M NaCl, 48 mM KCl, 2 mM EDTA, 0.5 mM EGTA) with 1% Tween-20 and 20 mM sodium azide. Samples were fixed for 2 minutes in 1% formaldehyde, transferred to HistoBond slides, and subsequently frozen. A second fixation step was performed in -20°C MeOH for 1 min. All wash steps were performed in PBST. Samples were blocked for a half hour in Blocking Reagent (Roche, Cat. No. 11 096 176 001). Primary and secondary antibody incubations were at least 2 hours to overnight. Rabbit anti-SYP-1 provided by Anne Villeneuve, guinea pig anti-HTP-3, rat anti-HIM-8, guinea pig anti-HIM-8, rat anti-Lamin, and anti-SUN-1 were all diluted in PBST. DNA was stained by incorporating 0.5 µg/ml DAPI in the second to last wash step. For *zyg-12* experiments, 18 hours post-L4 stage, animals were either temperature shifted to 25°C or were kept at 15°C for 6 hours. Hermaphrodites were immediately dissected after the 6-hour period.

When performing FISH, samples were first taken through the immunofluorescence protocol. After secondary antibody incubation and subsequent PBST washes, samples were fixed again in 3.7% formaldehyde. Samples were left overnight in 50% formamide/TBST at 37°C. Fifteen to 50 ng of the appropriate FISH probe were applied to samples, which were placed in a Ted Pella BioWave microwave oven attached to a ColdSpot circulating waterbath. Samples were denatured for 3 minutes at 95°C and placed in the microwave for a total of 1 hour for the hybridization step. Samples were washed again in 50% formamide/TBST. Finally, washes were done in TBST, with 10 µg/ml DAPI (4′-6-diamidino-2-phenylindole) included in the second to last wash step. The right-end X probe was previously described (Phillips et al. 2005). Slides were mounted in glycerol-NPG mounting media.

Imaging was performed using the Deltavision deconvolution microscopy system (Applied Precision, Issaquah, WA). Datasets were taken through gonads with 0.2 µm spacing between sections. Datasets were deconvolved and projected in 3D using *Softworx* (Applied Precision).

Scoring of pairing and synapsis

For the synapsis assay, hermaphrodite gonads were divided into five regions of equal length, starting in the premeiotic region and extending until the end of pachytene. Synapsis was assessed in three gonads of each genotype. Nuclei were considered to have fully synapsed chromosomes if there was complete colocalization of HTP-3 and SYP-1.

In *sun-1* strains, late pachytene nuclei from three gonads of each genotype were assessed for pairing of the X chromosome. A nucleus was considered to have paired Xs when FISH signals were ≤0.7 µm apart (distance measured using *Softworx*).

References

Colaiacovo, M.P. (2006). The many facets of SC function during C. elegans meiosis. Chromosoma *115*, 195-211.

Couteau, F., Nabeshima, K., Villeneuve, A., and Zetka, M. (2004). A component of C. elegans meiotic chromosome axes at the interface of homolog alignment, synapsis, nuclear reorganization, and recombination. Curr Biol *14*, 585-592.

Ding, X., Xu, R., Yu, J., Xu, T., Zhuang, Y., and Han, M. (2007). SUN1 is required for telomere attachment to nuclear envelope and gametogenesis in mice. Dev Cell *12*, 863-872.

Fung, J.C., Rockmill, B., Odell, M., and Roeder, G.S. (2004). Imposition of crossover interference through the nonrandom distribution of synapsis initiation complexes. Cell *116*, 795-802.

Herman, R.K., and Kari, C.K. (1989). Recombination between small X chromosome duplications and the X chromosome in Caenorhabditis elegans. Genetics *121*, 723-737.

Hodgkin, J., and Albertson, D.G. (1995). Isolation of dominant XO-feminizing mutations in Caenorhabditis elegans: new regulatory tra alleles and an X chromosome duplication with implications for primary sex determination. Genetics *141*, 527-542.

Leu, J.Y., Chua, P.R., and Roeder, G.S. (1998). The meiosis-specific Hop2 protein of S. cerevisiae ensures synapsis between homologous chromosomes. Cell *94*, 375-386.

Lynn, A., Soucek, R., and Borner, G.V. (2007). ZMM proteins during meiosis: crossover artists at work. Chromosome Res *15*, 591-605.

MacQueen, A.J., Phillips, C.M., Bhalla, N., Weiser, P., Villeneuve, A.M., and Dernburg, A.F. (2005). Chromosome sites play dual roles to establish homologous synapsis during meiosis in C. elegans. Cell *123*, 1037-1050.

Malone, C.J., Misner, L., Le Bot, N., Tsai, M.C., Campbell, J.M., Ahringer, J., and White, J.G. (2003). The C. elegans hook protein, ZYG-12, mediates the essential attachment between the centrosome and nucleus. Cell *115*, 825-836.

Martinez-Perez, E., and Villeneuve, A.M. (2005). HTP-1-dependent constraints coordinate homolog pairing and synapsis and promote chiasma formation during C. elegans meiosis. Genes Dev *19*, 2727-2743.

Niwa, O., Shimanuki, M., and Miki, F. (2000). Telomere-led bouquet formation facilitates homologous chromosome pairing and restricts ectopic interaction in fission yeast meiosis. EMBO J *19*, 3831-3840.

Penkner, A., Tang, L., Novatchkova, M., Ladurner, M., Fridkin, A., Gruenbaum, Y., Schweizer, D., Loidl, J., and Jantsch, V. (2007). The nuclear envelope protein Matefin/SUN-1 is required for homologous pairing in C. elegans meiosis. Dev Cell *12*, 873-885.

Penkner, A.M., Fridkin, A., Gloggnitzer, J., Baudrimont, A., Machacek, T., Woglar, A., Csaszar, E., Pasierbek, P., Ammerer, G., Gruenbaum, Y*., et al.* (2009). Meiotic chromosome homology search involves modifications of the nuclear envelope protein Matefin/SUN-1. Cell *139*, 920-933.

Phillips, C.M., and Dernburg, A.F. (2006). A family of zinc-finger proteins is required for chromosome-specific pairing and synapsis during meiosis in C. elegans. Dev Cell *11*, 817-829.

Phillips, C.M., Wong, C., Bhalla, N., Carlton, P.M., Weiser, P., Meneely, P.M., and Dernburg, A.F. (2005). HIM-8 binds to the X chromosome pairing center and mediates chromosome-specific meiotic synapsis. Cell *123*, 1051-1063.

Sato, A., Isaac, B., Phillips, C.M., Rillo, R., Carlton, P.M., Wynne, D.J., Kasad, R.A., and Dernburg, A.F. (2009). Cytoskeletal forces span the nuclear envelope to coordinate meiotic chromosome pairing and synapsis. Cell *139*, 907-919.
Smolikov, S., Eizinger, A., Schild-Prufert, K., Hurlburt, A., McDonald, K., Engebrecht, J., Villeneuve, A.M., and Colaiacovo, M.P. (2007). SYP-3 restricts synaptonemal complex assembly to bridge paired chromosome axes during meiosis in Caenorhabditis elegans. Genetics *176*, 2015-2025.
Villeneuve, A.M. (1994). A cis-acting locus that promotes crossing over between X chromosomes in Caenorhabditis elegans. Genetics *136*, 887-902.

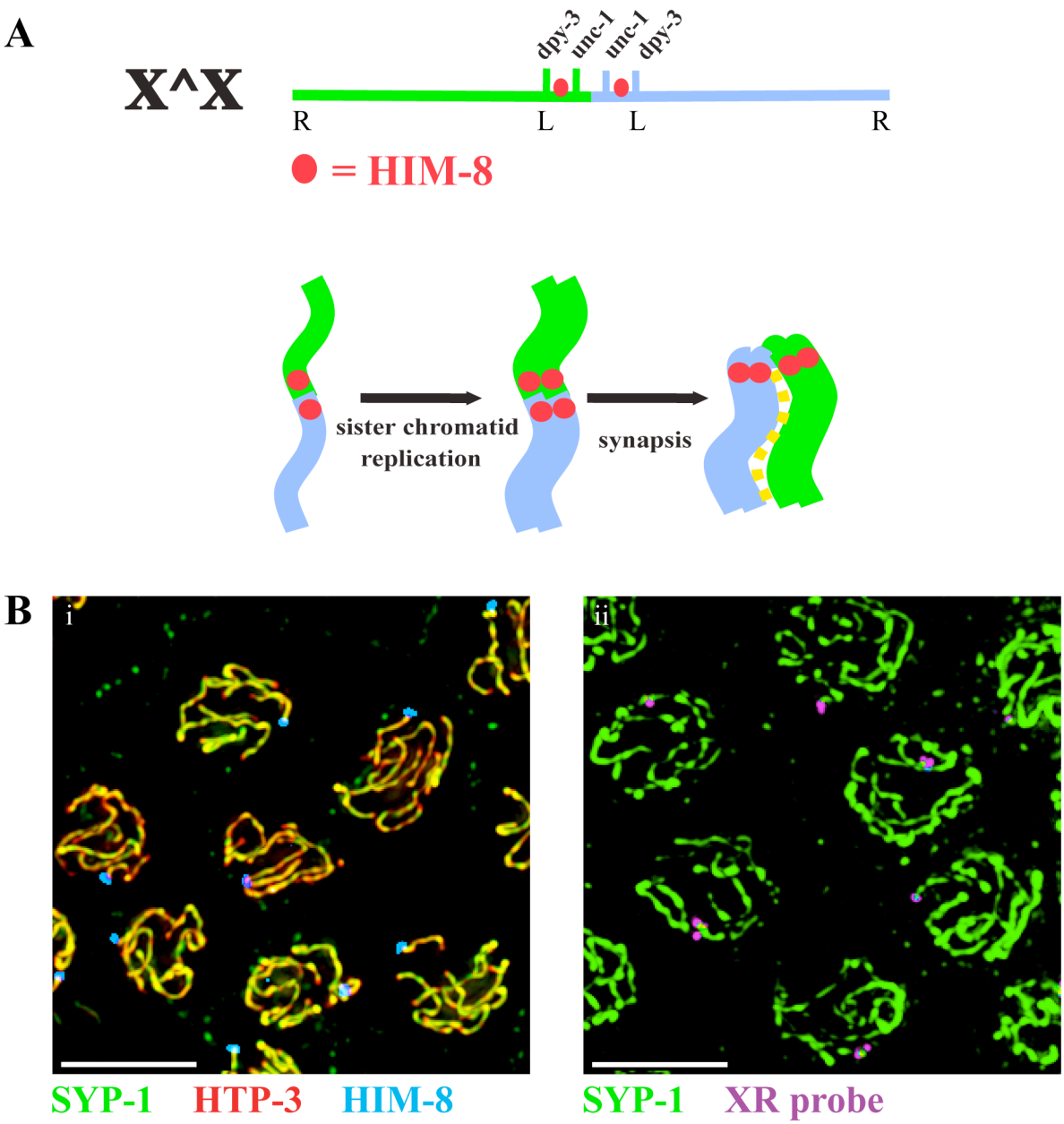

Figure 1: The *X^X* strain is a tool for studying synapsis independently of pairing.
(A) Structure of the X^X. The X^X is comprised of two X chromosomes fused at their PC ends. HIM-8 binds to the regions proximal to the attachment site and thus, appears paired in premeiotic and meiotic cells. If synapsis proceeds appropriately, the X^X will fold over on itself. (B) (i) Pachytene nuclei from an *X^X;mIs11* animal showing HIM-8 (blue) and the synaptonemal complex proteins HTP-3 (red) and SYP-1 (green). The X^X loads SYP-1 appropriately and synapses. (ii) Pachytene nuclei from an *X^X;mIs11* animal showing SYP-1 (green) and a FISH probe to the right end of X (purple). Although a continuous piece of DNA (as opposed to two independent homologs), the X^X folds over at the site of attachment and synapses. Scale bars are 5 µm.

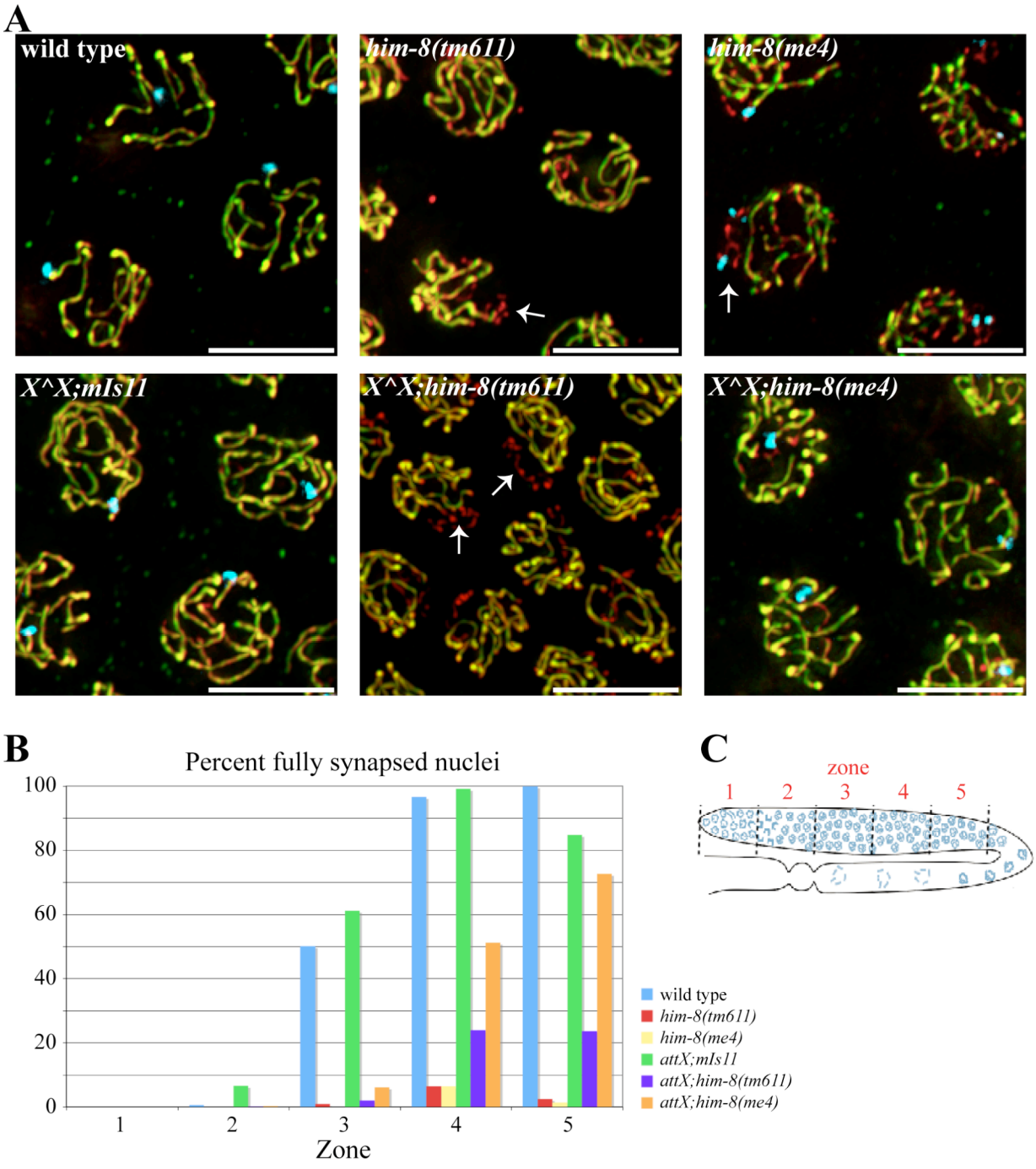

Figure 2: HIM-8 is required for synapsis initiation, but the X^X partially rescues the synapsis defect in the *him-8(me4)* point mutant.

(A) Pachytene nuclei from wild type and mutants showing HTP-3 in red, SYP-1 in green, and HIM-8, marking the X chromosome, in blue. Unsynapsed chromosomes (marked by arrows) load only HTP-3 and appear red in mutants. The *tm611* mutation disrupts binding of mutant HIM-8 protein to the X PC; thus, no HIM-8 focus is detected along the X chromosome in this background. Scale bars are 5 µm. (B) Quantification of synapsis time course in wild type and mutants. The number of nuclei with synapsed chromosomes was averaged in each region of the gonad. Nuclei were considered fully synapsed if there was complete colocalization of HTP-3 and SYP-1. (C) Cartoon of the *C. elegans* gonad. For quantification of synapsis in (B), the gonads of hermaphrodites were divided into 5 regions of equal length, starting in the premeiotic region and extending until the end of pachytene.

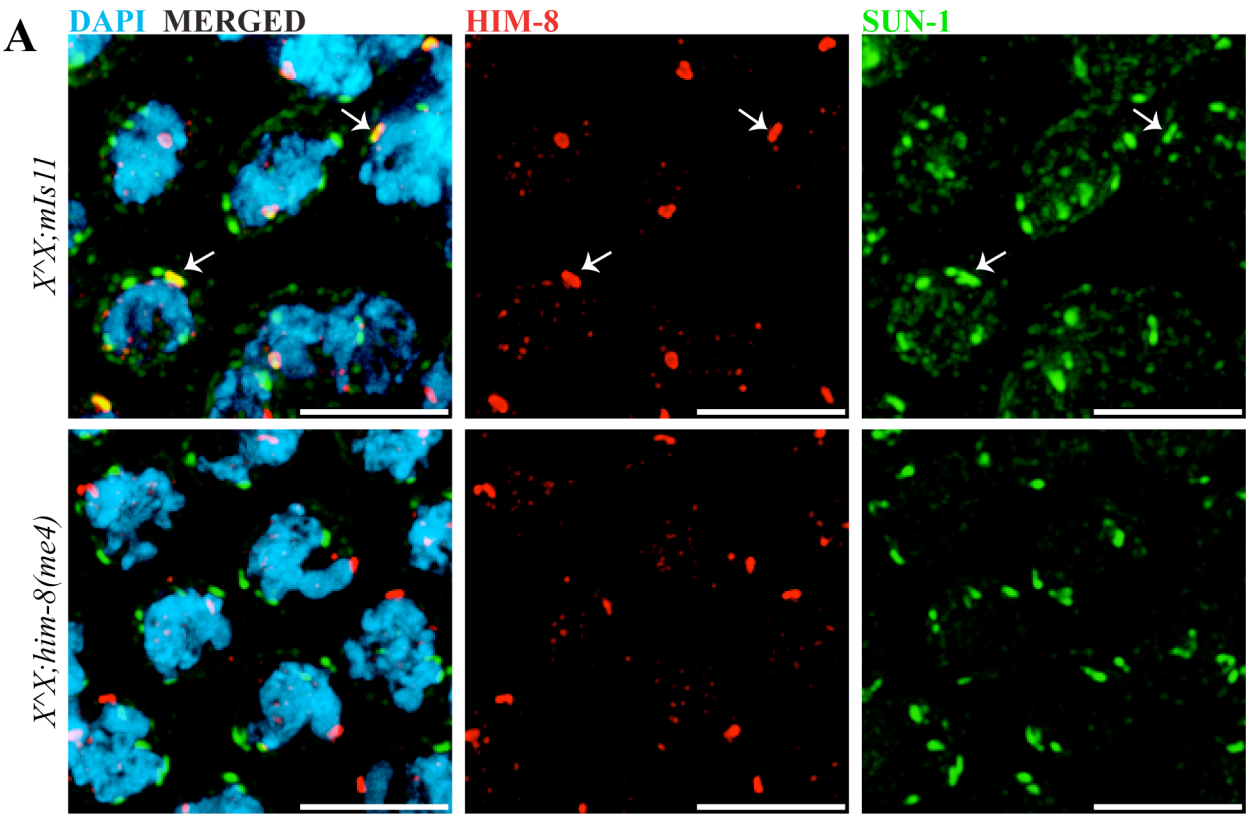

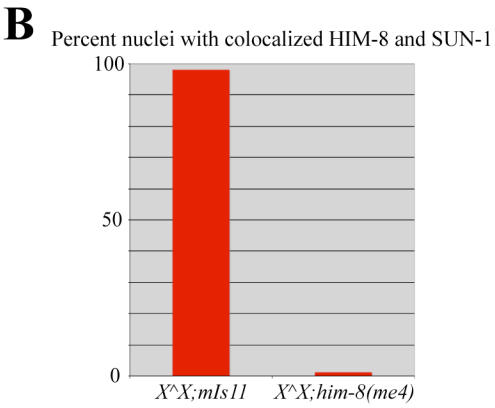

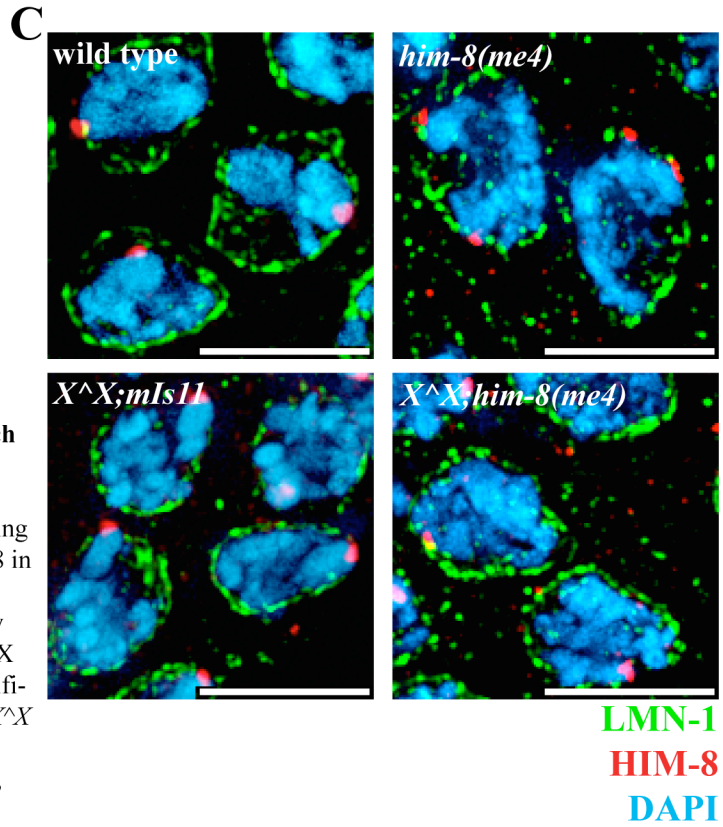

Figure 3: Nucleation of a nuclear envelope patch is not required for the X^X to synapse in the *him-8(me4)* mutant.
(A) Transition zone nuclei from *X^X* strains showing DAPI (DNA) in blue, SUN-1 in green, and HIM-8 in red. In a wild type background, X^X PCs are always associated with a SUN-1 patch (marked by arrows), while in the *him-8(me4)* background, X^X PCs are never associated with a patch. (B) Quantification of colocalization of HIM-8 and SUN-1 in *X^X* strains. (C) Transition zone nuclei from wild type and mutant strains, showing DAPI (DNA) in blue, LMN-1 in green, and HIM-8 in red. In wild type and all mutant conditions, HIM-8 is found at the nuclear envelope. All scale bars are 5 µm.

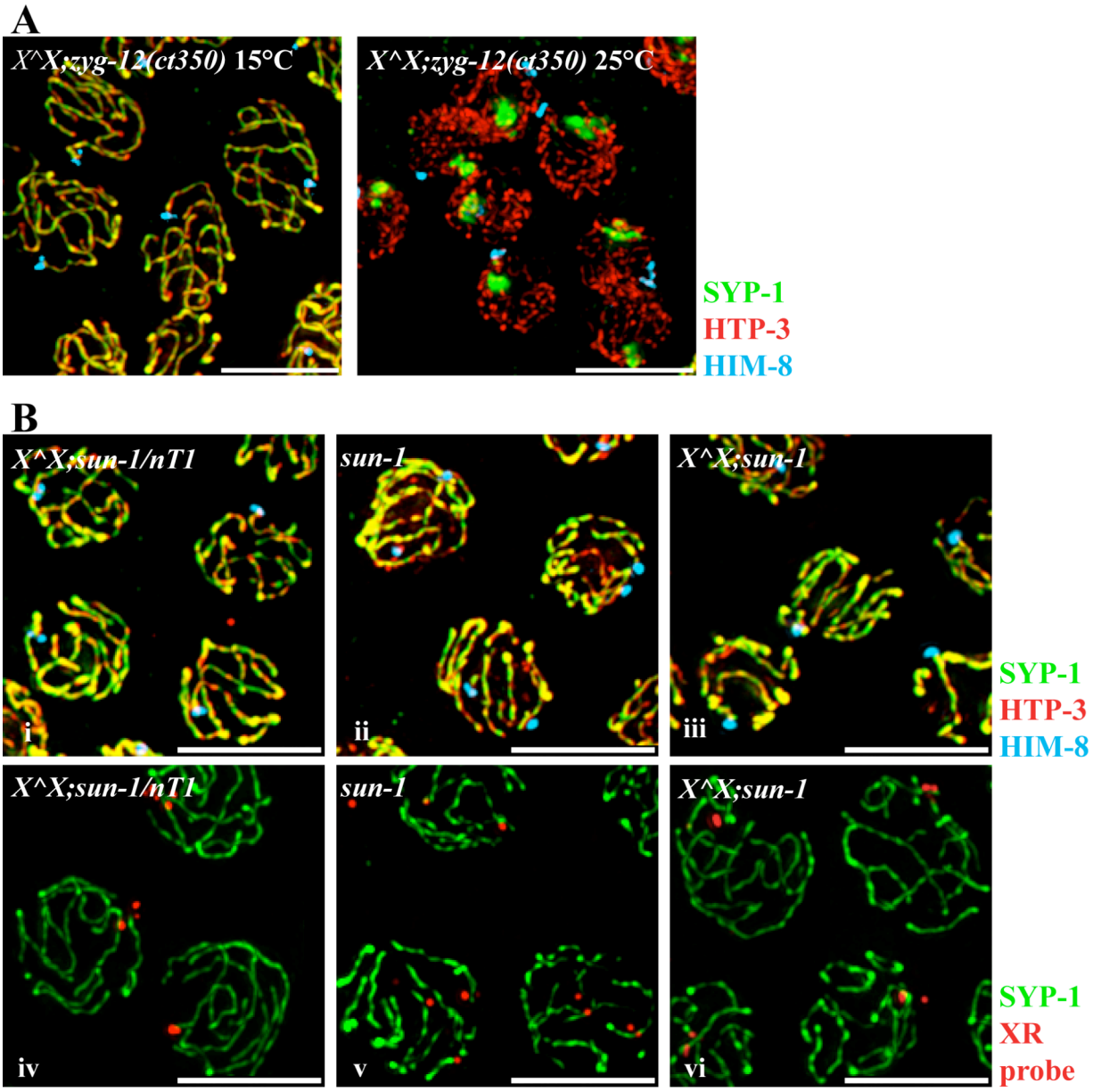

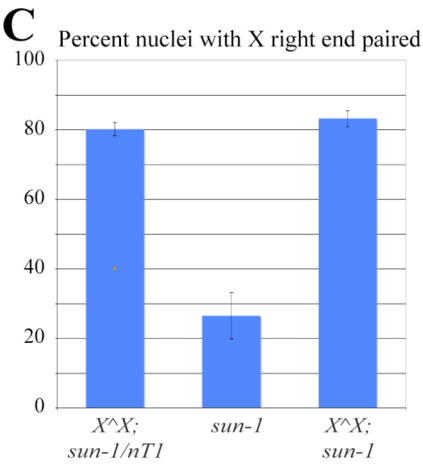

Figure 4: Mutations in nuclear envelope components differentially affect synapsis of the X^X.
(A) Nuclei from the mid-pachytene region of *X^X;zyg-12(ct350)* animals at permissive (15°C) and non-permissive (25°C) temperatures, showing HTP-3 in red, SYP-1 in green, and HIM-8 in blue. In the *zyg-12(ct350)* mutant at the non-permissive temperature, the X^X (and autosomes) does not synapse. Scale bars are 5 µm. (B) (i-iii) Pachytene nuclei from *X^X* animals and *sun-1(jf18)* mutants showing HTP-3 in red, SYP-1 in green, and HIM-8 in blue. The X^X synapses in the absence of *sun-1*. (iv-vi) Pachytene nuclei from *X^X* animals and *sun-1(jf18)* mutants showing SYP-1 in green and a FISH probe to the right end of the X chromosome in red. The X^X rescues the *sun-1(jf18)* nonhomologous synapsis phenotype. Scale bars are 5 µm. (C) Quantification of X chromosome right-end pairing in *X^X* and *sun-1(jf18)* mutants.

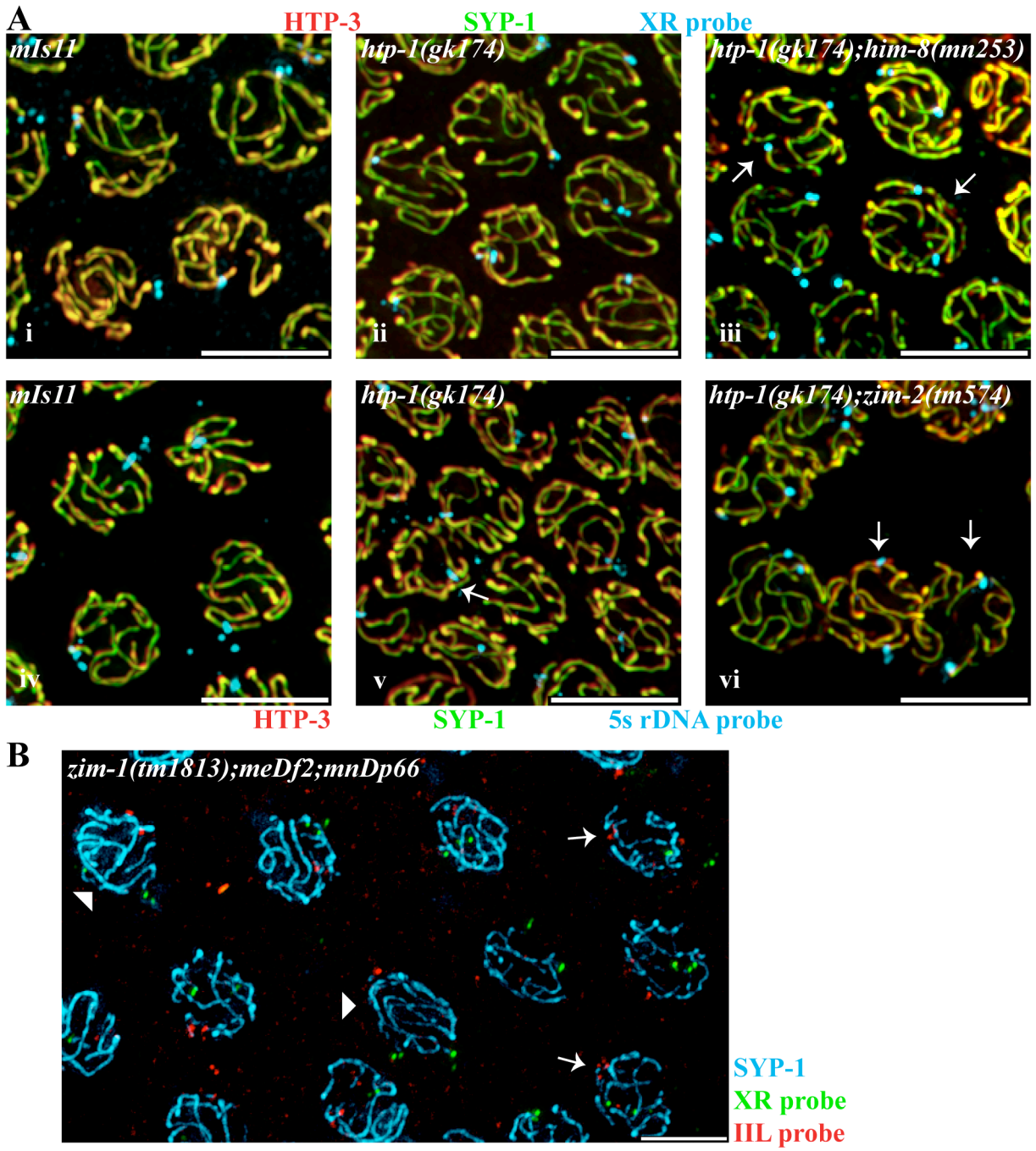

Figure 5: Pairing Center proteins are not required for initiating nonhomologous synapsis.
(A) (i-iii) Pachytene nuclei from a wild type (*mIs11*) animal and mutants showing HTP-3 in red, SYP-1 in green, and a FISH probe to the right end of X in blue. Arrows indicate instances of nonhomologous synapsis, where two X chromosome probe signals are unpaired and attached to two different stretches of the SC. (iv-vi) Pachytene nuclei from a wild type animal and mutants showing HTP-3 in red, SYP-1 in green, and a FISH probe to the 5srDNA locus on chromosome V in blue. Arrows indicate instances of nonhomologous synapsis, where two chromosome V probe signals are unpaired and attached to two different stretches of the SC. All scale bars are 5 µm. (B) Pachytene nuclei from a *zim-1(tm1813);meDf2;mnDp66* mutant showing SYP-1 in blue, a FISH probe to the right end of X in green, and a FISH probe to the left end of chromosome II in red. Nuclei exhibit nonhomologous synapsis where the XR (arrowhead) and/or IIL (arrow) FISH probes are unpaired and are attached to two different stretches of the SC. Scale bar is 5 µm.

Chapter 2: Attempts to isolate the Pairing Center complex

Summary

The *him-8/zim* gene family is required for proper homolog pairing, and as shown in Chapter 1, *him-8* is also required for synapsis initiation. To gain a clearer understanding of the mechanism by which *him-8/zim*s coordinate pairing and synapsis, I sought to identify protein interactors of Pairing Center (PC) proteins. In this chapter, I will describe my attempts to biochemically isolate PC proteins and their interactors. PC proteins are expressed at very low levels in *C. elegans*. HIM-8 is expressed in the gonad in the mitotic region through the end of pachytene, while expression of ZIMs is restricted to the transition zone. Ultimately, HIM-8 and ZIM-1-3 were not consistently detected or purified, which was likely due to a low abundance of them in whole worm lysates.

Introduction

In the previous chapter, I identified that HIM-8 is required for synapsis initiation. The *X^X;him-8(me4)* result where synapsis was occurring without PCs being connected to a nuclear envelope patch was quite intriguing. To date, this is the first instance of such robust synapsis occurring between homologs that are not connected to an NE patch in *C. elegans*. In fact, recent investigations into the meiotic role of dynein, a component of the NE patch, led to the conclusion that dynein is required for licensing synapsis (Sato et al., 2009). Clearly, there is still more to be uncovered about the molecular mechanisms governing homologous pairing and synapsis.

In order to further our understanding of the coordination of homolog pairing and synapsis, I sought to identify protein interactors of the HIM-8/ZIM family of proteins. Following isolation of protein interactors, I planned to use well-established genetic and cytological techniques that already existed in the lab to characterize the meiotic function of a novel interactor. As a graduate student, Aya Sato performed a yeast two-hybrid screen against a *C. elegans* cDNA library and found that HIM-8 and ZIM-3 interact with DPY-30, an essential component of the dosage compensation complex that serves to equalize X chromosome gene expression in males and hermaphrodites (Hsu and Meyer, 1994); however, further functional analysis does not indicate that DPY-30 plays a critical role in meiosis (A. Sato and A.F. Dernburg unpublished data). Furthermore, additional meiosis-specific protein interactors of PC proteins were not identified by yeast-two hybrid. In this chapter, I will describe my attempts of taking a biochemical approach to isolate PC proteins and their interactors.

From the onset, there were a variety of classes of protein interactors that I expected to identify. One potential class of interactors was NE proteins. Sato et al. (2009) genetically and cytologically characterized a network of proteins linking microtubles to PCs via the nuclear envelope, but it is still unknown what molecule directly tethers PC proteins to this network. In *C. elegans*, PCs do not interact with SUN-1 or ZYG-12 by yeast two-hybrid. This is a negative result, and thus, it is possible that the context of a yeast cell is not the appropriate environment for a protein-protein interaction to be detected. In budding yeast, the meiotic telomere protein Ndj1 interacts directly with Mps3, the budding yeast SUN-1 homolog (Conrad et al., 2007). This tethering of homologs via Ndj1 to the nuclear envelope is necessary for the rapid movements that chromosomes undergo while pairing and synapsis of homologs is initiated (Conrad et al., 2008). In fission yeast, Bqt1 and Bqt2 function as a bridge to connect the telomere protein Rap1 to Sad1, the fission yeast SUN-1 homolog, during the initiation of meiosis (Chikashige et al., 2006). While SUN-1 may not directly interact with PC proteins in *C. elegans*, there could be yet-to-be-identified chromatin interactors linking PCs to the SUN-1/ZYG-12 network.

In Chapter 1, I showed that HIM-8 is required for initiating synapsis of the X chromosome; thus, HIM-8/ZIMs may perform their function of coupling pairing and synapsis by physically interacting with and recruiting SC components (e.g., SYP-1), following pairing of homologous HIM-8/ZIM foci. To date, four central element proteins, SYP-1-4, have been identified in *C. elegans* (Colaiacovo et al., 2003; MacQueen et al., 2002; Smolikov et al., 2007; Smolikov et al., 2009). In addition, a host of axial element proteins are known in *C. elegans*, including HIM-3 and its three paralogs, HTP-1, HTP-2, and HTP-3 (Couteau and Zetka, 2005; Goodyer et al., 2008; Martinez-Perez and Villeneuve, 2005; Zetka et al., 1999). PC proteins could interact with any number of these SC components to initiate synapsis.

Another class of HIM-8/ZIM interactors may specifically be involved in mediating protein-protein interactions between two PCs. Yeast two-hybrid data indicate that full-length HIM-8 and ZIMs are unable to self-associate (A. Sato and A.F. Dernburg unpublished data). While negative evidence of self-association may be an artifact in the context of a yeast cell, it may also indicate that additional proteins are required for stabilizing interactions between two homologous PCs.

I expected the above 3 classes of interactors to be conserved among HIM-8/ZIM family members (i.e., factors associating with ZIM-2 at the Chromosome V PC would also interact with HIM-8 at the X PC). I expected conserved interactions because HIM-8/ZIMs all play the same primary role of mediating pairing via PCs. A final class of interactors I could find is specific to ZIM-1 and ZIM-3. Both ZIMs bind to two different autosomal PCs and thus, must not be sufficient for assessing homolog identity. It is possible that additional interacting proteins may provide further specificity. It is also possible that additional proteins are not needed and that homolog identity is finalized through homology search of one homolog invading another.

Potential PC interactors are of course not restricted to the expected classes of interactors listed above. By taking an unbiased biochemical approach, I sought to identify expected and novel classes of protein interactors. In this chapter, I will describe my attempts to immunoprecipitate endogenous PC proteins, as well as a tagged version of HIM-8 from whole worm lysates. Due to PC proteins being of low abundance in whole worm lysates, I was unable to successfully isolate PC proteins or their interactors.

Results

HIM-8 and ZIM proteins are likely present at too low levels to detect in worm lysates

Before trying to biochemically isolate the PC protein complex, the first basic step was to identify PC proteins by western blot of whole worm lysates. Antibodies that were specific to endogenous HIM-8/ZIMs had previously been generated and worked successfully for immunofluorescence (Phillips and Dernburg, 2006; Phillips et al., 2005). Mutants were also available for *him-8/zims*, providing appropriate negative controls for westerns.

Multiple HIM-8 antibodies that worked well for immunofluorescence were unable to recognize specific bands in whole worm lysate from wild type worms compared to lysate from the *him-8(tm611)* mutant (Figure 1A). The *him-8(tm611)* strain carries a 413 bp deletion that should cause a 5 kD band shift from the predicted molecular weight of 40 kD. While many background bands appeared in both samples, a difference between wild type lysates and *tm611* whole worm lysates was never clearly detected. Anti-HIM-8 antibodies did successfully detect a recombinant bacterially-expressed fragment of HIM-8, indicating that the antibody does work for westerns (Figure 1A, lane 1). Thus, it is likely that HIM-8 is not present in whole worm lysate at a concentration high enough that is detectable by western.

Anti-ZIM-1 and ZIM-3 westerns yielded similar results—specific target bands were not detectable above background levels (Figures 1B and 1D). Worm lysate from *zim-1(tm1479)* animals was an appropriate negative control to use for the anti-ZIM-1 western, since it carries a 737 bp deletion upstream of the antigenic region. The predicted molecular weight of ZIM-1 is 66 kD, but a band of this size was never specifically detected in wild type lysates. Lysates from *zim-3(tm2303)* and *glp-4(bn2ts)*, a mutant that produces no germline cells (Beanan and Strome, 1992), were used as negative controls for anti-ZIM-3 westerns. The *zim-3(tm2303)* strain

carries a 371 bp deletion upstream of the antigenic region. The expected molecular weight for ZIM-3 is 64 kD, but this was never detected specifically in wild type lysates. Recombinant ZIM-1 and ZIM-3 were not available as positive controls, so I could not determine if anti-ZIM-1 and/or anti-ZIM-3 were simply not good for westerns; however, ZIM-1 and ZIM-3 are expressed in even fewer cells than HIM-8, and thus, it is likely that they are also at too low concentrations in worm lysates to detect by western.

Westerns probed with anti-ZIM-2 seemed most promising at first, as a specific band was detected in wild type compared to mutant lysates (Figure 1C). Lysates from *zim-2(tm574)* served as a good negative control, since the mutation is a 415 bp deletion that results in an early stop codon upstream of the antigenic region. A specific band was detected in wild type around 40 kD that was not found in *zim-2(tm574)* lysates. This was lower than the predicted molecular weight of ZIM-2, which was 65 kD. In an effort to knockout expression of the entire *him-8/zim* operon, the promoter region upstream of *zim-1*, the first gene of this operon, was deleted (C.M. Phillips and A.F. Dernburg unpublished data). By immunofluorescence, only ZIM-1 expression was abrogated in the *zim-1 promoter* Δ line. Thus, if the wild type-specific band is in fact ZIM-2, it is not surprising that this band is also detected in lysates from the *zim-1 promoter* Δ line. Of all the PC proteins, this would be the best to follow up on, but even so, anti-ZIM-2 westerns were inconsistent, and often times, the specific band was not detected in wild type lysates. Again, ZIM-2 is expressed in a very restricted region—the transition zone of the gonad. Thus, for all PC proteins, westerns were unsuccessful or inconsistent, which was likely due to a low abundance of these proteins in whole worms.

Immunoprecipitation of endogenous HIM-8 and ZIM-1, -2, and -3 does not pull down targets

Despite westerns not working, I still attempted to immunoprecipitate (IP) endogenous PC proteins. Enrichment of targets by IP could allow for easier detection of low abundance proteins. Lysate preparation from wild type worms grown in liquid culture and immunoprecipitation experiments with anti-HIM-8 and ZIM-1-3 were carried out in Arshad Desai's lab with the help of Iain Cheeseman. Silver stain of IP samples looked promising, as specific bands were observed (Figure 2). IP samples were eluted with 0.1 M glycine, pH 2.6 or with 8 M urea and were sent off to be analyzed by Mud-PIT mass spectrometry. Mass spectrometry results revealed that none of the targets were isolated at detectable levels by IP.

Immunoprecipitation of a tagged version of HIM-8 is not successful

Since immunoprecipitation of endogenous PC proteins was not fruitful, I took a different approach and attempted to IP a tagged version of HIM-8. While a graduate student, David Wynne constructed a *GFP::HIM-8* strain (*ieIs24)* through biolistic transformation (D.J. Wynne and A.F. Dernburg unpublished data). This strain did not fully rescue the X pairing defect in a *him-8* mutant, but the tagged protein colocalized appropriately with endogenous HIM-8 protein, indicating that it likely interacts with at least some of the same proteins as endogenous HIM-8. Anti-GFP westerns inconsistently detected a band that was potentially GFP::HIM-8 (Figure 3A, lane 2). Lysate from *fem-2*, a strain that does not make sperm, served as a negative control, as it should not express the GFP::HIM-8 transgene. The band that was potentially GFP::HIM-8 ran at roughly 80 kD, while the predicted size is 67 kD; however, this GFP::HIM-8 80 kD band was inconsistently detected by western in whole worm lysates (Figure 3C, lanes 2 and 3). Anti-HIM-8 westerns on lysates from *GFP::HIM-8* worms failed to detect the same band, indicating that

either this was a spurious band or that the GFP prevents anti-HIM-8 from binding the tagged protein (Figure 3A, lane 4). The latter is unlikely, since the western was done on denatured proteins.

A spectrum of detergents was tested to solubilize what was thought to be GFP::HIM-8. Since HIM-8 colocalizes with nuclear envelope patches, it was expected that GFP::HIM-8 would come down in the insoluble fraction. Attempts were made to solubilize GFP::HIM-8 with 1% Triton and 0.1% sodium deoxycholate (Figure 3B), 1% NP-40 (Figure 3C), 1% digitonin, 1% Tween-20, and 1% octylgluocopyranoside (data not shown). In all cases, GFP::HIM-8 remained insoluble or was inconsistently detected in the soluble fraction. A line expressing the GFP::H2B transgene (strain AZ212) was used as a positive control, and a fraction of it was successfully solubilized with Triton and other detergents (Figure 3B and data not shown).

Despite the results of the solubility test, attempts were still made to immunoprecipitate GFP::HIM-8 with anti-GFP antibodies in case immunoprecipitation would allow for enough enrichment of GFP::HIM-8 to be detectable by western (Figure 3C). Triton and NP-40 were used to solubilize GFP::HIM-8. The positive control GFP::H2B was successfully immunoprecipitated (Figure 3, lane 7), but GFP::HIM-8 was not isolated (Figure 3, lanes 8 and 9)

Discussion

Low abundance of PC proteins likely makes it difficult to biochemically isolate them

By cytology, PC proteins are only detected in a subset of nuclei in the germline. HIM-8 is expressed as foci binding to the X chromosome Pairing Center in the pre-meiotic region through the end of pachytene. The ZIMs are only expressed and bound to their Pairing Centers in the transition zone, which contains roughly 40-80 nuclei in a typical adult hermaphrodite gonad (Carlton et al., 2006). Isolating proteins that are expressed at such low levels and that are also interacting with insoluble membranes, make biochemical isolation of them quite difficult. While inconsistently detected, ZIM-2 may be the best candidate to follow up on, since anti-ZIM-2 westerns occasionally led to clear detection of a band that was specifically depleted in the *zim-2* mutant.

Making a lysate specifically from meiotic nuclei would increase the concentration of PC proteins, which could potentially allow for easier detection and immunoprecipitation of targets. One possible approach would be to use a strain expressing an abundant meiosis-specific protein that is fluorescently labeled (e.g., a meiosis-specific histone tagged with GFP). These worms would need to be broken apart just enough so that nuclei are free but intact. Fluorescence-activated cell sorting (FACS) could be used to specifically isolate cells expressing GFP. The GFP-expressing fraction would be enriched for meiotic nuclei and thus, for meiotic proteins like HIM-8 and ZIMs, as well. Lysate could be made from this faction, which could then be used as the starting material for westerns and IPs.

Materials and methods

Strains

See chapter 2 for details on handling strains. Unless otherwise indicated, N2 Bristol was used as the wild type strain. *him-8(tm611)*, *zim-1(tm1479)*, *zim-2(tm574), zim-3(tm2903),* and *zim-1 promoter* Δ lines were all maintained as homozygotes. *glp-4(bn2)* is a temperature-sensitive mutant and was maintained at the permissive temperature of 16°C. To exhibit the mutant phenotype, *glp-4(bn2)* animals were shifted to the restrictive temperature of 25°C at the L4 stage.

Preparation of worm lysates for westerns

Worms were handpicked into worm lysis buffer (10 mM Tris, pH 7.4, 150 mM NaCl, 2 mM EDTA, 1.5 mM EGTA, 1.5 mM $MgCl_2$, 0.5 mM Na_3VO_4, Roche protease inhibitor tablets). Samples were flash frozen in liquid nitrogen and thawed on ice. Thawed samples were sonicated at 4°C in a Bioruptor (Diagenode) for 5 cycles of 10 sec on/10 sec off. Lysates were boiled in sample buffer and loaded on an SDS-PAGE gel.

Immunoprecipitation experiments

Synchronized wild type animals or GFP-tagged lines were grown up in liquid culture until hermaphrodites were gravid. Harvested adults were washed several times with M9/S basal, and a 30% sucrose float was done to recover only adults. After several more M9/S basal washes, worms were spun down and resuspended 50:50 in a buffer of 50 mM HEPES, pH 7.5, 1 mM EGTA, 1 mM $MgCl_2$, 100 mM KCl, 10% glycerol plus Roche protease inhibitor tablets. This 50:50 suspension of worms to buffer was pipetted small drops at a time into liquid nitrogen to make "worm popcorn" that was stored at -80°C. Lysate preparation and immunoprecipitation experiments were carried out as described previously (Cheeseman and Desai, 2005).

References

Beanan, M.J., and Strome, S. (1992). Characterization of a germ-line proliferation mutation in C. elegans. Development *116*, 755-766.

Carlton, P.M., Farruggio, A.P., and Dernburg, A.F. (2006). A link between meiotic prophase progression and crossover control. PLoS Genet *2*, e12.

Cheeseman, I.M., and Desai, A. (2005). A combined approach for the localization and tandem affinity purification of protein complexes from metazoans. Sci STKE *2005*, pl1.

Chikashige, Y., Tsutsumi, C., Yamane, M., Okamasa, K., Haraguchi, T., and Hiraoka, Y. (2006). Meiotic proteins bqt1 and bqt2 tether telomeres to form the bouquet arrangement of chromosomes. Cell *125*, 59-69.

Colaiacovo, M.P., MacQueen, A.J., Martinez-Perez, E., McDonald, K., Adamo, A., La Volpe, A., and Villeneuve, A.M. (2003). Synaptonemal complex assembly in C. elegans is dispensable for loading strand-exchange proteins but critical for proper completion of recombination. Dev Cell *5*, 463-474.

Conrad, M.N., Lee, C.Y., Chao, G., Shinohara, M., Kosaka, H., Shinohara, A., Conchello, J.A., and Dresser, M.E. (2008). Rapid telomere movement in meiotic prophase is promoted by NDJ1, MPS3, and CSM4 and is modulated by recombination. Cell *133*, 1175-1187.

Conrad, M.N., Lee, C.Y., Wilkerson, J.L., and Dresser, M.E. (2007). MPS3 mediates meiotic bouquet formation in Saccharomyces cerevisiae. Proc Natl Acad Sci U S A *104*, 8863-8868.

Couteau, F., and Zetka, M. (2005). HTP-1 coordinates synaptonemal complex assembly with homolog alignment during meiosis in C. elegans. Genes Dev *19*, 2744-2756.

Goodyer, W., Kaitna, S., Couteau, F., Ward, J.D., Boulton, S.J., and Zetka, M. (2008). HTP-3 links DSB formation with homolog pairing and crossing over during C. elegans meiosis. Dev Cell *14*, 263-274.

Hsu, D.R., and Meyer, B.J. (1994). The dpy-30 gene encodes an essential component of the Caenorhabditis elegans dosage compensation machinery. Genetics *137*, 999-1018.

MacQueen, A.J., Colaiacovo, M.P., McDonald, K., and Villeneuve, A.M. (2002). Synapsis-dependent and -independent mechanisms stabilize homolog pairing during meiotic prophase in C. elegans. Genes Dev *16*, 2428-2442.

Martinez-Perez, E., and Villeneuve, A.M. (2005). HTP-1-dependent constraints coordinate homolog pairing and synapsis and promote chiasma formation during C. elegans meiosis. Genes Dev *19*, 2727-2743.

Phillips, C.M., and Dernburg, A.F. (2006). A family of zinc-finger proteins is required for chromosome-specific pairing and synapsis during meiosis in C. elegans. Dev Cell *11*, 817-829.

Phillips, C.M., Wong, C., Bhalla, N., Carlton, P.M., Weiser, P., Meneely, P.M., and Dernburg, A.F. (2005). HIM-8 binds to the X chromosome pairing center and mediates chromosome-specific meiotic synapsis. Cell *123*, 1051-1063.

Sato, A., Isaac, B., Phillips, C.M., Rillo, R., Carlton, P.M., Wynne, D.J., Kasad, R.A., and Dernburg, A.F. (2009). Cytoskeletal forces span the nuclear envelope to coordinate meiotic chromosome pairing and synapsis. Cell *139*, 907-919.

Smolikov, S., Eizinger, A., Schild-Prufert, K., Hurlburt, A., McDonald, K., Engebrecht, J., Villeneuve, A.M., and Colaiacovo, M.P. (2007). SYP-3 restricts synaptonemal complex assembly to bridge paired chromosome axes during meiosis in Caenorhabditis elegans. Genetics *176*, 2015-2025.

Smolikov, S., Schild-Prufert, K., and Colaiacovo, M.P. (2009). A yeast two-hybrid screen for SYP-3 interactors identifies SYP-4, a component required for synaptonemal complex assembly and chiasma formation in Caenorhabditis elegans meiosis. PLoS Genet *5*, e1000669.
Zetka, M.C., Kawasaki, I., Strome, S., and Muller, F. (1999). Synapsis and chiasma formation in Caenorhabditis elegans require HIM-3, a meiotic chromosome core component that functions in chromosome segregation. Genes Dev *13*, 2258-2270.

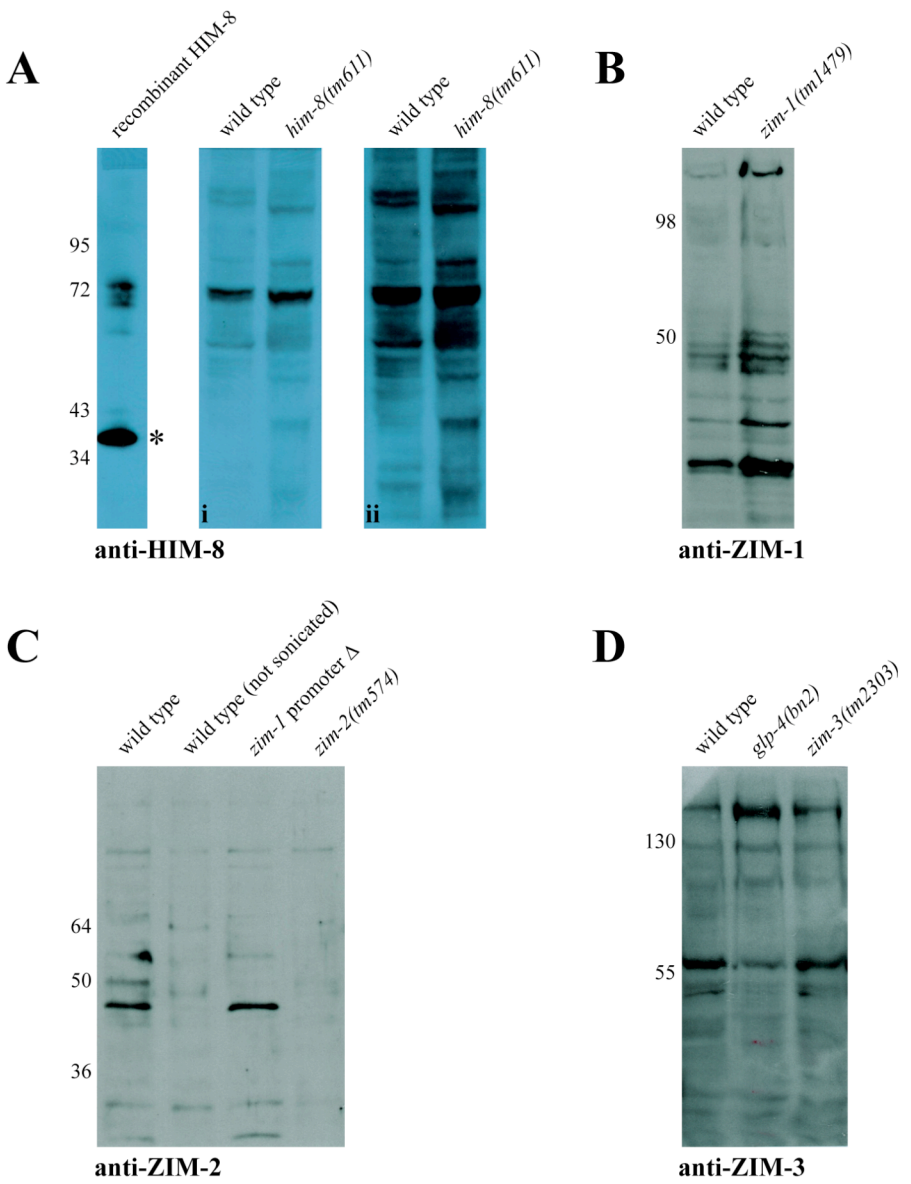

Figure 1: Endogenous HIM-8 and ZIM-1, -2, and -3 are difficult to detect on westerns on whole worm lysates. (A) Affinity-purified anti-HIM-8 recognizes purified recombinant HIM-8 fragment, but not endogenous HIM-8 from wild type whole worm lysates. Wild type HIM-8 is predicted to run at 40 kD, while the mutant protein from the *him-8(tm611)* deletion strain should run at 35 kD. The anti-HIM-8 antibody was generated against a region of the protein upstream of the deletion. The recombinant HIM-8 sample is the purified HIM-8 fragment that was used to generate the antibody. (i) and (ii) are the same western with film exposures of 2 and 10 minutes, respectively. (B) Anti-ZIM-1 does not recognize a specific band in wild type compared to *zim-1(tm1479)* lysates. ZIM-1's expected size is 66 kD. The *tm1479* mutation contains a ~400 bp deletion in an intron upstream of the antigenic region. (C) Affinity purified anti-ZIM-2 recognizes a specific band in wild type lysate that is not seen in *zim-2(tm574)*. This band also appears in the mutant strain that carries a deletion of the *him-8/zim* operon promoter. This is expected, as the promoter deletion strain only reduces expression of *zim-1* by immunofluorescence. The expected size of ZIM-2 is 65 kD, which is much higher than the band seen here. The wild type-specific ZIM-2 band was not consistently detected in subsequent experiments. The *tm574* deletion causes an early stop codon upstream of the antigenic region. (D) Affinity-purified anti-ZIM-3 does not recognize a specific band in wild type lysates compared to *zim-3(tm2303)* or to *glp-4(bn2)*, a temperature-sensitive mutant that does not have a germline when kept at the non-permissive temperature. The expected size of ZIM-3 is 64 kD. The *tm2303* mutation contains a deletion upstream of the antigenic region.

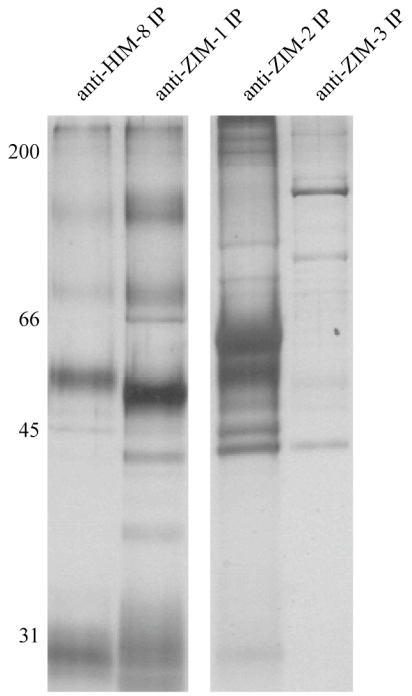

Figure 2: Immunoprecipitation experiments do not pull down HIM-8 and ZIM-1, -2, and -3.
Silver stain of anti-HIM-8, anti-ZIM-1, anti-ZIM-2, and anti-ZIM-3 immunoprecipitated samples. While specific bands do appear in IP lanes, Mud-PIT mass spectrometry analysis of immunoprecipitated samples revealed that targets were not isolated.

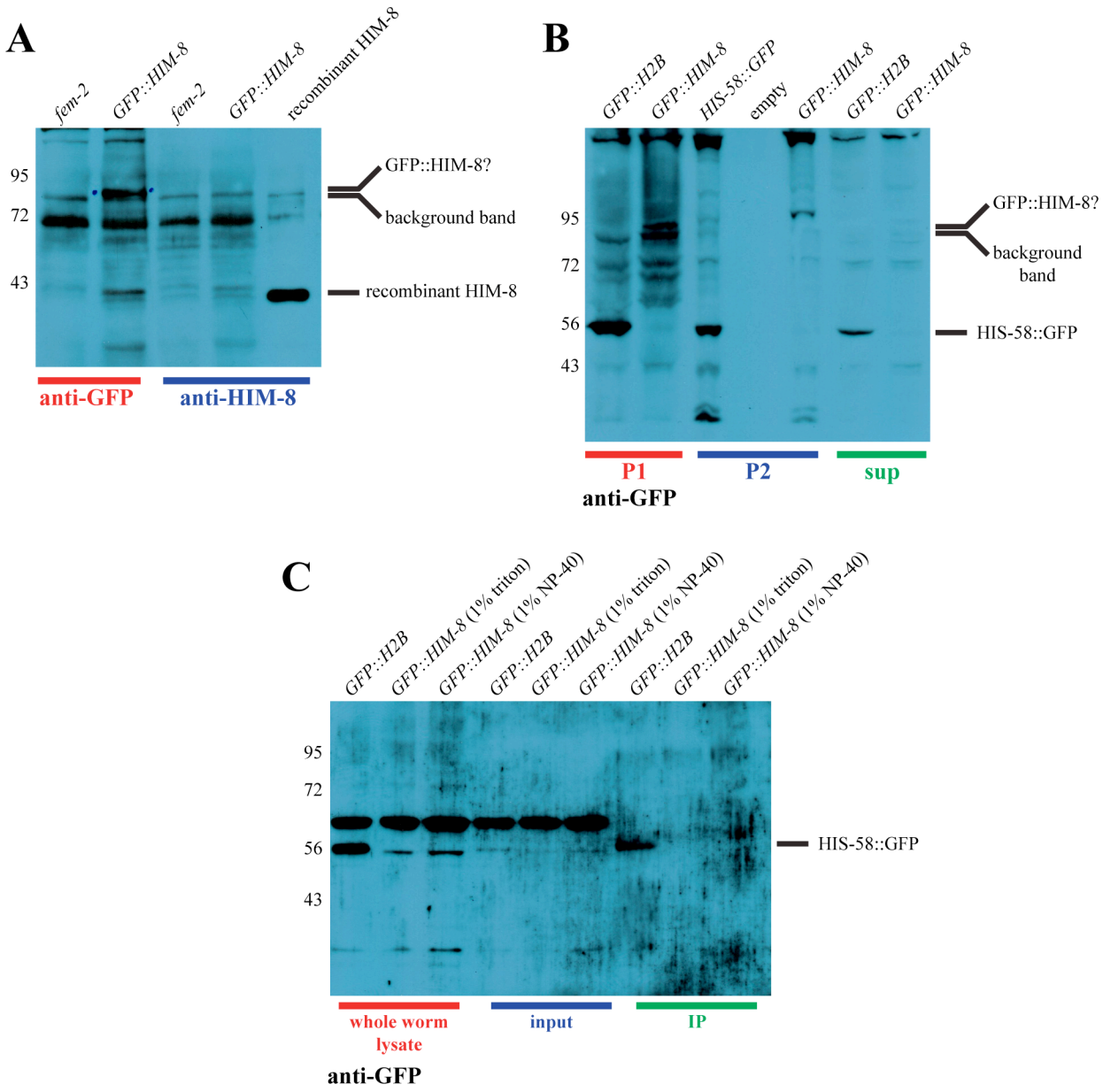

Figure 3: Immunoprecipitation of GFP::HIM-8 is not successful.
(A) Anti-GFP and anti-HIM-8 westerns detecting GFP-tagged HIM-8 in whole worm lysates from *fem-2* (a mutant that does not make sperm) and the *GFP::HIM-8* line that expresses GFP-tagged HIM-8 by immunofluorescence. A band that is specific to the *GFP::HIM-8* line may be GFP-tagged HIM-8, but it is not recognized by antibodies against HIM-8. This band was inconsistently detected in *GFP::HIM-8* lysates. (B) Anti-GFP western of *GFP::HIM-8* and *GFP::H2B* lysates solublized with 1% Triton and 0.1% sodium deoxycholate. "P1" represents the insoluble fraction from the first spin (9600g) after sonication, while "P2" represents the insoluble fraction from the second spin (81,000g). The "sup" sample represents the final soluble fraction. A fraction of HIS-58::GFP is solublized, while GFP::HIM-8 is not solublized. (C) Anti-GFP western/IP from *GFP::HIM-8* and *GFP::H2B* lysates solublized with 1% Triton or 1% NP-40. The GFP::H2B control IP worked successfully, while GFP::HIM-8 was not immunoprecipitated.

Chapter 3: GAK-1 plays a role in *C. elegans* meiosis

Summary

The *gak-1* gene was initially thought to play a role in meiosis because a reduction in its expression resulted in a Him phenotype, which is indicative of missegregation of the X chromosome. Subsequent analysis showed that *gak-1* mutants have ~80% embryonic lethality and elevated germline apoptosis, which are also both associated with defects in meiosis. Mutations in *gak-1* cause a range of subtle synapsis defects, none of which can easily account for the high levels of embryonic inviability. *gak-1* mutants are competent for homolog pairing and for forming crossovers. More detailed analysis revealed that mutations in *gak-1* lead to defects in disassembly of the synaptonemal complex prior to anaphase I. Additionally, mutations in *gak-1* result in an increased number of foci of RAD-51, which has previously been used to cytologically mark the double-strand breaks that initiate recombination; though, the implications of this result are unclear. GAK-1 localizes to chromatin and cytologically appears to be enriched on autosomes relative to the X chromosome, which is corroborated by ChIP-seq data. Interestingly, GAK-1 ChIP-seq signals overlap strongly with sites enriched for HIM-17, another chromatin-bound factor that has been implicated in making chromosomes competent for double-strand break formation. Both GAK-1 and HIM-17 are enriched at the transcription start sites of many meiosis-specific genes. This suggests that *gak-1* may be functioning as a transcription factor, which might explain the pleiotropic meiotic effects observed in the absence of *gak-1* function.

Introduction

I have been investigating how GAK-1, an AT-hook protein, is involved in meiosis. The *gak-1* gene was initially thought to play a role in meiosis because of the observation that loss of its function results in a Him (High incidence of males) phenotype (Kuervers et al., 1998). In *C. elegans,* the predominant sex is hermaphrodite, which is XX, while males are XO. Males result from defects in meiosis that cause nondisjunction of the X chromosome. In the wild type population, meiotic errors occur at a very low frequency, and only 0.2% are males (Hodgkin et al., 1979). In contrast, mutations in meiotic genes lead to a much higher incidence of males. Kuervers et al. (1998) injected a cosmid containing the *gak-1* gene and observed a Him phenotype. They originally thought this was due to overexpression of *gak-1*, but a later study showed that exogenous DNA in the germline cosuppresses (or reduces expression of) the endogenous gene (Dernburg et al., 2000). The *gak-1* gene also arose as a hit in an RNAi-based screen for genes required for the normal pattern of meiotic recombination (J. Yanowitz unpublished data). Recognizable homologs of *gak-1* are found only in other *Caenorhabditis* species.

GAK-1 contains two putative AT-hook domains, which are DNA-binding motifs that have been shown to bend DNA and to affect chromatin compaction *in vitro* (Falvo et al., 1995; Strick and Laemmli, 1995). The AT-hook motif was first identified in High mobility group (HMG) proteins, which are nonhistone chromosomal proteins that are involved in gene regulation (Reeves and Nissen, 1990). The AT-hook is a short motif that is centered around a glycine-arginine-proline (GRP) tripeptide that binds to AT-rich sequences at the minor groove of DNA. The AT-hook has been found in a variety of DNA-binding proteins, including transcription factors, chromatin architectural factors, and cofactors for other DNA-binding proteins (Aravind and Landsman, 1998). Previous studies have shown that DNA-binding proteins can alter chromatin structure, which can affect recombination (Mets and Meyer, 2009; Reddy and Villeneuve, 2004); thus, the putative DNA-binding properties of GAK-1 make it an interesting candidate meiotic gene.

Sara Jover-Gil, a former postdoctoral fellow in the lab, initiated detailed analysis of GAK-1 and found additional evidence for its role in meiosis. Two deletion alleles of *gak-1* were analyzed that appear to be functional nulls. In addition to the Him phenotype, *gak-1* loss-of-function mutations result in high levels of embryonic lethality, which is indicative of aneuploidy of autosomes. Germline apoptosis is also elevated, indicating that meiotic nuclei are being culled due to synapsis defects and/or unresolved meiotic DSBs. In the *C. elegans* germline, apoptosis can occur by three different means. There is physiological apoptosis, whereby nearly half of all oocytes are automatically targeted for apoptosis in the adult hermaphrodite (Gumienny et al., 1999). Additionally, the synapsis checkpoint and DNA damage checkpoint cull nuclei that have unsynapsed chromosomes and unrepaired DNA breaks, respectively (Bhalla and Dernburg, 2005; Gartner et al., 2000). Defects in meiosis lead to elevated apoptosis because one or both of these checkpoints is activated.

In my characterization of the *gak-1* gene, I found that it does not play a role in homolog pairing or forming crossovers. GAK-1 does play a subtle role in maintenance of the SC; though, this is not its primary role in meiosis, as an essential factor for SC formation would be required downstream for crossover formation, which is unaffected in *gak-1* mutants. More thorough analysis indicates a role for GAK-1 in SC disassembly. Additionally, an elevated number of RAD-51 foci, a marker for meiotic double-strand breaks, is seen in *gak-1* mutants. Antibodies

against GAK-1 show a broad distribution on meiotic chromosomes with weaker staining on the X chromosome relative to autosomes. Through ChIP-seq analysis, I obtained a detailed genome-wide profile of GAK-1 localization. I found that GAK-1 binding sites coincide with enrichment of HIM-17, a protein that has previously been implicated in making chromatin competent for DSBs (Reddy and Villeneuve, 2004; Tsai et al., 2008). Together, these proteins are enriched at transcription start sites for many meiosis-specific genes, which suggests that GAK-1 and HIM-17 might be playing a role in regulating expression of germline-specific genes.

Results

gak-1 mutants display typical characteristics of meiotic mutants

Two deletion alleles of *gak-1* are available (Figure 1A). The *ok708* allele contains a 599 bp deletion, while the *ok709* allele is a 399 bp insertion/1855 bp deletion. An obvious indication of a gene playing a role in meiosis is a Him phenotype in the mutant (Hodgkin et al., 1979). A former post-doc in the lab, Sara Jover-Gil, confirmed the reported Him phenotype in *gak-1* animals by quantifying the number of male progeny generated by animals carrying the *ok708* and *ok709* alleles (Table 1). Wild type animals throw only 0.06% males, while *ok708* and *ok709* animals throw about 25% males. This Him phenotype is quite strong, as *him-8* mutants, which are defective in segregating the X chromosome, lay ~38% male progeny (Phillips et al., 2005). While aneuploidy of the X chromosome is viable, aneuploidy of autosomes leads to dead eggs. *gak-1* mutants throw between 76-85% dead eggs (Table 1).

In addition to strong Him and embryonic lethality phenotypes, Sara found that *gak-1* mutants also have high levels of germline apoptosis, which is an indicator of a defect in meiosis (Bhalla and Dernburg, 2005; Gartner et al., 2000). Apoptotic cells were identified using the CED-1::GFP marker, which engulfs cells that are about to undergo programmed cell death (Boulton et al., 2004). Wild type animals have roughly 8 apoptotic nuclei per gonad, while *ok708* and *ok709* animals have ~22 apoptotic nuclei (Figure 1B). This is quite a significant increase in apoptosis, as mutants that activate both the synapsis and DNA damage checkpoint have ~20-24 apoptotic nuclei and mutants that activate just the DNA damage or synapsis checkpoint have ~13 apoptotic nuclei per gonad arm (Bhalla and Dernburg, 2005). Since the *ok708* and *ok709* alleles behave fairly similarly in terms of their Him phenotypes and apoptosis counts, the majority of the further analysis was done with just the *ok708* allele.

Homolog pairing is normal in *gak-1* mutants

Homolog pairing was assessed in *gak-1(ok708)* to determine whether GAK-1 plays a role in stabilizing pairing. Pairing Center proteins can be used to monitor pairing cytologically, since they mark particular homolog pairs (Phillips and Dernburg, 2006; Phillips et al., 2005). ZIM-2 was used to examine pairing of chromosome V in *gak-1* mutants (Figures 2A and 2C). ZIM-2 binds to unpaired chromosome V Pairing Centers as discreet foci in the transition zone where pairing is initiated. Its expression ceases at the start of pachytene, by which point pairing of V (and other chromosomes) is completed and one ZIM-2 focus per nucleus is seen. In order to take a time-course of chromosome V pairing, the location in the gonad where ZIM-2 is expressed was divided into four regions of equal length (Figure 2B). Upon initial expression of ZIM-2 in zone 1, over 50% of nuclei already have achieved chromosome V pairing in wild type animals (Figure 2C). By the end of the transition zone in zone 4, almost all nuclei have paired chromosome Vs.

gak-1 mutants have no difficulty in pairing of chromosome V, as a 100% of nuclei in zone 4 have paired ZIM-2 foci.

Similarly, HIM-8 was used to monitor pairing of the X chromosome (Figures 2D and 2E). HIM-8 is expressed as foci bound to the X Pairing Center starting in the mitotic region all the way to the end of pachytene. All pachytene nuclei observed in *gak-1(ok708)* animals had paired HIM-8 foci, similar to wild type. Thus, defects in pairing of the X or autosomes cannot account for the strong meiotic phenotype seen in *gak-1* mutants.

Crossovers form in *gak-1* mutants

As mentioned above, there are prior findings linking *gak-1* to a role in meiotic recombination. To assess whether crossover recombination among all homologs was taking place, I quantified the number of homolog pairs seen in diakinesis, which is the final stage of meiotic prophase. Upon reaching diakinesis, the chromatin undergoes compaction to a point where individual homolog pairs can be distinctly identified. In a wild type animal, a majority of diakinesis nuclei have six DAPI-stained bodies, representing the six homolog pairs that are held together by a crossover. Similarly, the majority of diakinesis nuclei in *gak-1* mutants have six DAPI-stained bodies, indicating that *gak-1* is not required for crossover recombination (Figure 3). Thus, most chromosome pairs undergo at least one CO. This indicates that if GAK-1 affects recombination, it does so in a more subtle way than blocking COs entirely. Therefore, I chose to look at markers in the CO pathway to see if any sub-stage was affected.

An elevated number of RAD-51 foci is seen in *gak-1* mutants

An early stage at which recombination is regulated is at the level of DSB formation. I assayed the number of DSBs cytologically by counting RAD-51 foci (Figure 4). RAD-51 coats the single-strand overhang that is left after a DSB is made and allows for strand invasion of its homolog during recombination (Neale and Keeney, 2006). Meiotic double-strand breaks marked by RAD-51 first appear in the transition zone (Alpi et al., 2003). They peak in early to mid-pachytene and disappear by late pachytene, by which point DSBs have been resolved into crossovers or noncrossovers. A time-course of DSBs was taken in *gak-1* mutants by quantifying the average number of RAD-51 foci per nucleus as they progressed through the gonad. The gonad was divided into five regions: the mitotic zone, the transition zone, early pachytene, mid-pachytene, and late pachytene (Figure 4B). The mitotic zone, transition zone, and pachytene were delineated based on chromatin morphology as done previously (Carlton et al., 2006). The pachytene region was then further divided into three regions of equal length. On average, *gak-1(ok708)* animals had more RAD-51 foci per nucleus compared to wild type. In the transition zone, *gak-1* animals have 3-fold more RAD-51 foci compared to wild type (Figure 4C). One caveat is that *gak-1* animals seem to have an extended region of transition-zone like nuclei, and thus, this particular zone spanned a larger region of the gonad in mutants compared to wild type. This may affect the quantification results; however, even in the region considered early pachytene in *gak-1* mutants, there is a 3-fold increase of RAD-51 foci compared to wild type. By late pachytene, RAD-51 foci disappear, indicating that meiotic breaks are being resolved in a timely fashion. This is consistent with the appearance of 6 distinct DAPI-stained bodies.

A greater number of RAD-51 foci does not necessarily imply that an increased number of DSBs are being generated in *gak-1* animals. Since these are fixed animals, more RAD-51 foci in any given nucleus could imply that RAD-51 is not turning over fast enough and that breaks are not being processed in a timely fashion in early pachytene. To determine the primary defect, I

looked at RAD-51 foci in the *rad-54* mutant. In *rad-54* mutants, repair of DSBs is blocked and RAD-51-bound DSBs are "trapped" (Mets and Meyer, 2009). Therefore, quantification of the total number of RAD-51 foci per nucleus gives an indication of how many total breaks are made at the point of formaldehyde fixation of samples. In the *rad-54* background, an average of 12 RAD-51 foci are observed in any given pachytene nucleus (Mets and Meyer, 2009; Youds et al., 2010). Based on this assay, it was determined that meiotic nuclei experience about twelve DSBs. Since we know that most homolog pairs undergo only one crossover, half the DSBs that form are being shunted down the noncrossover pathway in a wild type animal.

I looked at the *gak-1(ok708);rad-54(ok615)* mutant to see whether more or less than twelve breaks were being made per nucleus (Figure 4A). To my surprise, I observed a different result than what was reported for the *rad-54(ok615)* single mutant. In pachytene, upwards of 20 and sometimes 30 RAD-51 foci were seen in *rad-54(ok615)* animals. For the time being, the number of foci was not quantified in *rad-54(ok615)* versus *rad-54(ok615);gak-1(ok708)* because such a large number of foci per nucleus led to difficulties in manually quantifying foci number; though, by eye, it does appear that *rad-54(ok615);gak-1(ok708)* animals have more RAD-51 foci than *rad-54(ok615)* single mutants.

Crossover interference is unaffected in *gak-1* mutants

In most organisms, including *C. elegans*, each chromosome must undergo at least one crossover (CO) event during meiosis to create a chiasma (linkage) that will allow proper segregation. Most organisms also employ a mechanism known as interference that tightly regulates CO formation in a spatial fashion, such that the location of one CO inhibits the formation of another CO nearby (Hillers, 2004). Crossover interference is tightly regulated in *C. elegans*, such that even when multiple chromosomes are fused together, each fusion experiences only one CO (Hillers and Villeneuve, 2003). MSH-5 and ZHP-3 are two proteins required for CO completion (Jantsch et al., 2004; Kelly et al., 2000). At the end of pachytene, when DSBs are resolved into either COs or noncrossovers, these two proteins colocalize at the sites of crossovers (Bhalla et al., 2008). Six MSH-5/ZHP-3 foci per nucleus appear by the end of pachytene in a wild type animal, representing the single crossover between each of the six homolog pairs. If *gak-1* mutants have an increase in CO formation, this could potentially be assayed cytologically by quantifying the number of ZHP-3/MSH-5 foci per cell. In wild type and *gak-1* mutants, the majority of nuclei had an average of six MSH-5/ZHP-3 foci (Figures 5A and 5B); thus, based on this assay, *gak-1* is not required for regulating crossover interference. An independent assay was needed to verify *gak-1*'s role in crossover interference, as situations where crossover interference is lost have not always correlated with an increase in the occurrence of crossover markers like ZHP-3 (Youds et al., 2010).

To examine crossover interference more directly, I undertook a genetic approach. I measured the global number and distribution of crossovers by single nucleotide polymorphism (SNP) mapping (Figure 5C). *gak-1(ok708)* animals were repeatedly backcrossed to the Hawaiian strain CB4856 to generate a *gak-1* line that was homozygous for Hawaiian alleles at each SNP. Concurrently, the *gak-1* balancer strain, *hT2* was repeatedly backcrossed to CB4856 and was used to balance the Hawaiianized *gak-1(ok708)* strain. Hawaiianized *gak-1(ok708)/hT2* animals were crossed to *gak-1(ok708)*/*hT2* animals in the N2 Bristol background, and meiotic recombination was assayed in F1 hermaphrodites and males by genotyping starved F2s and F3s (see Materials and methods for details).

SNP genotyping was done using the Illumina GoldenGate assay. One hundred and forty-four SNPs were chosen for interrogation. The majority of these SNPs were chosen as a subset of SNP assays that had previously worked successfully in the GoldenGate assay (Rockman and Kruglyak, 2009). The 144 SNPs were distributed across the *C. elegans* genome, but not completely evenly, as more SNPs were concentrated at putative recombination hot spots. Four SNP assays were removed because they did not perform well on the GoldenGate platform. Twenty-two SNP assays were removed because the Hawaiianized *gak-1* strain was not homozygous at those particular SNPs or the SNP was not a true SNP, as the allele was the same in Hawaiian and N2 control strains.

Recombination was assayed in 45 wild type males, 47 wild type hermaphrodites, 46 *gak-1(ok708)* males, and 46 *gak-1(ok708)* hermaphrodites; however, due to poor sample quality or samples not being the correct cross-progeny, a subset was disregarded in the final analysis. The final set assayed included: 45 wild type males, 28 wild type hermaphrodites, 36 *gak-1(ok708)* males, and 31 *gak-1(ok708)* hermaphrodites. As expected, roughly half the chromosomes analyzed were recombinant in both wild type and *gak-1(ok708)* animals. The exception was the X chromosome in males of both genotypes, which was never recombinant because the single X chromosome in males does not undergo genetic recombination. As predicted, complete interference was observed in wild type animals, as only two chromosomes analyzed (both in males) showed evidence of double crossovers. Unpublished results from Judith Yanowitz's lab indicated that *gak-1* animals exhibit a reduction in crossover interference, but this was not observed here, as only one chromosome in a *gak-1* male underwent a double crossover. One caveat is that very closely spaced crossovers will be missed using this assay, since the SNP markers were not densely spaced throughout the genome. Despite this limitation, the results of this assay suggest that *gak-1* does not play a role in regulating crossover interference.

GAK-1 plays a role in proper maintenance of the SC

I next examined whether *gak-1* mutants exhibit a synapsis defect. Depending on the method used for depleting *gak-1* function, a range of synapsis defects was observed. In the *gak-1(ok708)* mutant, the synapsis defect is subtle. Synapsis was assayed by looking at colocalization of HTP-3, an axial element of the SC, and SYP-1, the central element of the SC (Goodyer et al., 2008; MacQueen et al., 2002). Complete colocalization of the two markers indicates synapsis is complete. In mid-pachytene, where synapsis should be fully completed, the ratio of SC components on the X (marked by HIM-8) seems to be altered, as less SYP-1 is present compared to HTP-3 (Figure 6B). In a subset of *gak-1(ok708)* animals, the X chromosomes initiate SC disassembly earlier than in wild type animals where they remain fully synapsed until diplotene (data not shown). In *gak-1(ok709)* mutants, synapsis defects range from delayed loading of the SC to early disassembly of SYP-1 (Figures 6D-6F). In *ok709*, the affected chromosome is sometimes the X and sometimes not (data not shown).

Germline cosuppression was also used to knockdown *gak-1* function (Dernburg et al., 2000). Cosuppression of *gak-1* results in a variable synapsis defect, with some asynapsed regions appearing in late pachytene (Figure 6G). The most consistently severe synapsis defect seems to appear in *gak-1(ok708)* second-generation homozygotes (unless otherwise indicated, all experiments were conducted on homozygous mutant progeny of heterozygous animals to avoid looking at aneuploid animals, which would confound synapsis results). In the majority of second-generation *ok708* animals, SYP-1 seems to disassemble from the X early (Figure 6C). In all of the above methods of knockdown, GAK-1 was undetectable by immunofluorescence (data

not shown). A range of synapsis defects was observed, which overall indicates some instability in SC maintenance; however, this alone cannot explain the strong meiotic phenotype in *gak-1* mutants, since a true synapsis defect would prevent crossover recombination, which is not the case here.

GAK-1 plays a role in proper disassembly of the synaptonemal complex

The synaptonemal complex disassembles from bivalents in a stereotypical fashion that is dictated by the site of the crossover (Martinez-Perez et al., 2008). Bivalents are usually asymmetric, as crossover placement is biased away from the center of chromosomes towards the arms (Rockman and Kruglyak, 2009). Upon entry into diplotene, the SC central element SYP-1 forms reciprocal localization with the axial elements HTP-1/2 along the bivalent (Figures 7A, 7C, and 7E). SYP-1 localizes to the short arm of the bivalent, while HTP-1/2 localizes to the long arm. In wild type, by the -3 oocyte, SYP-1 has completely disassembled from both arms of the bivalent, while HTP-1/2 remains on the long arm up until the -1 oocyte (Figure 7A). In contrast, SYP-1 remains on bivalents even on the -2 oocyte in *gak-1* mutants (Figures 7B and 7D). What is more striking is that SYP-1 and HTP-1/2 do not always strictly maintain reciprocal localization patterns in diakinesis nuclei in *gak-1* mutants. In the -2 oocyte, SYP-1 and HTP-1/2 are both found on one arm of the bivalent (Figure 7D).

A defect in SC disassembly could cause chromosome missegregation, since proper loss of SYP-1 and cohesin between homologs is required for homologs to separate at anaphase I. Staining for tubulin and DAPI in the first embryonic divisions did not reveal any obvious segregation defects like lagging chromosomes in anaphase I or II (Figure 8); however, only three embryos of each stage were isolated from *gak-1* animals, and so higher numbers are needed to confirm this result. Additionally, while lagging chromosomes are not apparent, FISH would need to be done to determine whether homologs are in fact properly segregating to opposite poles.

GAK-1 localizes to chromatin in the germline and is less abundant on the X chromosome

To determine where GAK-1 is expressed in *C. elegans*, an antibody was developed against 100 amino acids in the N-terminus of the protein. By immunofluorescence, GAK-1 localizes to chromatin in the premeiotic region (mitotically dividing germ cells), transition zone, and pachytene (Figure 9A). GAK-1 has a punctate appearance along the chromosomes. GAK-1 signal drops to undetectable levels about 5 or 6 rows of nuclei before the end of pachytene. When co-staining with GAK-1 and HIM-8 to identify the X chromosome, GAK-1 appears to be depleted on the X compared to autosomes (Figure 9B). In addition to the germline, GAK-1 is also expressed in the two primordial germ cells (data not shown). GAK-1 signal is undetectable in both *ok708* and *ok709* animals (data not shown).

To get a more fine-scale profile of GAK-1's distribution within the *C. elegans* genome, ChIP-seq technology was used. GAK-1 antibodies were used to isolate GAK-1 from whole worm lysate, and DNA fragments that were associated with GAK-1 were sequenced. Two programs were used to analyze GAK-1 ChIP-seq data: MACS and SPP (Kharchenko et al., 2008; Zhang et al., 2008). Both MACS and SPP call peaks—sites of enriched ChIP-seq signal—on input-subtracted data, as strong biases are known to exist for sequencing data. The cytological results above were confirmed by ChIP-seq analysis (Figures 10 and 11). MACS and SPP peak calls correlate well with one another across the *C. elegans* genome (data shown for chromosome I and the X in Figure 11). Like the immunofluorescence data, GAK-1 ChIP-seq

data also show an enrichment of signal on autosomes compared to the X, as fewer peaks are found on the X chromosome (Figures 10 and 11C). Three GAK-1 ChIP-seq replicates were performed to confirm GAK-1's genomic profile (Figure 13A). ChIP experiments with Rb3179 and Rb3161 anti-GAK-1 antibodies correlated well with each other. The Rb3161 ChIP shares 91% of its peaks with the Rb3179 ChIP experiment. The Rb0813 ChIP is the outlier, as very few peaks were called overall; thus, this experiment was considered to fail.

GAK-1 and HIM-17 ChIP-seq signals strongly correlate with one another and are enriched at transcription start sites.

As part of the worm ModENCODE project, all meiosis-specific chromatin factors are being mapped within the *C. elegans* genome by ChIP-chip and/or ChIP-seq. As a staff scientist in the lab, Andrea Doce has conducted ChIP on a number of meiosis-specific proteins, including HIM-17. HIM-17 is a protein required for crossover recombination (Reddy and Villeneuve, 2004). Since GAK-1 plays a role in recombination, I looked at correlation of GAK-1 and HIM-17 ChIP-seq signals. Analysis of ChIP-seq data by MACS and SPP produced remarkably strong overlap between GAK-1 and HIM-17 peaks (Figures 12 and 13B). Overall, HIM-17 has less binding sites throughout the genome compared to GAK-1, but 70% of HIM-17 peaks are also enriched for GAK-1. Like GAK-1, HIM-17 is depleted on the X chromosome compared to autosomes by immunofluorescence and by ChIP-seq; however, the few peaks that are found on the X do not correlate well between the two data sets (Figures 9C and 12A, bottom panel). Reciprocal localization experiments show that HIM-17 and GAK-1 are not required for each other's localization (data not shown).

Surprisingly, when I looked at the distribution of ChIP regions across the *C. elegans* genome, both GAK-1 and HIM-17 were enriched at transcription start sites (Figures 14A and 14B). Input samples are known to have sequencing biases, depending on the sequencing platform and methods used for shearing the DNA (Kharchenko et al., 2008). Rather than having an even distribution of sequenced tags across the genome, certain regions are over- and under-represented. The bias for the input sample in this study is enrichment in gene bodies compared to promoter regions (Figure 14B, right panel); thus, enrichment of ChIP-seq signals at promoters must be quite significant to be detectable. Roughly 40% of HIM-17 and GAK-1 peaks are found within promoter regions (Figure 14A). Germline-enriched genes are known to be depleted from the X chromosome (Reinke et al., 2004). Taking this into account and that GAK-1 and HIM-17 are depleted from the X, I wondered whether these two chromatin-bound proteins were preferentially binding to promoters of germline-enriched genes.

By scanning the *C. elegans* genome for ChIP-seq signals at known meiotic genes, it is apparent that GAK-1 and/or HIM-17 peaks are found within the promoter regions of many meiotic genes, including the *him-8/zim* operon (Figure 14C). GAK-1 and/or HIM-17 signal is found at the promoters of many synaptonemal complex components (e.g., *syp-1*, *syp-2*, *syp-3*, *htp-1*, *htp-2*, and *htp-3*), genes involved in the recombination pathway (e.g., *spo-11*, *msh-5*, *rad-51*, *rad-54*, and *zhp-3*), and nuclear envelope patch components (e.g., *zyg-12* and *sun-1*) that aggregate in transition zone nuclei and facilitate pairing and synapsis (Alpi et al., 2003; Colaiacovo et al., 2003; Couteau and Zetka, 2005; Dernburg et al., 1998; Goodyer et al., 2008; Jantsch et al., 2004; Kelly et al., 2000; MacQueen et al., 2002; Martinez-Perez and Villeneuve, 2005; Mets and Meyer, 2009; Sato et al., 2009; Smolikov et al., 2007). GAK-1 is also found at its own gene promoter. Statistical analysis of ChIP-seq data will need to be performed to

determine whether GAK-1 and HIM-17 are in fact preferentially at the promoters of germline-expressed genes.

Since GAK-1 has AT-hook motifs, which are known to bind AT-rich regions, I used MDscan to see if GAK-1 peaks were enriched for an AT-rich motif (Liu et al., 2002). Surprisingly, MDscan did not identify an AT-rich sequence, but there was a high-scoring motif (score of 7.304) that was enriched at GAK-1 peaks (Figure 14E). The 15 bp sequence (TCTCACCACGATGGG) appears to repeat on itself. Incidentally, HIM-17 had a different motif, even though it is enriched at GAK-1 peaks. The HIM-17 11 bp motif TTAAAGGCGCA was also very strong with a score of 7.908.

R06F6.12 is a GAK-1 interactor that may also have a meiotic defect

Sara Jover-Gil, the postdoctoral fellow in my lab who previously worked on *gak-1*, carried out a yeast two-hybrid screen to find interacting proteins. An uncharacterized gene, *R06F6.12* was one of the interactors identified. The protein contains no known domains and is conserved only among other *Caenorhabditis* species and *Pristionchus pacificus*. A deletion allele of this gene, *tm1499*, was obtained from the Japanese knockout consortium (Figure 15A). Initial characterization of the germline in *tm1499* animals revealed an obvious defect in meiosis. The majority of diakinesis nuclei in *tm1499* mutants had more than six DAPI-stained bodies, indicating that some homolog pairs were not undergoing crossover recombination (Figure 15B). The *R06F6.12(tm1499)* mutant initially showed a very strong synapsis defect, which was monitored by HTP-3 and SYP-1 staining (Figure 15C, center panel). Many nuclei contained some chromosomes that did not load the central element SYP-1, indicating a synapsis defect. After the strain was extensively outcrossed to wild type to remove irrelevant mutations, this defect disappeared (Figure 15C, right panel). This outcrossed strain does have a smaller brood size than wild type (data not shown).

An antibody was made to R06F6.12, and it localizes to chromatin throughout the germline (Figure 16). The antibody appears to be specific for the target protein, as it is undetectable in mutant animals (data not shown).

Discussion

GAK-1's role in the distribution of crossovers

Preliminary unpublished results from J. Yanowitz's lab indicated that *gak-1* mutations lead to a reduction of crossover interference, but two results in this current study argue against that. First, cytological markers for recombination, MSH-5 and ZHP-3, were used to show that *gak-1* mutants still have the expected six crossovers per nucleus. Using SNP markers as a more direct genetic assay to monitor crossovers, *gak-1* mutants again exhibit six crossovers per meiosis. While other mutations lead to double crossovers, which are not detectable cytologically by ZHP-3 (Youds et al., 2010), the genetic SNP assay directly looks at double crossovers and is more conclusive. Therefore, *gak-1* does not seem to play an obvious role in crossover interference.

Further analysis is currently being done to determine whether the distribution of crossovers in *gak-1* mutants is also altered. *C. elegans* has a specific distribution of crossovers such that exchanges are suppressed at the gene-rich center of chromosomes and are elevated on chromosome arms (Barnes et al., 1995; Rockman and Kruglyak, 2009). SC disassembly along a

bivalent is dictated by the location of the obligate crossover (Martinez-Perez et al., 2008); thus, if the distribution of crossovers is altered in *gak-1* mutants, it could potentially contribute to the SC disassembly defect that was observed in *gak-1* mutants.

Mutations in *gak-1* result in an increase in RAD-51 foci

When I looked at an early step in recombination, *gak-1* mutants displayed a defect. Compared to wild type animals, mutations in *gak-1* on average lead to more RAD-51 foci per nucleus. Currently, counting RAD-51 foci is the best available method for quantifying double-strand breaks; however, there are caveats to this assay, since an increase in RAD-51 foci could mean that more DSBs are made or it could imply that breaks are simply delayed in being repaired (Mets and Meyer, 2009). Since RAD-51 foci clear in a timely manner in *gak-1* mutants (actually even faster than in wild type), it is possible that more breaks are being made in the mutant.

I tried to form a more definitive conclusion by quantifying RAD-51 foci in the *rad-54* background where RAD-51-bound DSBs are "trapped." Theoretically, in this mutant, an absolute number of DSBs can be quantified, since breaks are prevented from being repaired (Mets and Meyer, 2009). To my surprise, I saw an increase in RAD-51 foci in *rad-54* mutants compared to what Mets et al. and others have reported (Youds et al., 2010). It was thought that on average roughly twelve DSBs were made per nucleus. Because each homolog pair experiences one crossover, the RAD-51 data in *rad-54* mutants implied that half the breaks are shunted down the noncrossover pathway. In my analysis, I frequently saw upwards of 20 RAD-51 foci in *rad-54* single mutants, which indicates that well over 12 breaks are made per nucleus. This result needs to be confirmed, as a different antibody was used in this study. I have not yet quantified the results in *rad-54* single mutants versus *rad-54;gak-1* double mutants, but the preliminary raw data seem to indicate that *rad-54;gak-1* mutants have an elevated number of RAD-51 foci. If it turns out that *gak-1* mutants do make more DSBs, it is still difficult to rectify how an increase in DSBs alone could result in such a strong meiotic phenotype.

The finding that GAK-1 correlates so strongly with HIM-17 enrichment in the genome provides indication that GAK-1 may be playing a role in recombination. HIM-17 is a meiosis-specific protein that is required for proper accumulation of H3diMeK9, a marker for heterochromatin and other transcriptionally inactive DNA, on chromosomes in the germline (Reddy and Villeneuve, 2004). Reddy et al. present a model whereby HIM-17 makes chromosomes more condensed, which makes them competent for DSB induction. Further analysis needs to be done to determine GAK-1's role in DSB formation, but it is possible that it plays an opposing role to HIM-17 and that it restricts the number of DSBs made on meiotic chromosomes. Perhaps HIM-17 and GAK-1 balance each other to regulate DSB formation, such that neither too many nor too few DSBs are made. Analysis of the *him-17;gak-1* double mutant will provide more insight on this.

GAK-1 and HIM-17 overlap at sites of transcription initiation

It is curious that both GAK-1 and HIM-17 are highly enriched in promoters. Further analysis showed that GAK-1 and HIM-17 peaks are found at many meiosis-specific gene promoters. Careful statistical analysis remains to be done to determine whether these proteins are overrepresented at germline-enriched genes compared to somatically-expressed genes. If they are in fact at germline gene promoters, I favor the idea that GAK-1 and HIM-17 function as transcription factors during meiosis to control gene expression of key meiotic players. This

hypothesis could also account for why both proteins are enriched on autosomes compared to the X chromosome, as previous studies have shown that germline-enriched genes are conspicuously underrepresented on the X (Reinke et al., 2004).

Many proteins that contain the AT-hook motif play roles in gene regulation (Aravind and Landsman, 1998); though, curiously, the consensus site that GAK-1 (which is proposed to have two AT-hook motifs) binds to is not AT-rich. Thus, it is unclear whether GAK-1 does in fact have functional AT-hooks. What is just as surprising is that while GAK-1 and HIM-17 share enrichment sites within the genome, MDscan identified different DNA-binding motifs for the two proteins. HIM-17, itself, contains six internal repeats of the THAP domain, which is thought to be a DNA-binding motif (Clouaire et al., 2005). This domain consists of a C_2CH module that has zinc-dependent DNA-binding activity. It is found only in animals and was first identified as the site-specific DNA-binding motif within the *Drosophila* P element transposase (Lee et al., 1998). Recently, DmTHAP from the P element transposase was co-crystallized with its natural 10 bp binding-site (Sabogal et al., 2010). Sabogal et al. performed binding site assays and identified a consensus binding sequence for DmTHAP and hTHAP1: TXXGGGXA/T, which is different from the TTAAAGGCGCA motif found at HIM-17 binding sites. Further analysis will need to be done to confirm GAK-1 and HIM-17 motifs and to look at their coincidence at enrichment sites. Preliminary scans show that both motifs are at least occasionally found near each other.

R06F6.12 is another chromatin-binding factor that is germline-enriched

Preliminary data indicated that the *R06F6.12* gene played a role in meiosis, as the mutant displayed a strong synapsis defect. Subsequent outcrossing to wild type animals resulted in a loss of this phenotype; though, a smaller brood size was still observed in this mutant. The *R06F6.12(tm1499)* mutation was generated by random mutagenesis with TMP/UV (Gengyo-Ando and Mitani, 2000); thus, a likely explanation is that it contained a background mutation that just happened to affect synapsis. Trying to isolate the background mutation would be worthwhile, as the synapsis defect was interesting.

Concluding remarks—*gak-1* has pleiotropic effects in meiosis

The *gak-1* gene plays a subtle role in various stages of meiosis, including synapsis and recombination. Experiments are underway to distinguish whether the DNA damage and/or synapsis checkpoint is activated in *gak-1* mutants (Bhalla and Dernburg, 2005; Gartner et al., 2000). This could help in identifying what the critical function of *gak-1* is in meiosis—whether its targets are synapsis-related and/or recombination-related. The range of defects, including SC maintenance, improper SC disassembly, and elevated RAD-51 foci may be independently controlled by *gak-1*; however, individually, they cannot account for the Him phenotype or high levels of embryonic lethality. An alternative explanation could be that *gak-1* plays an indirect role in all these processes by functioning as a transcription factor for other meiosis-specific genes that govern these processes. If this is true, many other subtle phenotypes not detected in the assays described here could also contribute to the high levels of nondisjunction in *gak-1* mutants. Further analysis remains to be done to determine if GAK-1 is significantly enriched at germline gene promoters compared to promoters of somatically-expressed genes. If this is the case, subsequent experiments will need to be done to look at *gak-1*'s effect on transcript levels.

Materials and methods

Genetics and strains

Unless otherwise indicated, the N2 Bristol strain was used as the wild type control. See Chapter 1 for details on handling strains. *gak-1(ok708)* and *gak-1(ok709)* were both maintained as balanced heterozygotes, using the *hT2* balancer. All experiments were done on homozygous mutant progeny, unless otherwise indicated. *fem-2(b245ts) III; axIs1442[ppie1::gfp:his-58: nos-2 M1 UTR unc-119+]* is a temperature-sensitive strain that is wild type at 15°C and fails to produce sperm at 23°C. It also expresses GFP::H2B in the germline. In the text, this strain is simply referred to as *fem-2*.

To generate *gak-1(ok708)* with Hawaiian SNPs in the background, *gak-1(ok708)* hermaphrodites were backcrossed to CB4856 males. Individual F1 cross-progeny were plated and allowed to self. F2s were picked to individual plates, and plates with ~25% males in the F3 generation were saved for the subsequent backcross. After 5 backcrosses, the presence of the *gak-1(ok708)* deletion was confirmed by PCR. The *hT2/+* balancer strain was independently backcrossed to CB4856. *hT2/+* hermaphrodites were mated to CB4856 males. *hT2/+* cross progeny males were backcrossed to CB4856 hermaphrodites. This was repeated 6 times. Hawaiianized *gak-1* males were mated to Hawaiianized *hT2/+* hermaphrodites to generate *gak-1/hT2* in a Hawaiian background.

Immunofluorescence, FISH, and microscopy

See Chapter 2 for detailed protocols. The *unc-119* probe was made by digesting the pMM051 plasmid (contains *unc-119* rescue construct) with the following enzymes for 2 hours at 37°C: AluI, HaeIII, MboI, MseI, MspI, and RsaI. The tailing and labeling reactions were done as previously described (Phillips et al., 2009). For embryo staining, ~50 non-age-matched wild type and mutant gravid hermaphrodites were dissected by cutting down the middle of the worm to release embryos in M9 on a glass cover slip. The cover slip was picked up with an inverted HistoBond slide and excess liquid was wicked away with absorbent paper. Samples were then freeze-cracked on an aluminum block on dry ice. The cover slip was removed with a razor blade and samples were then fixed in 100% MeOH for 30 minutes at -20°C. Samples were washed three times in PBST and then taken through the immunofluorescence protocol described in Chapter 1. Tubulin staining was done with anti-Tubulin (Sigma, catalog #T9026) at 1:500.

Antibodies

The Rb0813 GAK-1 antibody was made against the following peptide by SDI: LIVDDDDETDS PPASSSNYEPKAHIGWASFGDSCLPPPPKPVKKATDPNLPRRKVYVIRSQNTDKSKSPLV VNNQQVTLEKAQNSPKNPNPVVSKPIVLT. Rb0813 was used primarily for immunofluorescence experiments. The Rb3179 and Rb3161 GAK-1 antibodies were made against the following peptide by SDI: RDIFRNSYDSDEEEFLRSRYQRAVTPPPILERQSGST RESVSEPSEGKILEEDATLGSEHTERVGKRIELEEINPSQLLRTKISASAIPILPLSKSIMER. Three ChIP replicate experiments were performed using all three anti-GAK-1 antibodies: Rb0813, Rb3179, and Rb3161. All subsequent analysis was done using data from the Rb3179 ChIP experiment. The R06F6.12 antibody was made against the following peptide by SDI: EAGKSTRSPIIGETVQIRTADGRLQDAVVKYVRGDSEYKIQLMNGEFAYATIDQMLVPQ RDRSDHEYQQVAPPVLLRRTDMASVRNAAQKRSANDDLCPP.

Scoring of pairing and synapsis

Pairing of chromosome V was scored in the transition zone of three animals of each genotype using ZIM-2 staining. The region of the gonad with ZIM-2 signal was divided into 4 equal regions, and a time course of pairing was done. Nuclei with one ZIM-2 focus were assessed as having paired chromosome Vs, while two foci indicated unpaired chromosome Vs. Similarly HIM-8 staining was used to assess pairing of the X chromosome in nuclei at the late-pachytene stage. Roughly 30-50 nuclei from three animals of each genotype were scored for HIM-8 pairing. Nuclei containing one HIM-8 focus were considered to have paired X chromosomes.

Cytological scoring of crossovers

To determine whether each homolog pair had undergone at least one crossover, DAPI-stained bodies were counted at the diakinesis stage using the Deltavision deconvolution microscopy system. One hundred nuclei of each genotype were scored, with data being taken from ~50 animals of each genotype.

To determine the number of crossovers occurring, the number of colocalized MSH-5/ZHP-3 foci was quantified in each nucleus. This quantification was done using nuclei at late pachytene where ZHP-3 had ceased to appear as stretches and was only forming foci. One hundred seventy five to 200 nuclei of each genotype were scored, with data being compiled from between 4 to 8 animals of each genotype.

Cosuppression experiments

Forward and reverse primers for the *gak-1* cosuppression construct were: ggcgagacgagacatctagg and taacaaatgtggggtcaacg, which amplifies the entire *gak-1* gene, as well as 659 bp upstream of the start codon. EG4322 *unc-119* animals were aged 20-24 hours post L4 stage at 20°C and were microinjected with pMM051 (*unc-119* rescuing vector) at a final concentration of 50 ng/µl and the *gak-1* cosuppression construct at a final concentration of 100 ng/µl in injection buffer (20% PEG, 200 mM potassium phosphate, pH 7.5; 30 mM potassium citrate, pH 7.5). Injected animals were picked onto NGM plates and placed at 20°C to recover. NonUnc F1s were plated individually, and lines throwing nonUnc F2s were followed up on with immunofluorescence and male counts. Cosuppressed lines were maintained by mating nonUnc cosuppressed males to EG4322 hermaphrodites and by picking nonUnc hermaphrodites for subsequent experiments and nonUnc males to continue maintenance of the cosuppressed line.

ChIP-seq experiments

An asynchronous population of *fem-2(b245ts) III; axIs1442[ppie1::gfp:his-58: nos-2 M1 UTR unc-119+]* worms was grown up in liquid culture at the permissive temperature of 15°C. A synchronized population was obtained by bleaching gravid hermaphrodites and allowing embryos to hatch without food until the L1 stage. Synchronized L1s were grown up in liquid culture at the restrictive temperature of 23°C and harvested as adults. Harvested adults were washed several times with M9/S basal, and a 30% sucrose float was done to recover only adults. After several more M9/S basal washes, worms were spun down and resuspended 50:50 in a buffer of 50 mM HEPES, pH 7.5, 1 mM EGTA, 1 mM $MgCl_2$, 100 mM KCl, 10% glycerol plus Roche protease inhibitor tablets. This 50:50 suspension of worms to buffer was pipetted small drops at a time into liquid nitrogen to form "worm popcorn" that was stored at -80°C.

To prepare lysates for ChIP, worm popcorn was first ground up using the Mixermill MM 400 (Retsch, Haan, Germany) until worms were broken into at least 3 or 4 parts. As soon as ground-up worms reached 4°C, the mixture was immediately resuspended in PBS with 1% formaldehyde. Samples were fixed on a nutator for 10 minutes at room temperature. The reaction was quenched with 125 mM glycine. Samples were washed in PBS and resuspended in FA buffer (50 mM HEPES, pH 7.5, 1 mM EDTA, 1% Triton, 0.1% sodium deoxycholate, 150 mM NaCl, plus protease and phosphatase inhibitors) with 0.5% SDS. Fixed samples were sonicated for 34 cycles of 30 sec on/1 min off at 4°C in a Bioruptor (Diagenode). The sonicated sample was centrifuged at 13,200 rpm in a microfuge, and the soluble portion was saved for subsequent ChIP experiments.

Worm lysate containing ~1.3mg of protein was pre-cleared with Protein G Dynabeads (Invitrogen) for 2 hours at 4°C. Concurrently, 40ul of Protein G Dynabeads were blocked with 20ug of BSA and 20ug of salmon sperm DNA in FA buffer (50 mM HEPES pH 7.5, 1 mM EDTA, 1% Triton, 0.1% sodium deoxycholate, 150 mM NaCl, plus protease and phosphatase inhibitors) for 2 hours at 4°C. The pre-cleared lysate was then incubated with 5 µg of affinity-purified antibody for 2 hours at 4°C. The beads were washed as follows at room temperature: 2x with FA buffer, 1x with FA buffer with 500 mM NaCl, 1x with FA buffer with 1M NaCl, 1x with TEL buffer (10 mM Tris, pH 8, 1 mM EDTA, 250 mM LiCl, 1% NP-40, 1% sodium deoxycholate, plus protease and phosphatase inhibitors), and 2x with TE pH 8. ChIP samples were eluted in TE with 1% SDS and 250 mM NaCl at 65°C. ChIP and input samples were treated with RNAse A, and crosslinking was reversed by incubating overnight with Proteinase K at 65°C. Libraries for sequencing were made from DNA from ChIP experiments using the Illumina ChIP-seq DNA Sample Prep Kit (Illumina, catalog # IP-102-1001). Sequencing was done at the Vincent J. Coates Genomics Sequencing Laboratory (University of California, Berkeley) on the Genome AnalyzerIIe (Illumina, San Diego, CA). Sequencing data was processed using MACS or SPP (Kharchenko et al., 2008; Zhang et al. 2008).

Recombination Assay

To generate *gak-1(ok708)* animals that were heterozygous for Hawaiian and N2 Bristol SNPs, *gak-1/hT2* hermaphrodites (carrying N2 SNPs) were mated to Hawaiianized *gak-1/hT2* males. Individual *gak-1* homozygote F1 males were mated to individual CB4856 hermaphrodites to assess recombination in *gak-1* males. Individual F2s were plated. Concurrently, individual *gak-1* homozygote F1 hermaphrodites were mated to CB4856 males to assess recombination in *gak-1* hermaphrodites. Individual F2s were plated. F2s that threw males in the first generation were discarded, as they were assessed to be self-progeny, instead of the desired cross-progeny. F2 cross-progeny were left to self for multiple generations until the plates starved. Within one day of starvation, the DNA isolation protocol was started. The DNA isolation protocol is based on a protocol communicated by Matthew Rockman (NYU). Starved worms were washed off plates with TNES (50 mM Tris-HCl (pH 8.0), 20 mM 0.5M EDTA (pH 8.0), 400 mM NaCl, 0.5% SDS, 1 mg/ml proteinase K). Samples were placed at -80°C for at least one hour, followed by an overnight incubation at 55°C. Another 400 µg of proteinase K was added, followed by a 2 hour 55°C incubation. Samples were placed at 95°C to inactivate proteinase K or were directly treated with 800 µg of RNAse A. NaCl was added to a final concentration of 1.3 M to precipitate out proteins. The precipitate was spun out, and the supernatant was taken through a standard EtOH precipitation to isolate DNA. Samples were re-suspended in TE and were quantified using PicoGreen (Invitrogen) or a spectrophotometer.

Samples were normalized to 50 ng/µl and were sent to the University of California, Davis Genome Center for the GoldenGate BeadXpress genotyping assay (Illumina). Genotyping results were analyzed using the Illumina GenomeStudio software.

References

Alpi, A., Pasierbek, P., Gartner, A., and Loidl, J. (2003). Genetic and cytological characterization of the recombination protein RAD-51 in Caenorhabditis elegans. Chromosoma *112*, 6-16.

Aravind, L., and Landsman, D. (1998). AT-hook motifs identified in a wide variety of DNA-binding proteins. Nucleic Acids Res *26*, 4413-4421.

Barnes, T.M., Kohara, Y., Coulson, A., and Hekimi, S. (1995). Meiotic recombination, noncoding DNA and genomic organization in Caenorhabditis elegans. Genetics *141*, 159-179.

Bhalla, N., and Dernburg, A.F. (2005). A conserved checkpoint monitors meiotic chromosome synapsis in Caenorhabditis elegans. Science *310*, 1683-1686.

Bhalla, N., Wynne, D.J., Jantsch, V., and Dernburg, A.F. (2008). ZHP-3 acts at crossovers to couple meiotic recombination with synaptonemal complex disassembly and bivalent formation in C. elegans. PLoS Genet *4*, e1000235.

Boulton, S.J., Martin, J.S., Polanowska, J., Hill, D.E., Gartner, A., and Vidal, M. (2004). BRCA1/BARD1 orthologs required for DNA repair in Caenorhabditis elegans. Curr Biol *14*, 33-39.

Carlton, P.M., Farruggio, A.P., and Dernburg, A.F. (2006). A link between meiotic prophase progression and crossover control. PLoS Genet *2*, e12.

Clouaire, T., Roussigne, M., Ecochard, V., Mathe, C., Amalric, F., and Girard, J.P. (2005). The THAP domain of THAP1 is a large C2CH module with zinc-dependent sequence-specific DNA-binding activity. Proc Natl Acad Sci U S A *102*, 6907-6912.

Colaiacovo, M.P., MacQueen, A.J., Martinez-Perez, E., McDonald, K., Adamo, A., La Volpe, A., and Villeneuve, A.M. (2003). Synaptonemal complex assembly in C. elegans is dispensable for loading strand-exchange proteins but critical for proper completion of recombination. Dev Cell *5*, 463-474.

Couteau, F., and Zetka, M. (2005). HTP-1 coordinates synaptonemal complex assembly with homolog alignment during meiosis in C. elegans. Genes Dev *19*, 2744-2756.

Dernburg, A.F., McDonald, K., Moulder, G., Barstead, R., Dresser, M., and Villeneuve, A.M. (1998). Meiotic recombination in C. elegans initiates by a conserved mechanism and is dispensable for homologous chromosome synapsis. Cell *94*, 387-398.

Dernburg, A.F., Zalevsky, J., Colaiacovo, M.P., and Villeneuve, A.M. (2000). Transgene-mediated cosuppression in the C. elegans germ line. Genes Dev *14*, 1578-1583.

Falvo, J.V., Thanos, D., and Maniatis, T. (1995). Reversal of intrinsic DNA bends in the IFN beta gene enhancer by transcription factors and the architectural protein HMG I(Y). Cell *83*, 1101-1111.

Gartner, A., Milstein, S., Ahmed, S., Hodgkin, J., and Hengartner, M.O. (2000). A conserved checkpoint pathway mediates DNA damage--induced apoptosis and cell cycle arrest in C. elegans. Mol Cell *5*, 435-443.

Gengyo-Ando, K., and Mitani, S. (2000). Characterization of mutations induced by ethyl methanesulfonate, UV, and trimethylpsoralen in the nematode Caenorhabditis elegans. Biochem Biophys Res Commun *269*, 64-69.

Goodyer, W., Kaitna, S., Couteau, F., Ward, J.D., Boulton, S.J., and Zetka, M. (2008). HTP-3 links DSB formation with homolog pairing and crossing over during C. elegans meiosis. Dev Cell *14*, 263-274.

Gumienny, T.L., Lambie, E., Hartwieg, E., Horvitz, H.R., and Hengartner, M.O. (1999). Genetic control of programmed cell death in the Caenorhabditis elegans hermaphrodite germline. Development *126*, 1011-1022.
Hillers, K.J. (2004). Crossover interference. Curr Biol *14*, R1036-1037.
Hillers, K.J., and Villeneuve, A.M. (2003). Chromosome-wide control of meiotic crossing over in C. elegans. Curr Biol *13*, 1641-1647.
Hodgkin, J., Horvitz, H.R., and Brenner, S. (1979). Nondisjunction Mutants of the Nematode CAENORHABDITIS ELEGANS. Genetics *91*, 67-94.
Jantsch, V., Pasierbek, P., Mueller, M.M., Schweizer, D., Jantsch, M., and Loidl, J. (2004). Targeted gene knockout reveals a role in meiotic recombination for ZHP-3, a Zip3-related protein in Caenorhabditis elegans. Mol Cell Biol *24*, 7998-8006.
Kelly, K.O., Dernburg, A.F., Stanfield, G.M., and Villeneuve, A.M. (2000). Caenorhabditis elegans msh-5 is required for both normal and radiation-induced meiotic crossing over but not for completion of meiosis. Genetics *156*, 617-630.
Kharchenko, P.V., Tolstorukov, M.Y., and Park, P.J. (2008). Design and analysis of ChIP-seq experiments for DNA-binding proteins. Nat Biotechnol *26*, 1351-1359.
Kuervers, L.M., Janke, D.L., and Baillie, D.L. (1998). Overexpression of a novel protein causes chromosome nondisjunction in Caenorhabditis elegans. Worm Breeder's Gazette *15*, 24.
Lee, C.C., Beall, E.L., and Rio, D.C. (1998). DNA binding by the KP repressor protein inhibits P-element transposase activity in vitro. EMBO J *17*, 4166-4174.
Liu, X.S., Brutlag, D.L., and Liu, J.S. (2002). An algorithm for finding protein-DNA binding sites with applications to chromatin-immunoprecipitation microarray experiments. Nat Biotechnol *20*, 835-839.
MacQueen, A.J., Colaiacovo, M.P., McDonald, K., and Villeneuve, A.M. (2002). Synapsis-dependent and -independent mechanisms stabilize homolog pairing during meiotic prophase in C. elegans. Genes Dev *16*, 2428-2442.
Martinez-Perez, E., Schvarzstein, M., Barroso, C., Lightfoot, J., Dernburg, A.F., and Villeneuve, A.M. (2008). Crossovers trigger a remodeling of meiotic chromosome axis composition that is linked to two-step loss of sister chromatid cohesion. Genes Dev *22*, 2886-2901.
Martinez-Perez, E., and Villeneuve, A.M. (2005). HTP-1-dependent constraints coordinate homolog pairing and synapsis and promote chiasma formation during C. elegans meiosis. Genes Dev *19*, 2727-2743.
Mets, D.G., and Meyer, B.J. (2009). Condensins regulate meiotic DNA break distribution, thus crossover frequency, by controlling chromosome structure. Cell *139*, 73-86.
Neale, M.J., and Keeney, S. (2006). Clarifying the mechanics of DNA strand exchange in meiotic recombination. Nature *442*, 153-158.
Phillips, C.M., and Dernburg, A.F. (2006). A family of zinc-finger proteins is required for chromosome-specific pairing and synapsis during meiosis in C. elegans. Dev Cell *11*, 817-829.
Phillips, C.M., McDonald, K.L., and Dernburg, A.F. (2009). Cytological analysis of meiosis in Caenorhabditis elegans. Methods Mol Biol *558*, 171-195.
Phillips, C.M., Wong, C., Bhalla, N., Carlton, P.M., Weiser, P., Meneely, P.M., and Dernburg, A.F. (2005). HIM-8 binds to the X chromosome pairing center and mediates chromosome-specific meiotic synapsis. Cell *123*, 1051-1063.
Reddy, K.C., and Villeneuve, A.M. (2004). C. elegans HIM-17 links chromatin modification and competence for initiation of meiotic recombination. Cell *118*, 439-452.

Reeves, R., and Nissen, M.S. (1990). The A.T-DNA-binding domain of mammalian high mobility group I chromosomal proteins. A novel peptide motif for recognizing DNA structure. J Biol Chem *265*, 8573-8582.
Reinke, V., Gil, I.S., Ward, S., and Kazmer, K. (2004). Genome-wide germline-enriched and sex-biased expression profiles in Caenorhabditis elegans. Development *131*, 311-323.
Rockman, M.V., and Kruglyak, L. (2009). Recombinational landscape and population genomics of Caenorhabditis elegans. PLoS Genet *5*, e1000419.
Sabogal, A., Lyubimov, A.Y., Corn, J.E., Berger, J.M., and Rio, D.C. (2010). THAP proteins target specific DNA sites through bipartite recognition of adjacent major and minor grooves. Nat Struct Mol Biol *17*, 117-123.
Sato, A., Isaac, B., Phillips, C.M., Rillo, R., Carlton, P.M., Wynne, D.J., Kasad, R.A., and Dernburg, A.F. (2009). Cytoskeletal forces span the nuclear envelope to coordinate meiotic chromosome pairing and synapsis. Cell *139*, 907-919.
Smolikov, S., Eizinger, A., Schild-Prufert, K., Hurlburt, A., McDonald, K., Engebrecht, J., Villeneuve, A.M., and Colaiacovo, M.P. (2007). SYP-3 restricts synaptonemal complex assembly to bridge paired chromosome axes during meiosis in Caenorhabditis elegans. Genetics *176*, 2015-2025.
Strick, R., and Laemmli, U.K. (1995). SARs are cis DNA elements of chromosome dynamics: synthesis of a SAR repressor protein. Cell *83*, 1137-1148.
Tsai, C.J., Mets, D.G., Albrecht, M.R., Nix, P., Chan, A., and Meyer, B.J. (2008). Meiotic crossover number and distribution are regulated by a dosage compensation protein that resembles a condensin subunit. Genes Dev *22*, 194-211.
Youds, J.L., Mets, D.G., McIlwraith, M.J., Martin, J.S., Ward, J.D., NJ, O.N., Rose, A.M., West, S.C., Meyer, B.J., and Boulton, S.J. (2010). RTEL-1 enforces meiotic crossover interference and homeostasis. Science *327*, 1254-1258.
Zetka, M.C., and Rose, A.M. (1995). Mutant rec-1 eliminates the meiotic pattern of crossing over in Caenorhabditis elegans. Genetics *141*, 1339-1349.
Zhang, Y., Liu, T., Meyer, C.A., Eeckhoute, J., Johnson, D.S., Bernstein, B.E., Nussbaum, C., Myers, R.M., Brown, M., Li, W.*, et al.* (2008). Model-based analysis of ChIP-Seq (MACS). Genome Biol *9*, R137.

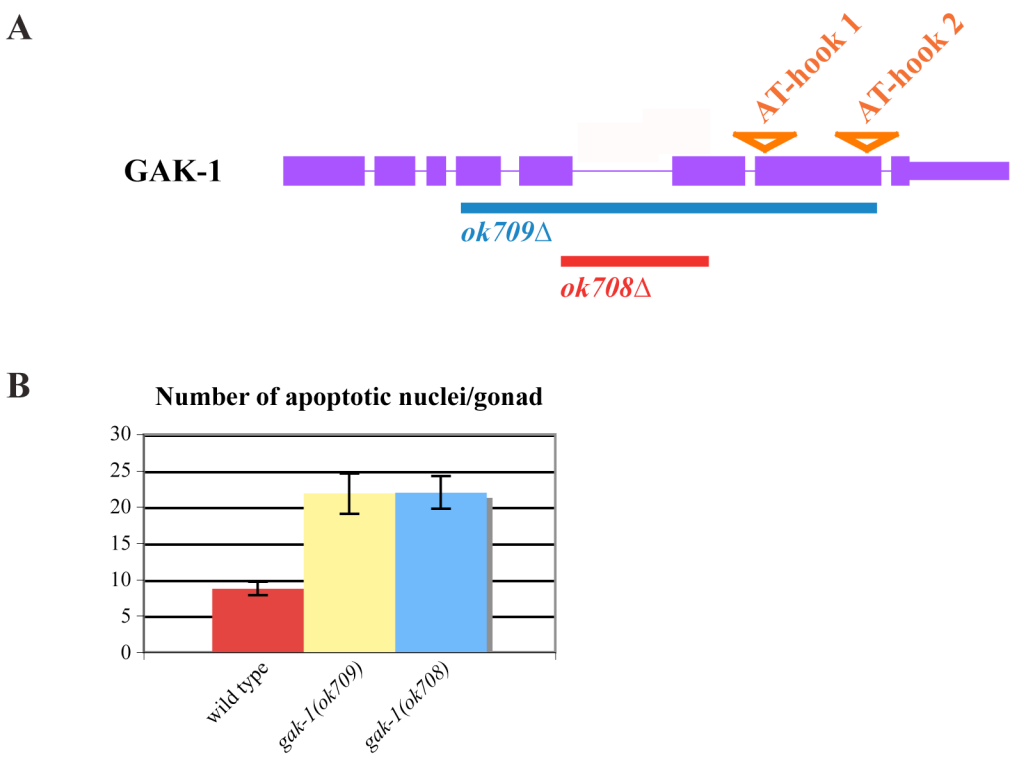

Figure 1: Mutations in *gak-1* lead to elevated levels of germline apoptosis.
(A) *gak-1* gene structure with location of mutations. *gak-1* contains two putative AT-hook domains. The *ok708* and *ok709* alleles are both deletion mutants. (B) Germline apoptosis was quantified in wild type and *gak-1* mutants using the CED-1::GFP marker. *gak-1* animals have elevated levels of apoptotic nuclei in the germline.

	Percent males	Percent dead eggs	n
N2	0.06	0.10	1755
gak-1(ok708)	25.40	76.90	940
gak-1(ok709)	23.45	84.33	517

Table 1: Phenotypes associated with aneuploidy are observed in *gak-1* mutants.
Quantification of embryonic lethality and male progeny in wild type (N2) and *gak-1* mutants. *gak-1* mutants exhibit high levels of embryonic lethality and a Him (High incidence of males) phenotype, which are indicative of aneuploidy of the autosomes and the X chromosome, respectively.

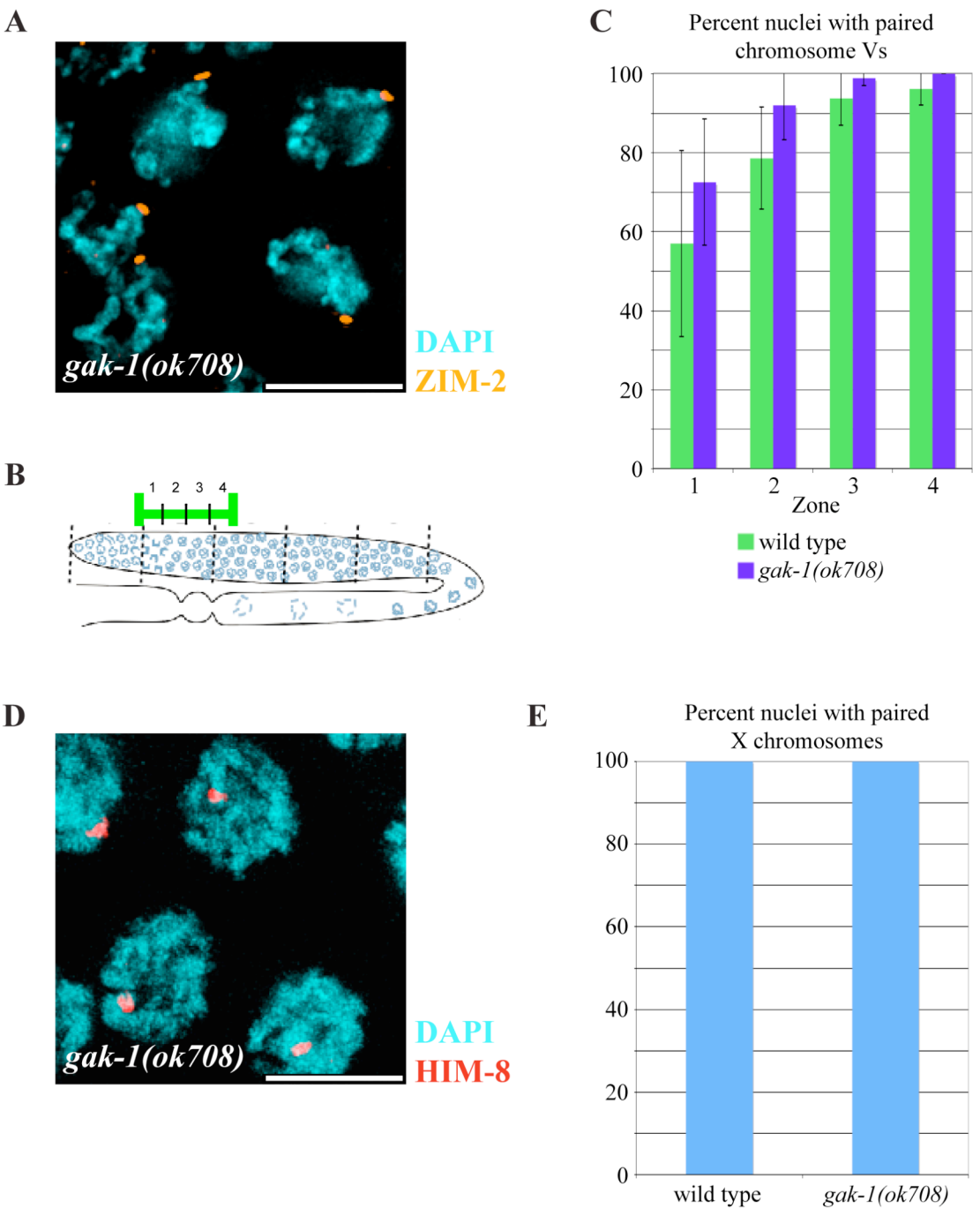

Figure 2: GAK-1 does not play a role in homolog pairing.
(A) Transition zone nuclei from a *gak-1(ok708)* mutant showing DAPI (DNA) in blue and ZIM-2 in orange. Scale bar is 5 µm. (B) Cartoon of the *C. elegans* gonad. For quantification of chromosome V pairing in (C), the region in the gonad where ZIM-2 is expressed (transition zone through early pachytene) was divided into four regions of equal length. (C) Quantification of chromosome V pairing in wild type and *gak-1(ok708)* mutants. Chromosome Vs were considered paired if ZIM-2 foci appeared as one and unpaired if two foci per nucleus were distinguishable. (D) Late pachytene nuclei from a *gak-1(ok708)* mutant showing DAPI (DNA) in blue and HIM-8 in red. Scale bar is 5 µm. (E) Quantification of X chromosome pairing in wild type and *gak-1(ok708)* mutants in pachytene. The X chromosomes were considered paired if HIM-8 foci appeared as one and unpaired if two foci per nucleus were distinguishable.

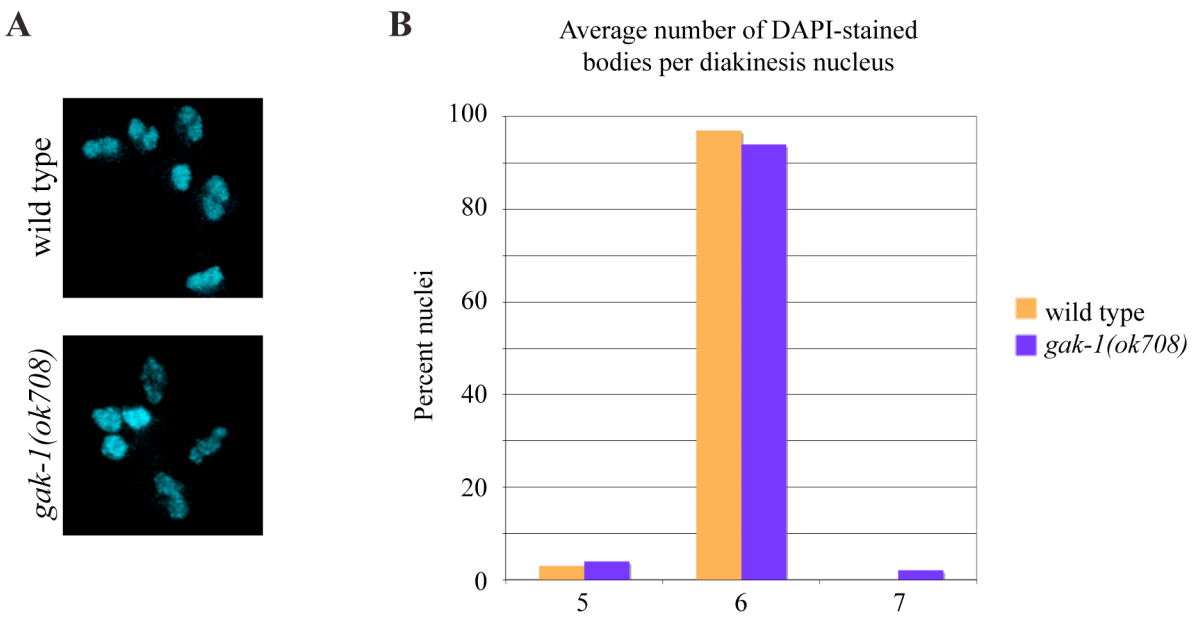

Figure 3: *gak-1* mutants form crossovers.
(A) Diakinesis nuclei from a wild type and a *gak-1(ok708)* animal showing DAPI (DNA) in blue. Wild type and *gak-1* nuclei contain 6 bivalent chromosomes. (B) Quantification of DAPI-stained bodies in diakinesis for wild type and *gak-1(ok708)* animals. *gak-1* mutants have mostly 6 DAPI-stained bodies, indicating that all 6 homolog pairs are undergoing crossovers.

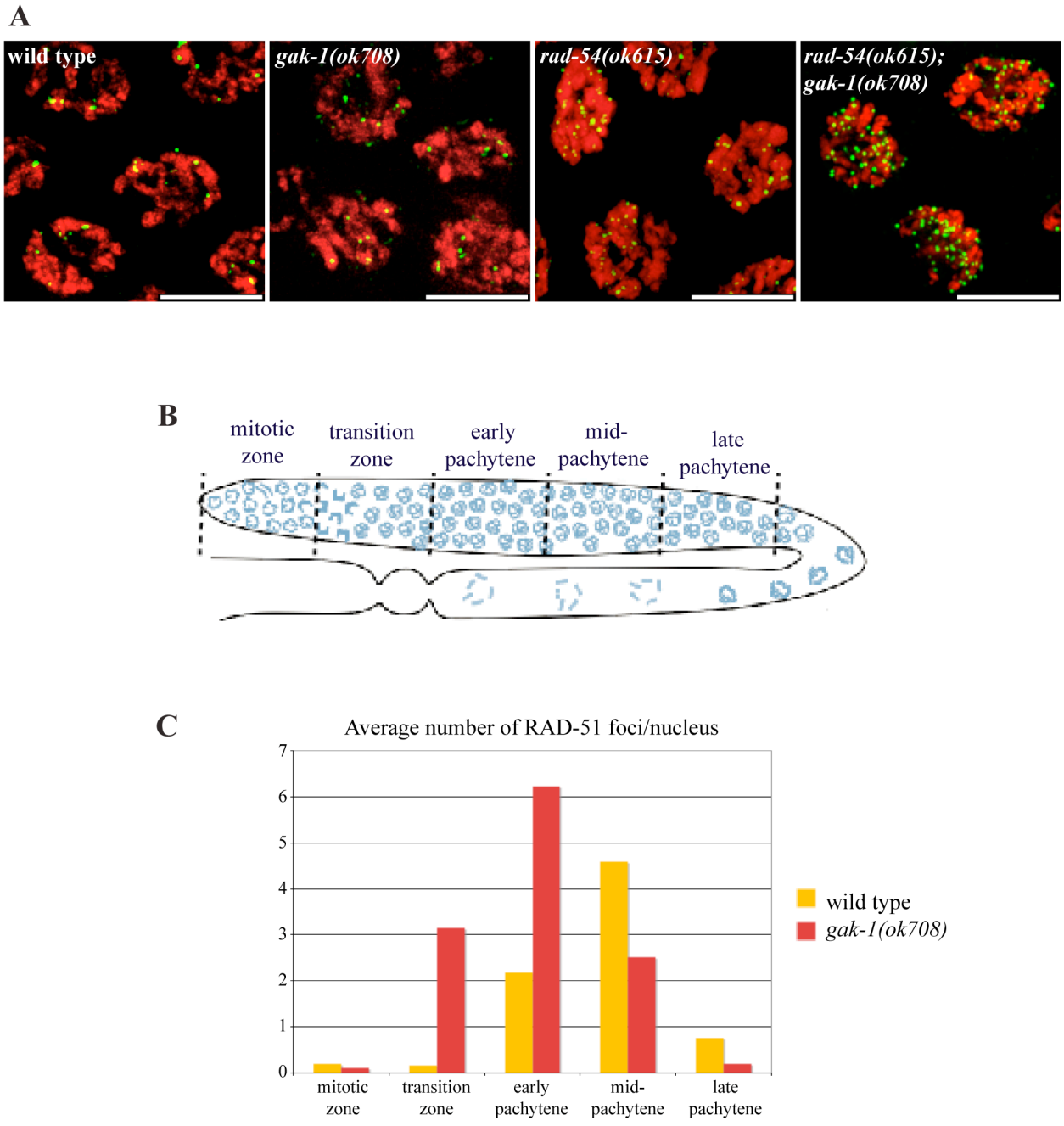

Figure 4: An elevated number of RAD-51 foci is observed in *gak-1* mutants.
(A) Pachytene nuclei from a wild type and mutant animals showing DAPI (DNA) in red and RAD-51 foci in green. Scale bars are 5 µm. (B) Cartoon of the *C. elegans* gonad. For quantification of RAD-51 foci in (C), the gonad was divided into five regions: the mitotic zone, the transition zone, early pachytene, mid-pachytene, and late pachytene. (C) Quantification of average number of RAD-51 foci per nucleus in wild type and *gak-1(ok708)* mutants.

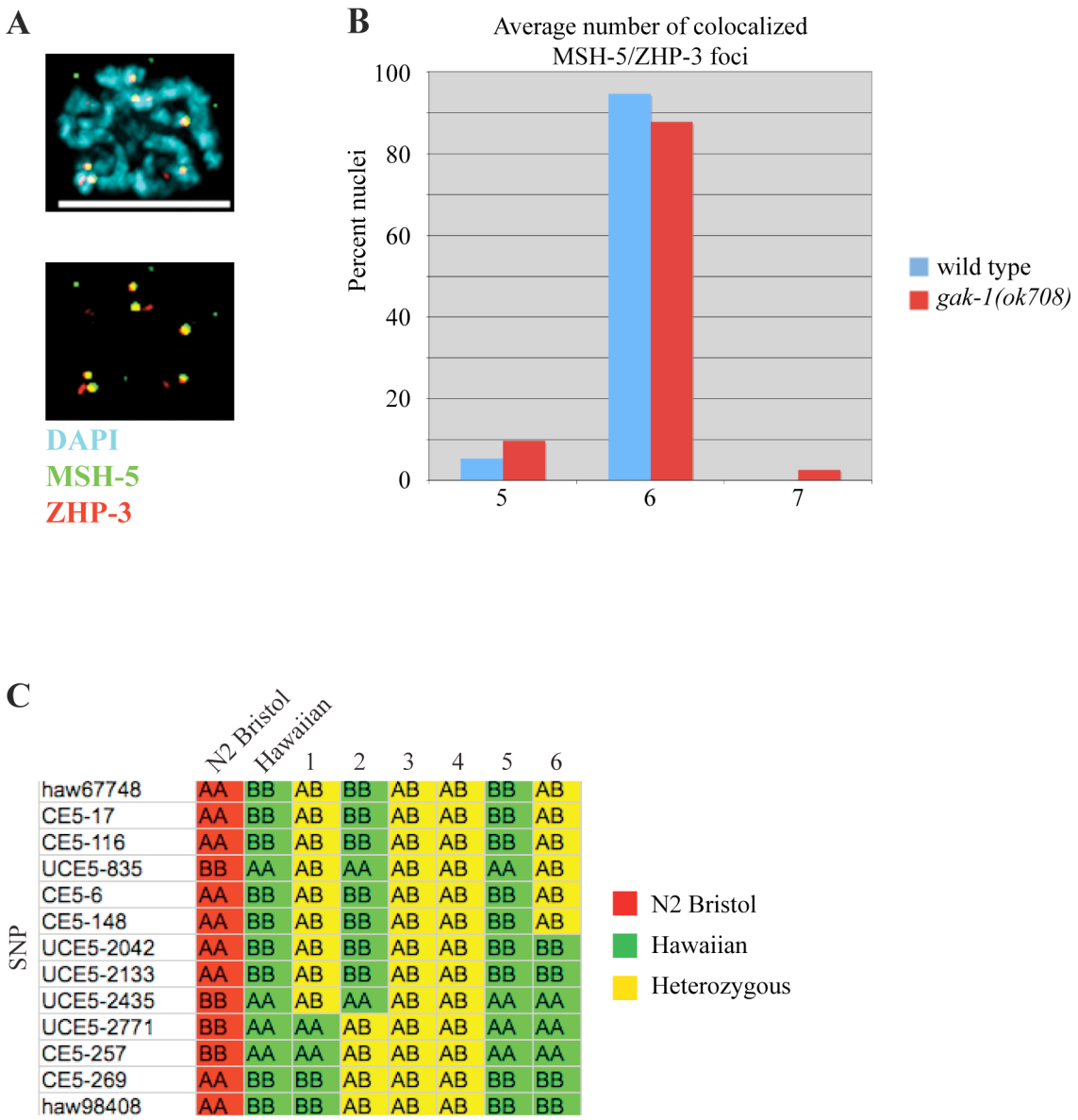

Figure 5: GAK-1 does not play a role in crossover interference.
(A) Diplotene nucleus from a wild type animal showing DAPI (DNA) in blue and markers for crossovers, MSH-5 (green) and ZHP-3 (red). Six MSH-5/ZHP-3 foci represent the single crossover that occurred on each bivalent. Scale bar is 5 µm. (B) Quantification of average number of MSH-5/ZHP-3 foci in diplotene nuclei in wild type and *gak-1* animals. Like wild type, *gak-1* mutants almost always have 6 ZHP-3/MSH-5 foci. (C) Sample genotyping data from recombination assay. The recombination assay was designed such that F2/F3 test samples should be either homozygous for the Hawaiian allele (shaded in green) or heterozygous (shaded in yellow) at each SNP, but not homozygous for the N2 allele (shaded in red). The first column indicates the SNPs tested on chromosome V in syntenic order. The second and third columns represent the N2 and Hawaiian genotypes at each SNP, respectively, while 1 through 6 represent the genotypes of test samples. Among test samples, half the chromosomes should be recombinant, and the other half should be non-recombinant. Samples 1, 2, and 6 have recombinant chromosome Vs, indicated by a switch from the heterozygous genotype to being homozygous for Hawaiian alleles.

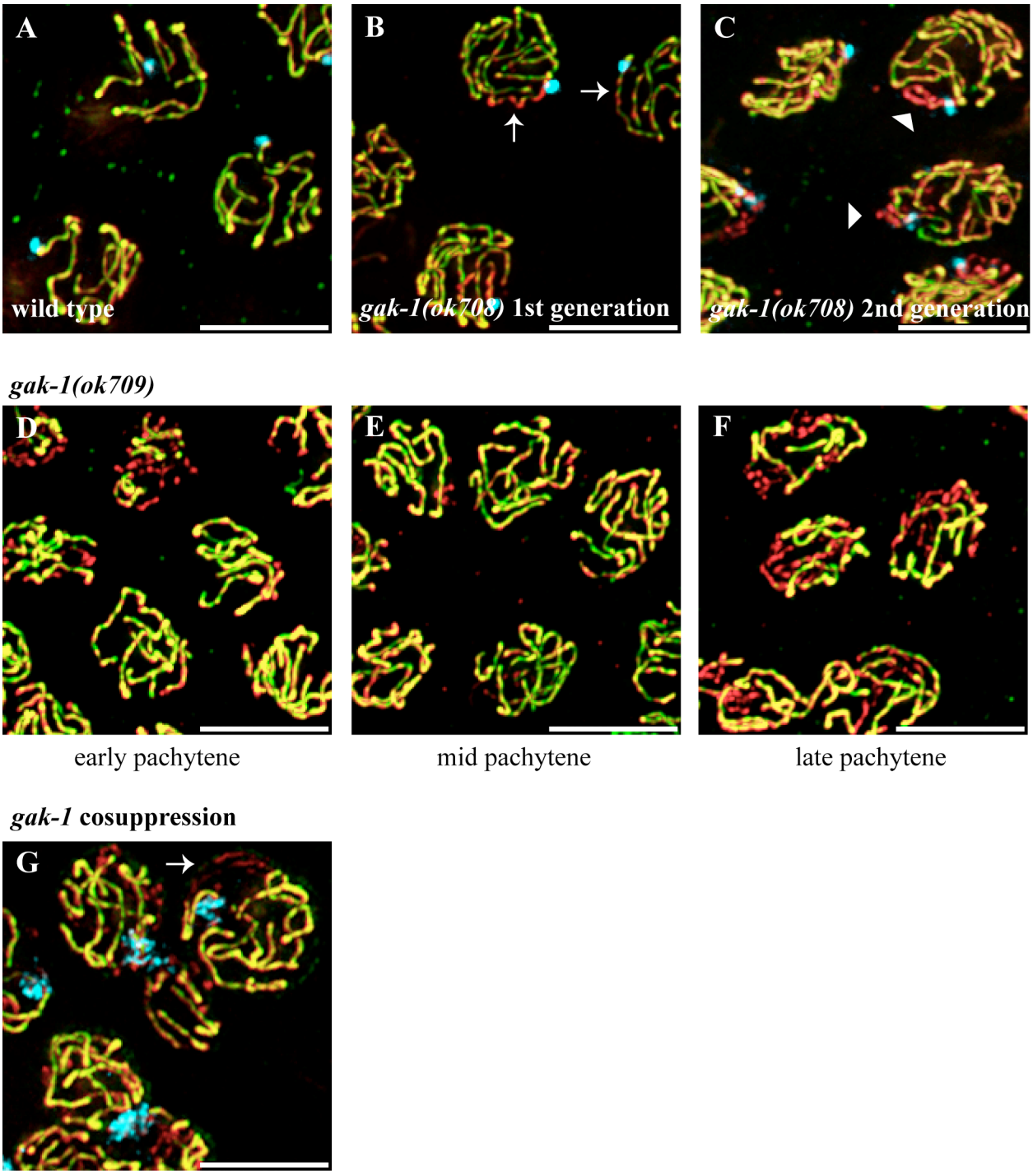

Figure 6: SC maintenance is defective in *gak-1* mutants.
(A-C) Late pachytene nuclei from wild type and *gak-1* mutants showing HIM-8 (blue) and the synaptonemal complex proteins HTP-3 (red) and SYP-1 (green). At late pachytene in *gak-1(ok708)* mutants, the X chromomsome occasionally has less SYP-1 loaded compared to HTP-3 (marked by arrows) or no SYP-1 loaded (marked by arrowheads). (D-F) Various stages of pachytene nuclei in a *gak-1(ok709)* mutant showing HTP-3 (red) and SYP-1 (green). In a subset of animals, there is a synapsis delay. In a subset of animals, SYP-1 falls off homolog pairs at the end of pachytene. (G) Late pachytene nuclei from *gak-1* cosuppression line showing HTP-3 in red, SYP-1 in green, and FISH probe to cosuppression array in blue. In addition to unsynapsed regions on the array, some chromosomal regions lack SYP-1 loading (marked by arrow). All scale bars are 5 μm.

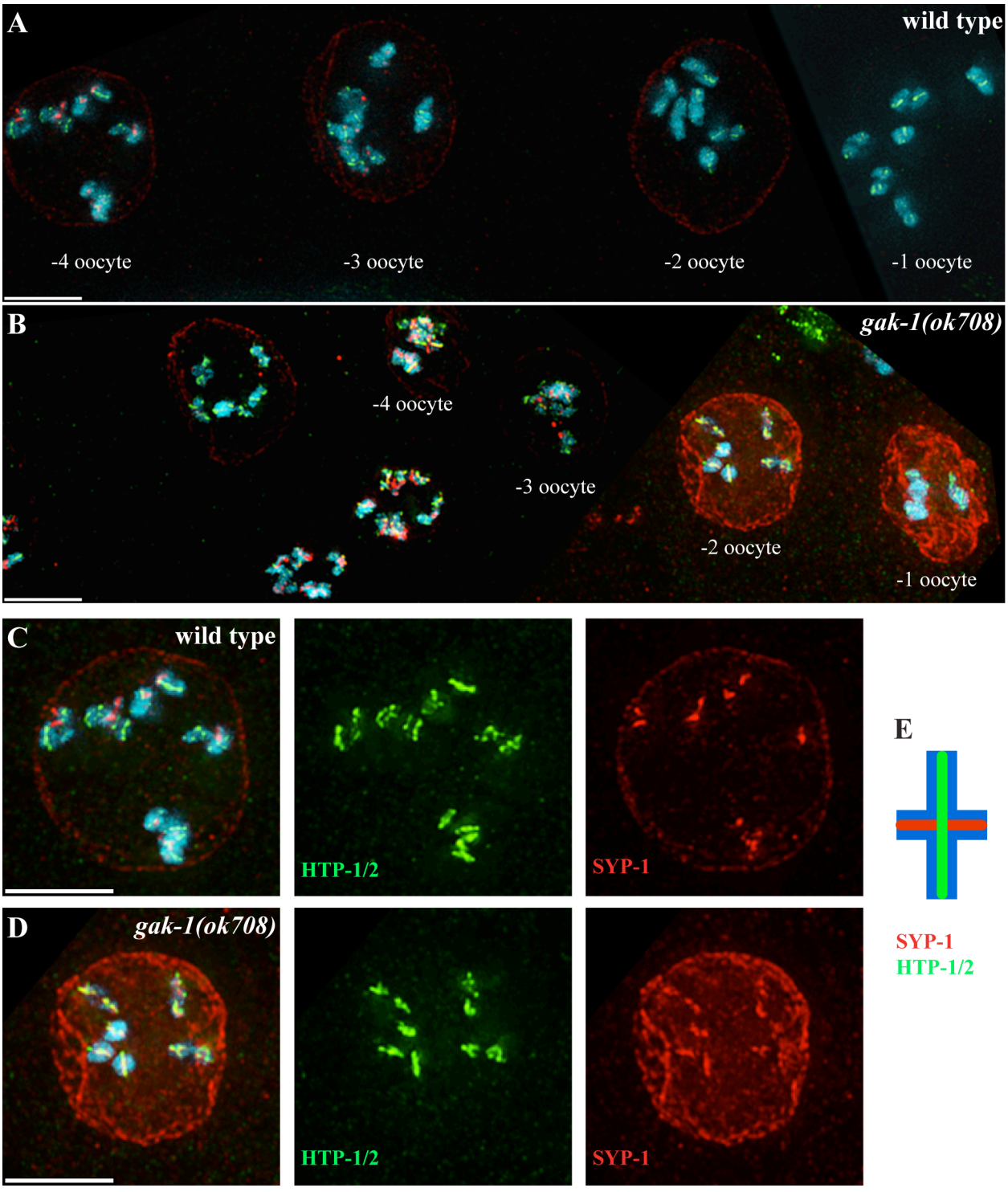

Figure 7: Mutations in *gak-1* lead to an SC disassembly defect.
(A-B) Diakinesis nuclei maturing from left to right from wild type and a *gak-1(ok708)* mutant with DAPI (DNA) in blue, SYP-1 in red, and HTP-1/2 in green. The synaptonemal complex (SC) disassembles in a stereotypical fashion, such that SYP-1 is lost at the long arm of the bivalent and HTP-1/2 is lost at the short arm of the bivalent. In *gak-1* mutants, the SC disassembles aberrantly, as SYP-1 and HTP-1/2 do not maintain strict reciprocal localization. (C-D) Zoomed-in sections from (A) and (B). All scale bars are 5 μm. (E) Cartoon of SC disassembly along a bivalent.

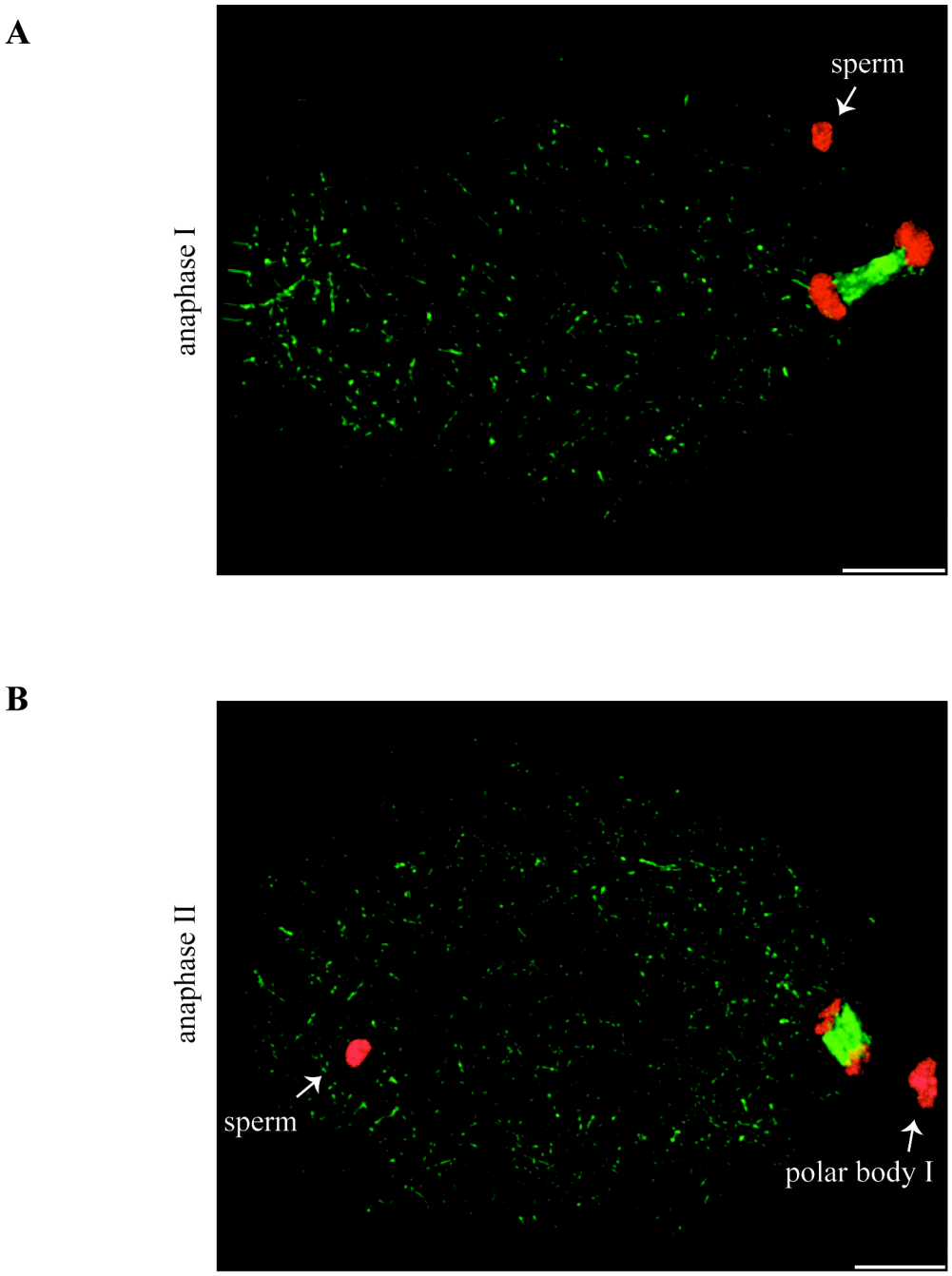

Figure 8: Gross segregation defects are not observed in early *gak-1* embryos.
(A) Anaphase I in *gak-1(ok708)* embryo with DAPI (DNA) in red and tubulin in green. (B) Anaphase II in *gak-1(ok708)* embryo with DAPI (DNA) in red and tubulin in green. All scale bars are 5 μm.

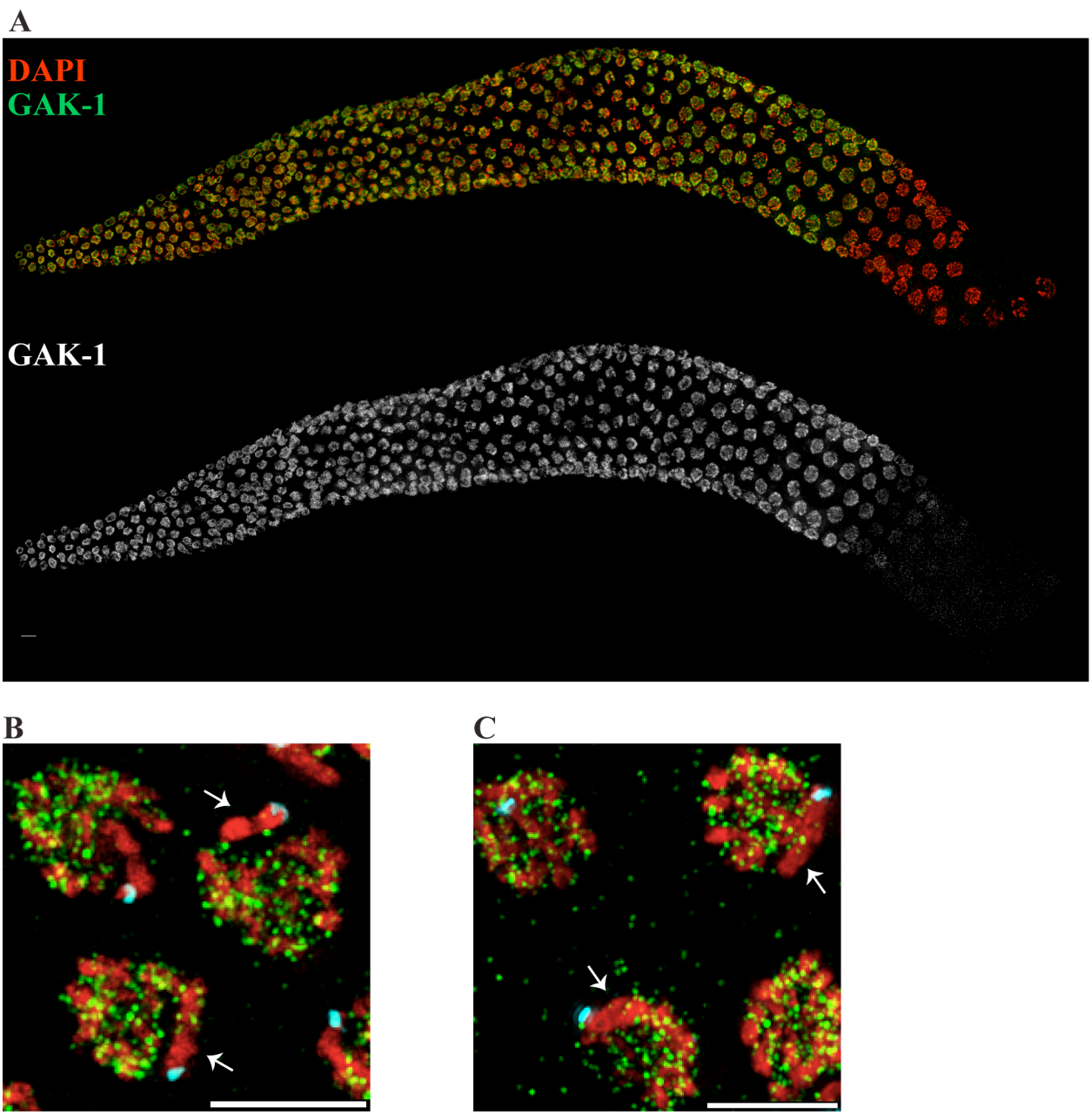

Figure 9: GAK-1 localizes to chromatin in germline nuclei.
(A) Wild type hermaphrodite gonad showing DAPI (DNA) in red and GAK-1 in green. The gonad is oriented such that meiosis is proceeding from left to right, with premeiotic nuclei on the left and diakinesis nuclei to the right. Scale bar is 5 µm. (B) Late pachytene nuclei from a wild type animal showing DAPI in red, GAK-1 in green, and HIM-8 (marking the X chromosome) in blue. GAK-1 is enriched on autosomes compared to the X (marked by arrows). Scale bar is 5µm. (C) Late pachytene nuclei from a wild type animal showing DAPI in red, HIM-17 in green, and HIM-8 (marking the X chromosome) in blue. HIM-17 is enriched on autosomes compared to the X (marked by arrows). Scale bar is 5µm.

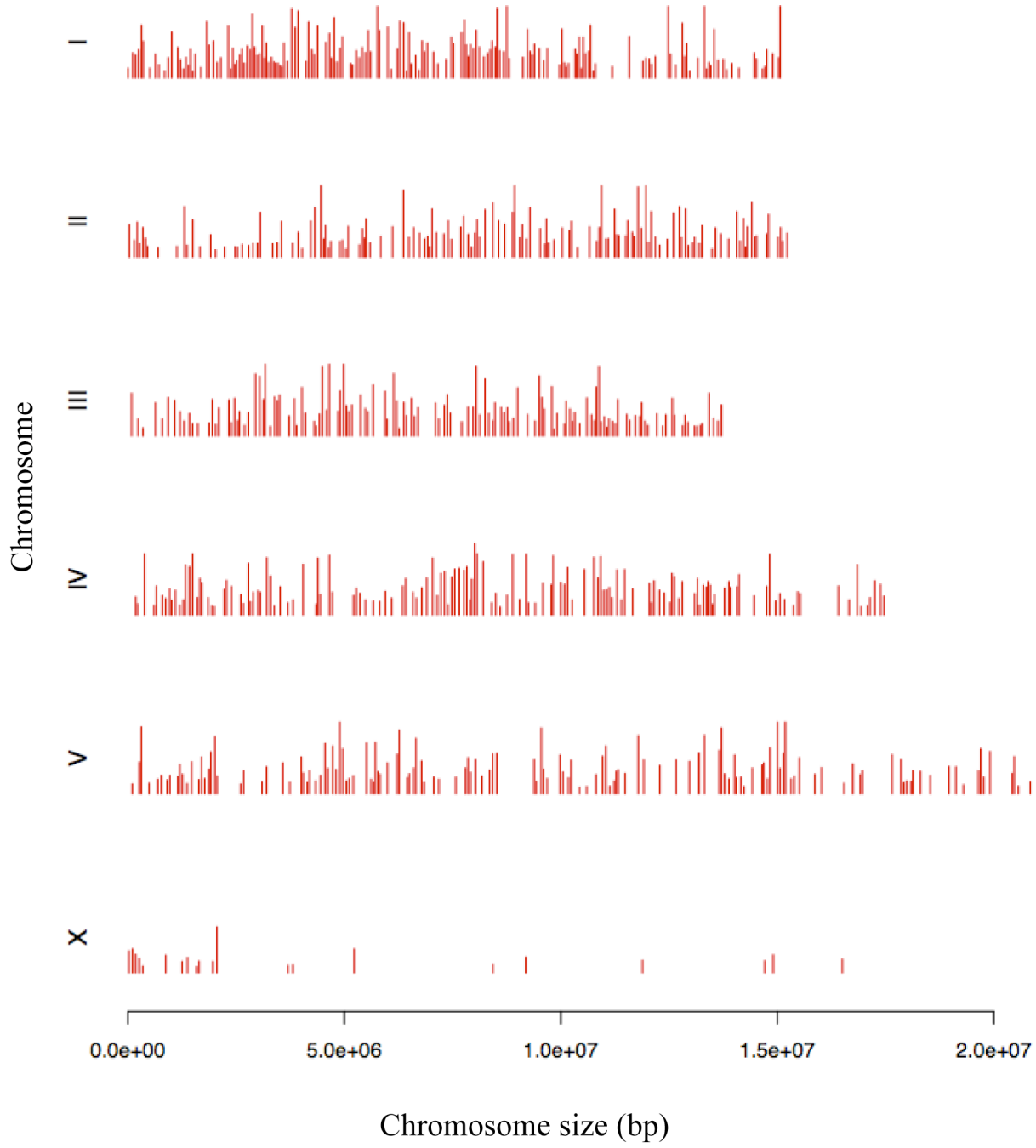

Figure 10: GAK-1 ChIP-seq data confirm that GAK-1 is enriched on autosomes compared to the X chromosome.
Global profiles of relative enrichment of GAK-1 within the *C. elegans* genome. ChIP-seq peaks were called using MACS.

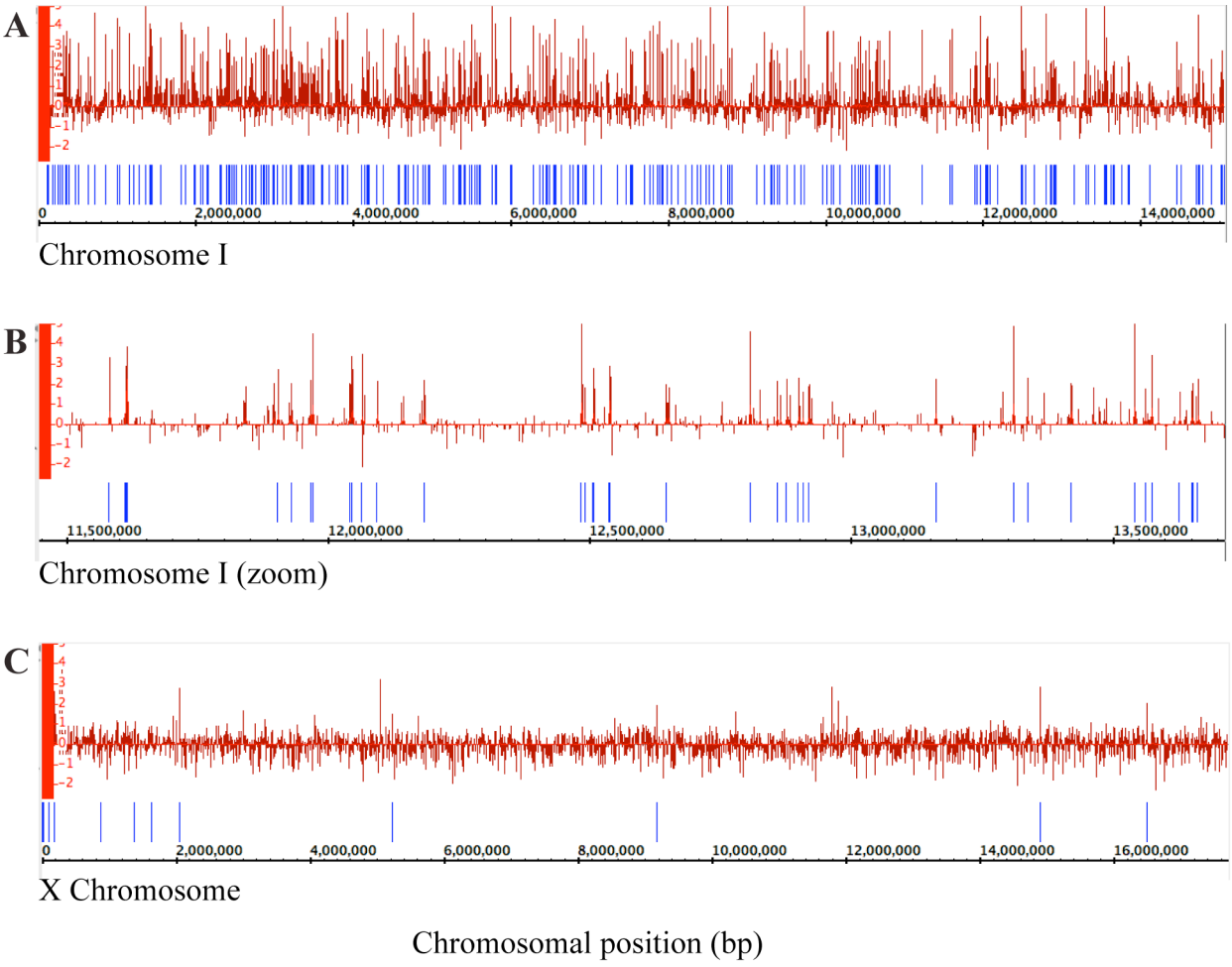

Figure 11: GAK-1 ChIP-seq data look similar when analyzed by two peak-calling programs.
GAK-1 peak-calls by MACS (blue bars) and SPP (red plot) for chromosomes I and X viewed on the Integrated Genome Browser. Relative enrichment of GAK-1 on chromosome I (A), a zoomed-in 2-megabase region at the right end of chromosome I (B), and the X chromosome (C). Relative enrichment of GAK-1 is plotted as a function of position in the *C. elegans* genome. Like MACS, SPP-processed ChIP-seq data also shows fewer peaks called on the X chromosome.

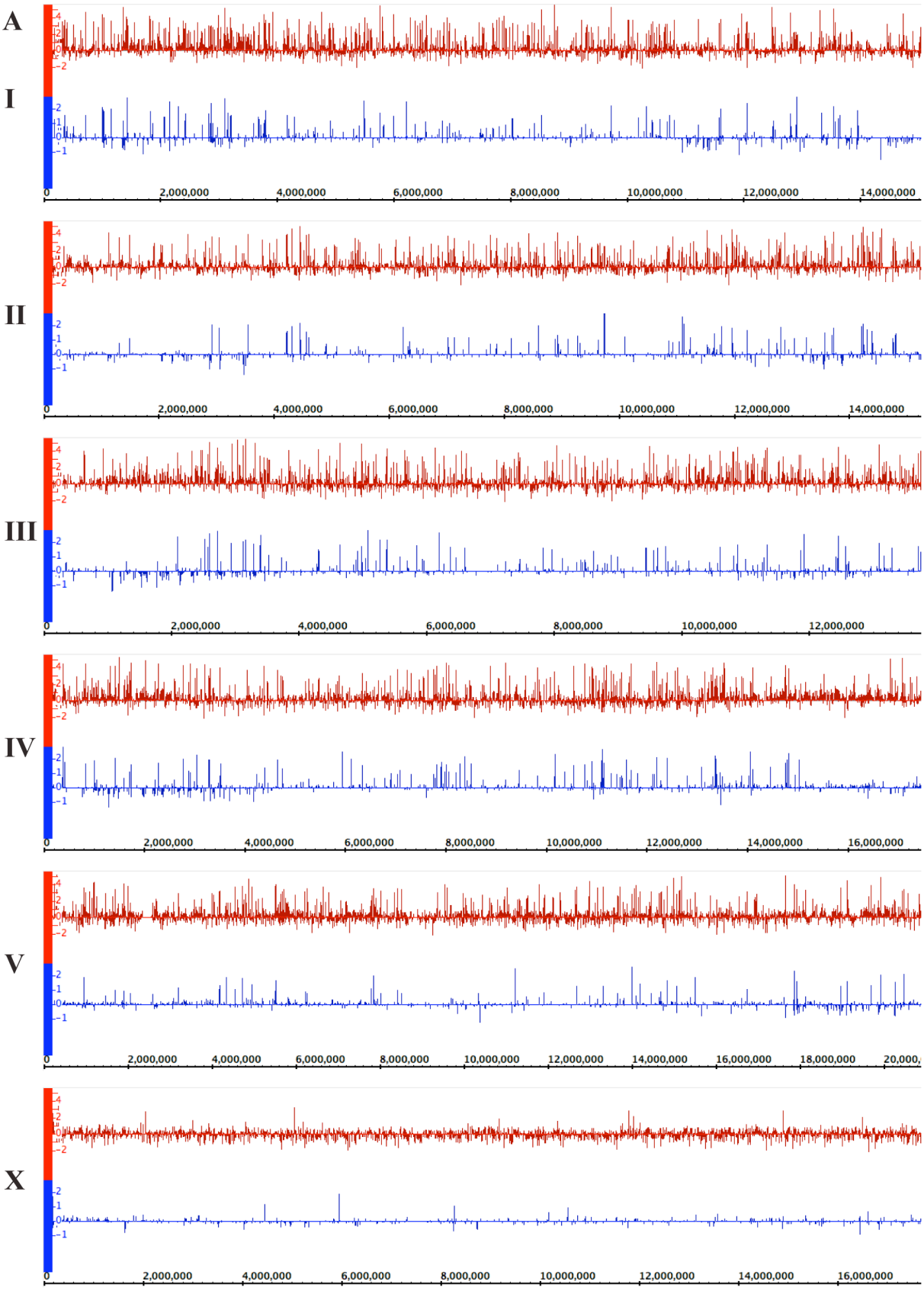
A
I
II
III
IV
V
X
Chromosomal position (bp)

B

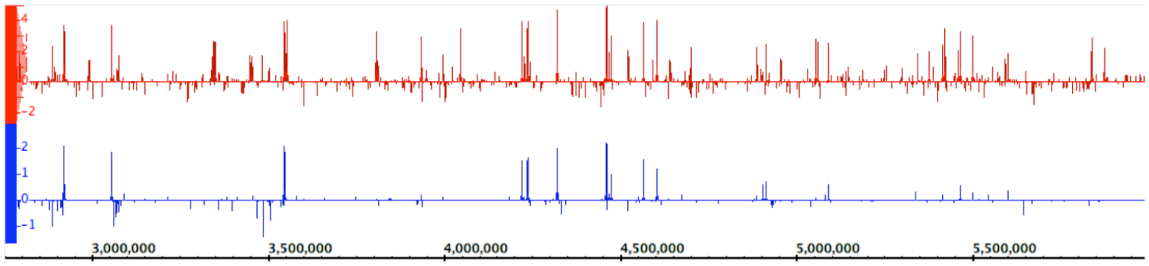

Figure 12: GAK-1 shares a subset of binding sites throughout the genome with the recombination protein HIM-17.
(A) Global profiles of GAK-1 (plots in red) and HIM-17 (plots in blue) enrichment within the *C. elegans* genome. ChIP-seq peaks were called using SPP and viewed in the Integrated Genome Browser. Relative enrichment of GAK-1 and HIM-17 is plotted as a function of position in the *C. elegans* genome. HIM-17 enrichment sites overlap with a subset of GAK-1 peaks. Like GAK-1, HIM-17 is also enriched on autosomes compared to the X chromsome. (B) A zoomed-in 2.5-megabase region towards the left end of chromosome II shows clear overlap between SPP-called GAK-1 and HIM-17 peaks.

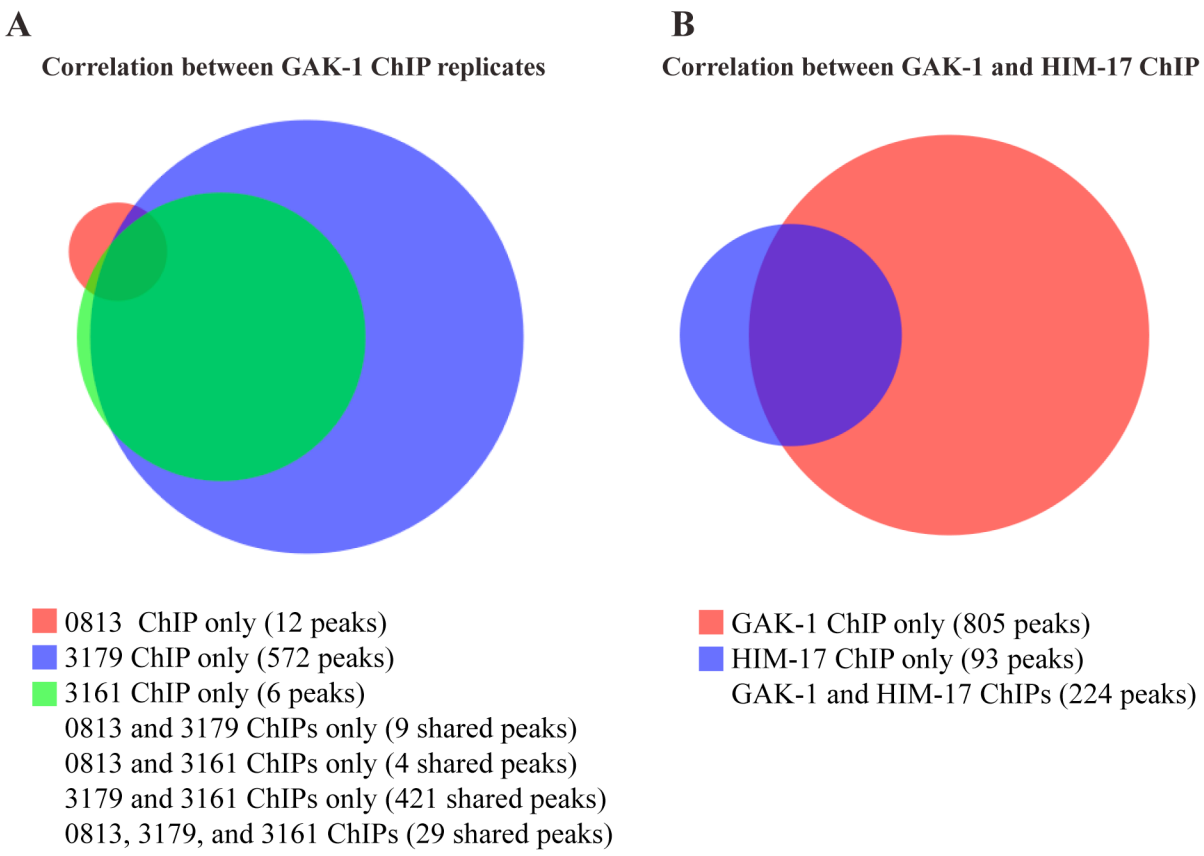

Figure 13: GAK-1 ChIP-seq replicates and HIM-17 ChIP-seq results show strong correlation with one another.
(A) Two GAK-1 ChIP-seq replicates yield similar genome-wide binding sites. Three ChIP-seq experiments with three different GAK-1 antibodies were performed. Antibodies 3179 and 3161 were made against the same region of GAK-1, and their respective ChIP-seq experiments give overlapping results. Antibody 0813 was made against a different region of GAK-1 and had very few peaks called. Thus, it was considered a failed experiment. ChIP-seq peaks were called by MACS. All GAK-1 ChIP data shown in other figures is based on the 3179 ChIP experiment. (B) A high percentage of HIM-17 binding sites are occupied by GAK-1 peaks. ChIP-seq peaks were called by MACS.

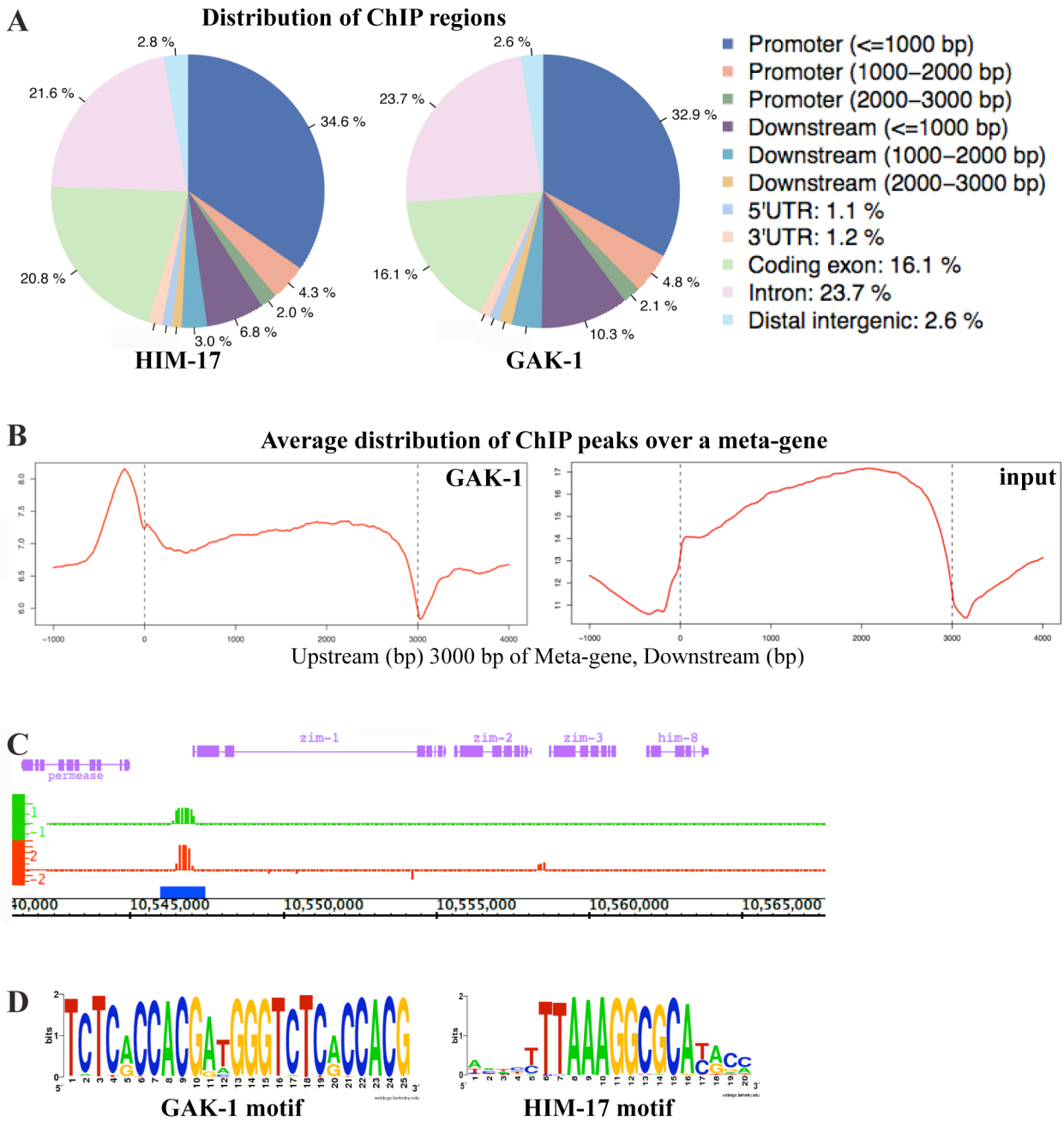

Figure 14: GAK-1 and HIM-17 are enriched at gene promoters and are associated with specific DNA motifs. (A) Distribution of GAK-1 and HIM-17 ChIP-seq peaks throughout the genome. ChIP-seq peaks were called by MACS. (B) Average distribution of GAK-1 and input peaks over a meta-gene. These graphs describe the average distribution of sequenced tags from GAK-1 ChIP and input samples over any given gene. Position 0 bp is the location of the transcription start site, while position 3000 bp is the location of the stop codon in an average gene. ChIP-seq peaks were called by MACS. (C) GAK-1 and HIM-17 are enriched at the promoter of the *zim/him-8* operon. ChIP-seq peaks were called by SPP (GAK-1 in red and HIM-17 in green) and MACS (GAK-1 in blue) and viewed on the Integrated Genome Browser. (D) Consensus binding motifs for GAK-1 and HIM-17. MDscan was used on MACS-called peaks to identify potential binding site motifs. GAK-1 and HIM-17 motifs had significantly high MDscan scores of 7.304 and 7.908, respectively.

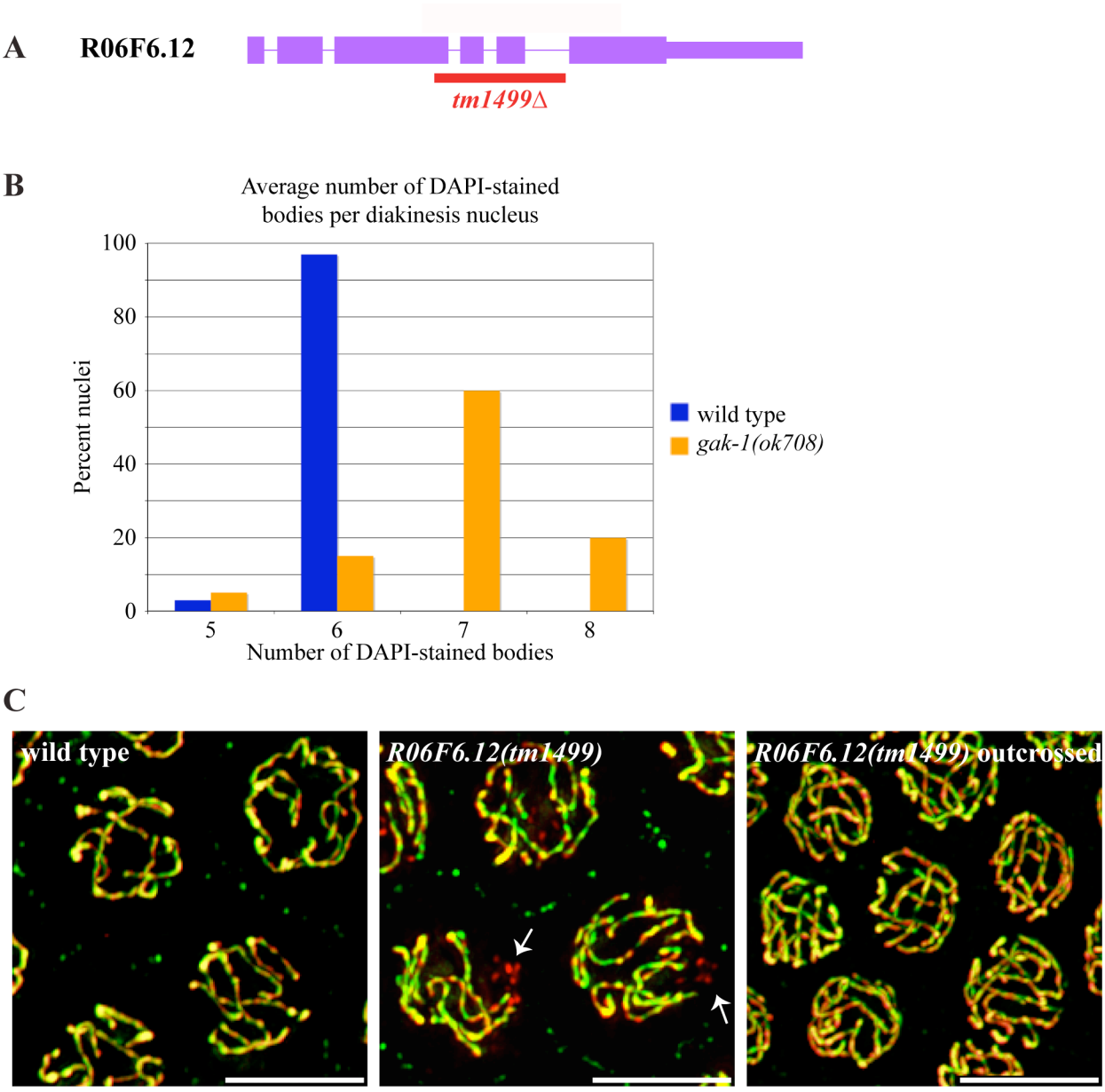

Figure 15: Characterization of the GAK-1 interactor R06F6.12.
(A) *R06F6.12* gene structure with location of *tm1499* deletion. (B) Quantification of DAPI-stained bodies in diakinesis for wild type and non-outcrossed *R06F6.12(tm1499)* animals. Non-outcrossed *R06F6.12* mutants often have more than 6 DAPI-stained bodies, indicating that some homolog pairs are not undergoing crossovers. (C) Pachytene nuclei from wild type and *R06F6.12(tm1499)* mutants showing HIM-8 (blue) and the synaptonemal complex proteins HTP-3 (red) and SYP-1 (green). The original mutagenized *R06F6.12* line has some unsynapsed chromosomes (marked by arrows), while the outcrossed strain has no synapsis defect. Scale bars are 5 µm.

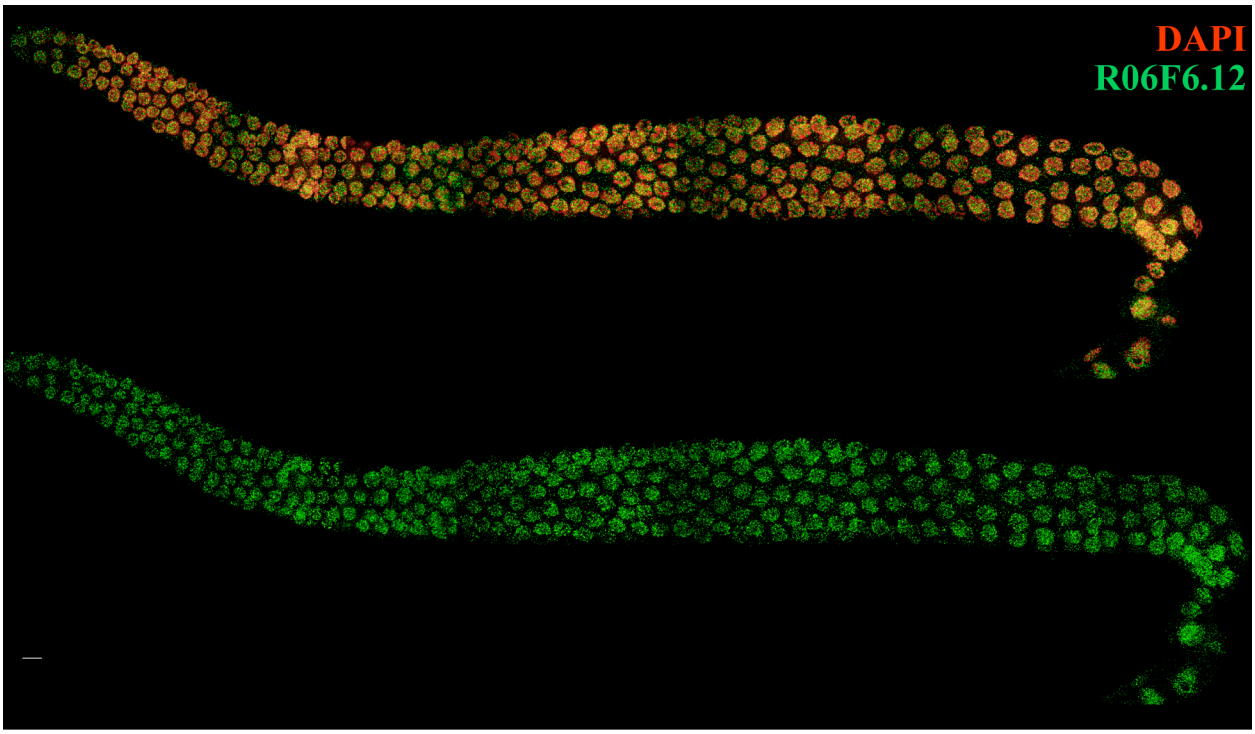

Figure 16: R06F6.12 localizes to chromatin throughout the *C. elegans* germline.
Wild type hermaphrodite gonad showing DAPI (DNA) in red and R06F6.12 in green. The gonad is oriented such that meiosis is proceeding from left to right, with premeiotic nuclei on the left and diakinesis nuclei to the right. Scale bar is 5 μm.